

SYNTHESES OF CONDUCTING POLYMERS OF 3-ESTER SUBSTITUTED
THIOPHENES AND
CHARACTERIZATION OF THEIR ELECTROCHROMIC PROPERTIES

A THESIS SUBMITTED TO
THE GRADUATE SCHOOL OF NATURAL AND APPLIED SCIENCES
OF
MIDDLE EAST TECHNICAL UNIVERSITY

BY

PINAR ÇAMURLU

IN PARTIAL FULFILLMENT OF THE REQUIREMENTS
FOR
THE DEGREE OF DOCTOR OF PHILOSOPHY
IN
CHEMISTRY

SEPTEMBER 2006

Approval of the Graduate School of Natural and Applied Sciences

Prof. Dr. Canan Özgen
Director

I certify that this thesis satisfies all the requirements as a thesis for the degree of Doctor of Philosophy.

Prof. Dr. Hüseyin İşçi
Head of Department

This is to certify that we have read this thesis and that in our opinion it is fully adequate, in scope and quality, as a thesis and for the degree of Doctor of Philosophy.

Prof. Dr. Levent Toppare
Supervisor

Examining Committee Members

Prof. Dr. Zuhâl Küçükyavuz (METU, CHEM)

Prof. Dr. Levent Toppare (METU, CHEM)

Prof. Dr. Leyla Aras (METU, CHEM)

Prof. Dr. Teoman Tinçer (METU, CHEM)

Prof. Dr. Kadir Pekmez (Hacettepe.Üniv., CHEM)

I hereby declare that all information in this document has been obtained and presented in accordance with academic rules and ethical conduct. I also declare that, as required by these rules and conduct, I have fully cited and referenced all material and results that are not original to this work.

Name, Last name:

Signature :

ABSTRACT

SYNTHESES OF CONDUCTING POLYMERS OF 3-ESTER SUBSTITUTED THIOPHENES AND CHARACTERIZATION OF THEIR ELECTROCHROMIC PROPERTIES

Çamurlu, Pinar

Ph.D., Department of Chemistry

Supervisor: Prof. Dr. Levent Toppare

September 2006, 132 pages

In this study three different 3-ester substituted thiophene monomers were synthesized via esterification reaction of 3-thiophene ethanol with adipoyl chloride or sebacoyl chloride or octanoyl chloride in the presence of triethylamine at 0°C. Characterizations of the monomers were performed by ¹H-NMR, ¹³C-NMR, FTIR, DSC, TGA techniques. Electrochemical behavior of the monomers both in presence or absence of BFEE were studied by cyclic voltammetry. Results showed the astonishing effect of BFEE on the polymerization, where free standing films of the homopolymers could be synthesized. Copolymers of the monomers with thiophene or 3-methyl thiophene were synthesized at constant potential electrolysis and the resultant polymers were characterized by FTIR, DSC, TGA, SEM and conductivity measurements. Second part of the study was devoted to investigate the one of most interesting property of conducting polymers, the ability to switch reversibly between the two states of different optical properties, 'electrochromism'. In recent years there has been a growing interest in application of conducting polymers in electrochromic devices. Thus, electrochromic properties of the synthesized conducting polymers were investigated by several methods like spectroelectrochemistry, kinetic and colorimetry studies. Spectroelectrochemistry

experiments were performed in order to investigate key properties of conjugated polymers such as band gap, maximum absorption wavelength, the intergap states that appear upon doping and evolution of polaron and bipolaron bands. Switching time and optical contrast of the homopolymers and copolymers were evaluated via kinetic studies. Results implied the possible use of these materials in electrochromic devices due to their satisfactory electrochromic properties like short switching time and stability. Generally the homopolymers displayed color changes between yellow, green and blue colors upon variation of applied potentials. Fine tuning of the colors of the polymers were accomplished by techniques like copolymerization and lamination. These studies were supported with experiments like spectroelectrochemistry and FTIR. Results showed the possible control of the color of the electrochromic material in a predictable, controlled and reproducible manner. Yet, it was possible to achieve different tones of yellow, green, orange color in neutral state of these materials. As the last part of the study, dual type electrochromic devices based on polymers of 3-ester substituted thiophenes with poly(3,4-ethylenedioxythiophene) were constructed, where the former and the later functioned as anodically and cathodically coloring layers respectively. Spectroelectrochemistry, switching ability, stability, open circuit memory and color of the devices were investigated and the results revealed that these devices have satisfactory electrochromic parameters.

Keywords: Electropolymerization, Electrochromic polymers, Conducting polymers, Electrochromic Devices, Copolymerization, 3-ester substituted thiophenes

ÖZ

ESTER SÜBSTİTÜYE TİYOFENLERİN İLETKEN POLİMERLERİNİN SENTEZİ VE ELEKTROKROMİK ÖZELLİKLERİNİN KARAKTERİZASYONU

Çamurlu, Pınar

Doktora, Kimya Bölümü

Tez Yöneticisi: Prof. Dr. Levent Toppare

Eylül 2006, 132 sayfa

Bu çalışmada üç farklı 3-ester sübstitüe tiyofen monomerleri, trietilamin varlığında 3-tiyofen ethanol ile adipoil klorür veya sabasoil klorür veya oktanoil klorür ile 0°C deki esterifikasyon reaksiyonu ile sentezlenmiştir. Monomerlerin karakterizasyonu ¹H-NMR, ¹³C-NMR, FTIR, DSC, TGA teknikleri kullanılarak yapılmıştır. Monomerlerin elektrokimyasal davranışı dönüşümlü voltametre ile BFEE'nin varlığında ve yokluğunda incelenmiştir. Sonuçlar BFEE'nin polimerizasyona olan önemli etkisini ortaya koymuş ve elektrottan filim olarak kolayca ayrılabilen homopolimerler sentezlenmiştir. Sabit potansiyel elektroliz yöntemi kullanılarak monomerlerin tiyofen veya 3-metil tiyofen varlığında kopolimerleri sentezlenmiş ve elde edilen polimerler FTIR, NMR, GC-MS, DSC, TGA, SEM ve iletkenlik ölçümleri gibi yöntemler kullanılarak karakterize edilmiştir. Son yıllarda iletken polimerlerin elektrokromik cihazlarda kullanılması ilgi çeken bir konu haline gelmiştir. Bu sebeple çalışmanın ikinci kısmı, tersinir olarak iki farklı optik özellik arasında değişim yapma özelliğine, yani iletken polimerlerin en ilginç özelliklerinden biri olan elektrokromizme adanmıştır. Sentezlenen iletken polimerlerin özellikleri, spektroeletrokimya, kinetik ve kolorimetrik çalışmalar gibi yöntemlerle araştırılmıştır. Spektroeletrokimya deneyleri bant aralığı, maksimum soğurma

dalga boyu, katkılama sonucu ortaya çıkan arabant halleri ve polaron , bipolaron bantları gibi iletken polimerlerin anahtar özelliklerini ortaya çıkarmak için yapılmıştır. Homopolimerlerin ve kopolimerlerin tepki zamanı ve optik kontrast özellikleri kinetik çalışmalarla incelenmiştir. Sonuçlar bu malzemelerin önemli elektromik özellikler olan kararlılık ve kısa tepki zamanlarına sahip olduğunu ve elektromik cihaz uygulamaları için uygun olduğunu göstermiştir. Genel olarak uygulanan farklı voltajlarda homopolimerlerin sarı, yeşil ve mavi renkler arasında değişim gösterdiği gözlenmiştir. Kopolimerizasyon ve laminasyon teknikleri kullanılarak polimerlerin renkleri hassas bir biçimde ayarlanabilmiştir. Bu çalışmalar spektroeletrokimya ve FTIR deneyleriyle desteklenmiştir. Çalışmalar elektrokromik malzemenin renginin önceden belirlenebilir ve tekrarlanabilir bir biçimde kontrol edilebildiğini göstermiştir. Malzemelerin nötral hallerinde farklı tonlarda sarı, yeşil ve turuncu renkleri elde edilmiştir. Çalışmanın son kısmında ise 3-ester sübtitüye tiyofen polimerleri ve poli(3,4-etilendioksitiyofen) kullanılarak elektrokromik cihazlar kurulmuştur. Bu cihazlarda 3-ester sübtitüye tiyofen polimerleri yükseltgendiğinde, poli(3,4-etilendioksitiyofen) ise indirgendiğinde renklenen katman olarak kullanılmıştır. Bu cihazların spektroeletrokimya, tepki özellikleri, kararlılıkları, açık devre hafızaları ve renkleri araştırılmış ve tatmin edici elektrokromik özellikler göstermişlerdir.

Anahtar Kelimeler: İletken polimerler, elektrokimyasal polimerleşme, elektrokromik özellikler, elektrokromik cihazlar, 3-ester substitue tiyofenler

TO MY DEAR FAMILY

ACKNOWLEDGMENTS

It is a great pleasure to thank my supervisor Prof. Dr. Levent Toppare for his valuable guidance, support, advices for the completion of this work.

I would like to thank to Dr. Ali ırpan for introducing the field of work and for his valuable discussions and friendship.

I would like to thank to Prof. Dr. Ahmet nal, Dr. Atilla Cihaner for their help during ESR studies.

I would like to express my special thanks to, Metin Ak, Dr. Senem Kıralp, Grkem Gnbař, Simge Tarku, Bařak Yiğitsoy, Serhat Varıř, zlem Trkarılan, Yusuf Gner, Canan Biran, Bahar Bingl and Yusuf Nur for their cooperation and their kind friendships.

Words fail to express my eternal gratitude to my parents Oya and Hasan řanlı and my brother ner řanlı, for giving me the intellectual and emotional guidance that made me who I am, and for their never-ending support, encouragement along with understanding for my frequent absences.

Finally, my special thanks goes to Erdem amurlu for his continuous support, love and patience to my long working hours, absence at weekends and quickly prepared dinners. Without him none of this work could be accomplished.

TABLE OF CONTENTS

ABSTRACT	iv
ÖZ.....	vi
ACKNOWLEDGMENTS	ix
TABLE OF CONTENTS	x
LIST OF FIGURES	xiii
LIST OF TABLES	xx
ABBREVIATIONS.....	xxi
CHAPTERS	
1.INTRODUCTION.....	1
1.1. Conducting Polymers	1
1.2. Band Theory.....	2
1.3. Conduction in Conducting Polymers	4
1.3.1. Solitons, Polarons, Bipolarons	4
1.3.2. Doping Types in Conducting Polymers.....	6
1.4. Polythiophenes.....	8
1.4.1. Chemical polymerization.....	9
1.4.2. Electrochemical Polymerization	11
1.4.2.1. Mechanism of Electropolymerization	12
1.4.2.2. Factors Affecting Electropolymerization	13
1.4.2.3. Polythiophene Paradox.....	16
1.4.2.4. Effect of Substitution on Thiophene.....	17
1.5. Application Areas of Conducting Polymers	20
1.5.1. Light Emitting Diodes	21
1.5.2. Solar Cells.....	23
1.5.3. Organic Field Effect Transistors.....	24
1.5.4. Sensors.....	26
1.5.4.1. Biosensors	27
1.6. Chromism	28
1.6.1. Thermochromism	28
1.6.2. Photochromism	28
1.6.3. Halochromism	30
1.6.4. Piezochromism	30
1.6.5. Solvatochromism	30
1.6.6. Electrochromism	31
1.7. Electrochromism in Conducting Polymers.....	32
1.7.1. Factors Affecting the Band Gap and Color of Conducting Polymer	35
1.8. Electrochromic Devices.....	39
1.8.1. Types of Electrochromic Devices.....	40

1.8.2. Dual Type Transmissive /Absorptive Type Electrochromic Devices	40
2.EXPERIMENTAL	45
2.1. Materials.....	45
2.2. Equipment	45
2.3. Procedure.....	46
2.3.1.Synthesis of monomers	46
2.4. Synthesis of Conducting Polymers.....	47
2.4.1. Electrochemical Polymerization	47
2.4.1.1. Homopolymerization	47
2.4.1.2. Copolymerization	47
2.4.1.2.1. Copolymers of HABTE.....	47
2.4.1.2.2. Copolymer of DATE: P(DATE-co-Th)	48
2.4.1.2.3. Copolymer of OTE with 3-methyl thiophene : P(OTE-co-MeTh)	48
2.4.2. Chemical Polymerization	48
2.5. Characterization of Conducting Polymers	48
2.5.1. Cyclic Voltammetry (CV).....	48
2.5.2. Conductivity	52
2.5.3. Electrochromic Properties of the Conducting Polymers.....	53
2.5.3.1. Spectroelectrochemistry	53
2.5.3.2. Switching Studies	55
2.5.3.3. Colorimetry	55
2.6. Device Construction	56
2.6.1. Preparation of Gel Electrolyte	58
2.7. Characterization of the Electrochromic Devices.....	59
2.7.1. Spectroelectrochemistry Studies of Electrochromic Devices.....	59
2.7.2. Switching Properties of Electrochromic Devices.....	59
2.7.3. Open Circuit Stability	59
2.7.4. Stability of the Electrochromic Devices.....	60
3.RESULTS AND DISCUSION	61
3.1. Conducting Polymers of HABTE	61
3.1.1. Synthesis and Characterization of HABTE	61
3.1.2. Cyclic Voltammetry	62
3.1.3. FTIR.....	64
3.1.4. Thermal Properties	66
3.1.5. Morphologies of the Films.....	68
3.1.6. Conductivities of the Films	69
3.2. Conducting Polymers of OTE.....	69
3.2.1. Characterization of OTE	69
3.2.2. Cyclic Voltammetry	70
3.2.3. FTIR.....	71
3.2.4. Thermal analysis.....	73
3.2.5.Morphology of the films.....	74
3.2.6. Conductivity Measurements.....	75
3.3. Conducting Polymers of DATE.....	75
3.3.1. Characterization of DATE	75
3.3.2. Cyclic Voltammetry	76

3.3.3. FTIR Spectra.....	77
3.3.4. Thermal Behavior of Samples.....	78
3.3.5. Conductivity Measurements.....	79
3.3.6. Morphologies of the films.....	80
3.4. Electrochromic Properties of Polymers.....	81
3.4.1. Electrochromic Properties of Polymers of HABTE.....	81
3.4.2. Electrochromic Properties of POTE.....	88
3.4.3. Electrochromic Properties of Polymers of DATE.....	90
3.5. Fine Tuning of Color.....	93
3.5.1. Copolymerization.....	93
3.5.2. Green: The Missing Color- Lamination.....	96
3.6. Electrochromic Device Application.....	100
3.6.1. Electrochromic Devices of HABTE Based Polymers.....	100
3.6.1.1. Spectroelectrochemistry.....	101
3.6.1.2. Switching Characteristics.....	102
3.6.1.3. Electrochromic Memory.....	105
3.6.1.4. Stability.....	105
3.6.2. Electrochromic Devices of POTE and PDATE.....	107
3.6.2.1. Spectroelectrochemistry.....	108
3.6.2.2. Switching.....	110
3.6.2.3. Stability.....	111
3.6.2.4. Open Circuit Stability.....	112
4.CONCLUSIONS.....	115
REFERENCES.....	118
APPENDIX A.....	126
VITA.....	132

LIST OF FIGURES

Figures

Figure 1.1 Simple band picture explaining the difference between an insulator, a semiconductor and a metal.....	2
Figure 1.2 Generation of bands in polyacetylene.....	3
Figure 1.3 (a) Degenerate polyacetylene; and (b) non-degenerate polypyrrole.....	5
Figure 1.4 Charge carries in PPy and its corresponding energy bands in the mid gap.....	6
Figure 1.5 Doping mechanisms and related applications	7
Figure 1.6 Schematic respresentation of doping a) p-doping and b) n-doping of conducting polymer.....	8
Figure 1.7 Typical cyclic voltammogram for a conducting polymer exhibiting p-doping, the structure of polyacetylene is shown only for illustrational purpose.....	9
Figure 1.8 Synthesis of polythiophene via a) metal catalyzed coupling and b) chemical oxidation	10
Figure 1.9 McCullough method for the synthesis of regioregular poly(alkylthiophenes)	11
Figure 1.10 Electropolymerization mechanism. a) Polymerization of heterocycles (X = S, O, NH), b) Competitive reaction pathways in unsubstituted poly(heterocycles).....	14
Figure 1.11 Variation of monomer oxidation potential with Hammett constant for β -substituted thiophene monomers; where β = Me, H, Br and COOH from left to right, respectively	19
Figure 1.12 a) Schematic representation of a single-layer polymer electroluminescent diode b) Successive steps to electroluminescence	22

Figure 1.13 a) Formation of a bulk heterojunction and subsequent photoinduced electron transfer inside a composite formed from the interpenetrating donor/acceptor network plotted with the device structure for such a kind of junction b) Typical I-V characteristics of a solar cell, with the three characteristic parameters: short circuit current I_{sc} , open-circuit voltage V_{oc} , and Fill factor $FF = P_{max}/(V_{oc} * I_{sc})$; P_{max} is the electrical power delivered by the cell at the maximum power point MPP .	24
Figure 1.14 Typical a) bottom contact OFET architecture b) Current-Voltage curves of an OFET with different gate voltages	25
Figure 1.15 Schematic diagram showing the main components of a biosensor. The biocatalyst (a) converts the substrate to product. This reaction is determined by the transducer (b), which converts it to an electrical signal. The output from the transducer is amplified (c), processed (d) and displayed (e)	27
Figure 1.16 Schematic representation of photochromism	29
Figure 1.17 The three common viologen redox states, dication, radical cation, neutral species from left to right respectively.	32
Figure 1.18 Polaron and bipolarons in non-degenerate ground state polymers: band diagrams for neutral (left), positive polaron (center) and positive bipolaron (right); B) neutral (left), lightly doped (center) and heavily doped (right).	34
Figure 1.19 Schematic representation of parameters that play a determining role on E_g	35
Figure 1.20 Some examples of commercial applications of ECDs	39
Figure 1.21 The principles of four different applications of electrochromic devices.	41
Figure 1.22 Schematic illustration of Dual Type Transmissive /Absorptive Type Electrochromic Device configurations.	41
Figure 1.23 Schematic illustration of electrochemistry in ECDs	42
Figure 1.24 Schematic representation of the visible spectra for both anodically and cathodically coloring polymer demonstrating the concept of dual polymer ECDs for absorptive/ transmissive windows	43
Figure 2.1 Synthesis route of monomers	46

Figure 2.2 Typical (a) Potential–time excitation signal in CV (b) cyclic voltammogram of a reversible $O + ne^- \leftrightarrow R$ redox process	49
Figure 2.3 Concentration distribution of the oxidized and reduced forms of the redox couple at different times during cyclic voltammetric experiment correspond to a) the initial potential, b) the formal potential during the forward scan and c) zero reactant concentration at the surface	50
Figure 2.4 Cyclic Voltammogram of a representative type of electroactive monomer	51
Figure 2.5 Four-probe conductivity measurement setup	53
Figure 2.6 Schematic representation of electrochemical used in spectral studies.	54
Figure 2.7 CIELAB color space.	56
Figure 2.8 Schematic representation of the transmissive/absorptive type ECD....	57
Figure 2.9 Redox site charge vs synthesis charge graph for PEDOT synthesized at 1.5 V.....	58
Figure 3.1 $^1\text{H-NMR}$ of HABTE	61
Figure 3.2 Cyclic voltammogram of (a) monomer (HABTE), (b) HABTE in the presence of BFEE, (c) HABTE in the presence of thiophene and BFEE, (d) thiophene in the presence of BFEE, with platinum working and counter electrodes and a Ag/Ag^+ reference electrode in 0.1 M TBAFB/ACN with 500mV/s scan rate	63
Figure 3.3 Electrochemical polymerization of HABTE.....	65
Figure 3.4 FTIR spectra of a) PHABTE b) P(HABTE-co-Th) c)PTh.....	66
Figure 3.6 Chemically synthesized PHABTE (a) DSC thermogram (b) TGA thermogram.....	67
Figure 3.7 SEM micrographs of (a) PHABTE (b) P(HABTE/Th) c)P(HABTE-co-Th) d)PTh/BFEE.....	68
Figure 3.8 $^1\text{H-NMR}$ spectrum of OTE	70
Figure 3.9 Cyclic Voltammogram of (a) OTE in TBAFB/ACN and (b) OTE in TBAFB/ACN/BFEE (c) OTE in pure BFEE (d) OTE in the presence of 3-methyl thiophene and e) 3-methyl thiophene in TBAFB/ACN (Multi scans reveal the polymer chain growth).	72
Figure 3.11 Thermogram of (a) P(OTE/MeTh), (b) P(MeTh) and (c) POTE.....	73
Figure 3.12 SEM images of (a) P(OTE), (b) P(OTE-co-MeTh) and (c)P(MeTh). ..	74
Figure 3.13 $^1\text{H-NMR}$ of DATE.....	75

Figure 3.14 Cyclic Voltammogram of (a) DATE in 0.1M TBAFB in ACN (b)P(DATE) (c)(PDATE-co-Th) (d) PTh in 0.1M TBAFB in BFEE / ACN	76
Figure 3.15 FTIR spectra of (a) DATE (b) P(DATE-co-Th) (c)P(DATE).....	78
Figure 3.16 TGA thermogram (a) DATE (b) P(DATE-co-Th) (c)P(DATE).....	79
Figure 3.17 SEM micrographs of (a) P(DATE) (b) P(DATE-co-Th) c)PTh	80
Figure 3.18 Optoelectrochemical spectrum of PHABTE as at applied potentials between -1.0 and +1.0 V in 0.1 M TBAFB/ACN in the presence of BFEE: (a) -1.0 V, (b) -0.4 V, (c) 0.0 V, (d) +0.2 V, (e) +0.4 V, (f) +0.6 V , (g) +1.0 V	82
Figure 3.19 The ESR spectrum of PHABTE at a)-1.2, b)-1.0, c)-0.6, d)0.2, e)0.7, f) 1.0 , g)1.3, h)1.5, i)2.0, ,j)2.3, k) 2.5 V (3 min) and at 3V with duration of l) 3, m) 12, n) 20, o)30 min.....	83
Figure 3.20 Optoelectrochemical spectrum of P(HABTE-co-Th) as at applied potentials between 0.4 and +1.0 V in 0.1 M TBAFB/ACN in the presence of BFEE: (a) 0.4 V, (b) 0.5 V, (c) 0.6 V, (d) 0.7 V, (e) 0.8 V, (f) +0.9 V , (g) +1.0 V.....	84
Figure 3.21 Electrochromic switching, a) applied potential for PHABTE in TBAFB/BFEE/ACN.	85
Figure 3.21 Electrochromic switching, b) optical absorbance change monitored at 385 nm for PHABTE in TBAFB/BFEE/ACN.	86
Figure 3.22 Electrochromic switching, optical absorbance change monitored at 470 nm for P(HABTE-co-Th) in TBAFB/BFEE/ACN.	87
Figure 3.23 Optoelectrochemical spectrum of POTE at applied potentials between 0.4 ,0.7 and 1.2 V (from top to bottom) in 0.1 M TBAFB/ACN in the presence of BFEE.....	88
Figure 3.24 Electrochromic switching: Optical absorbance change monitored at 434 nm for POTE in TBAFB/ BFEE / ACN.....	89
Figure 3.25 Optoelectrochemical spectrum of P(DATE) at applied potentials between 0.5 and +1.0 V in 0.1 M TBAFB/ACN in the presence of BFEE: (a) 0.5 V, (b) 0.6 V, (c) 0.7 V, (d) 0.8 V, (e) 0.9 V, (f) +1.0 V ,..	91
Figure 3.26 Optoelectrochemical spectrum of P(DATE-co-Th) at applied potentials between 0.4 and +1.0V in 0.1 M TBAFB/ACN in the presence of BFEE: (a) 0.4 V, (b) 0.6 V, (c) 0.8 V, (d) 1.0 V, (e) 1.2 V, (f) +1.4 V ,	91

Figure 3.27 Electrochromic switching of P(DATE-co-Th)	92
Figure 3.28 UV-Vis spectra of the dedoped conducting polymers synthesized with feed ratio of a) 0, b) 0.1, c) 0.15, d) 0.25, e)1 (w/w) in 0.1 M TBAFB/ACN in the presence of BFEE at 1.5 V.	94
Figure 3.29 Colors of the polymers synthesized with feed ratio of 1, 0.5, 0.25, 0.15, 0.1, 0 % (w/w) in 0.1 M TBAFB/ACN in the presence of BFEE at 1.5 V (from left to right).....	94
Figure 3.30 FTIR spectra of a) pure homopolymer, copolymer synthesized with the feed ration of c).0.15. d) 0.25 e) 0.5 and e) pure polythiophene.	95
Figure 3.31 Schematic representation of lamination and color of the lectrochromic layer at +1.0 and -0.75 V.....	96
Figure 3.32 a) Spectroelectrochemistry studies of laminated electrode in 0.1 M TBAFB containing ACN b) colors of the electrochromic electrode at different potentials.....	98
Figure 3.33 Colors of the electrochromic electrodes of HABTE based polymers at different comonomer ratios and potentials.....	99
Figure 3.34 Colors of the electrochromic electrodes of DATE based polymers at different comonomer ratios and potentials.....	99
Figure 3.35 Colors of the electrochromic electrodes of POTE at different potentials	99
Figure 3.36 Optoelectrochemical spectra of (a) PHABTE/PEDOT ECD at applied potentials between 0.2 and +1.8 V (b) P(HABTE-co-Th)/PEDOT ECD at applied potentials between 0.0 and +1.6 V	103
Figure 3.37 (a) Electrochromic switching, optical absorbance change monitored at 619 nm for PHABTE/PEDOT ECD between 0.0 V and 1.4 V (b) Electrochromic switching, optical absorbance change monitored at 646 nm for P(HABTE-co-Th)/PEDOT between 0.0 V and 1.4 V.....	104
Figure 3.38 Open Circuit Memory of (a) P(HABTE-co-Th)/PEDOT (b) PHABTE/PEDOT monitored by single-wavelength absorption spectroscopy at a) 646 nm +1.6 and 0.0 V b) 619 nm +1.8 and 0.2V, pulses are applied for 1 second for every 200 seconds to recover the initial transmittance	106

Figure 3.39 Cyclic Voltammogram of (a) PHABTE/PEDOT (b) P(HABTE-co-Th)/PEDOT electrochromic devices as a function of repeated scans 500 mV/s: 1 st cycle and after 1000 th cycles	107
Figure 3.40 Optoelectrochemical spectrum of a) P(OTE)/PEDOT ECD at applied potentials between 0.0 and +1.4 V (a)+ 0.0 V, (b)+ 0.2 V, (c)+ 0.4 V, (d)+ 0.6 V, (e)+ 0.8 V, (f)+ 1.0 V , (g)+ 1.2V, (h)+ 1.4 V b) Optoelectrochemical spectrum of PDATE/PEDOT ECD at applied potentials between 0.0 and +1.4 V (a) + 0.0 V, (b)+ 0.2 V, (c)+ 0.4 V, (d) + 0.6 V, (e)+ 0.8 V, (f)+ 1.0 V , (g)+ 1.2 V (h)+ 1.3 V (i)+ 1.4 V....	109
Figure 3.41 a) Electrochromic switching, optical absorbance change monitored at 632 nm for POTE/PEDOT ECD between 0.0 V and 1.4 V b) Electrochromic switching, optical absorbance change monitored at 427 nm for PDATE/PEDOT between 0.0 V and 1.4 V	111
Figure 3.42 Cyclic Voltammogram of a) POTE/PEDOT b) PDATE/PEDOT electrochromic devices as a function of repeated scans 500 mV/s: after 1 st cycle (plain), after 1000 th cycles (dash)	113
Figure 3.43 Open Circuit memory of a POTE/PEDOT ECD monitored by single-wavelength absorption spectroscopy at 430 nm. +1.4 and 0.0 V pulses are applied for 1 second every 200 seconds to recover the initial transmittance	114
Figure A 1. ¹³ C-NMR of HABTE.....	126
Figure A 2.FTIR of HABTE	127
Figure A 3. ¹³ C-NMR of OTE	127
Figure A 4. FTIR of OTE.....	128
Figure A 5. ¹³ C-NMR of DATE	128
Figure A 6. FTIR of DATE	129
Figure A 7. FTIR of TBAFB	129
Figure A 8. Spectroelectrochemistry of PTh as a function of applied voltage: (a)0.2V, (b)0.4V, (c)0.5V, (d)0.6V, (e)0.7V, (f)0.8V, (g)1.0V, (h)1.2V	130
Figure A 9. Electrochromic switching at $\lambda_{\max} = 500\text{nm}$ as the voltage is stepped between -0.5V and 1.5V	130
Figure A 10. Spectroelectrochemistry of PEDOT as a function of applied voltage: (a)- 1.0 V, (b) -0.5 V, (c) -0.3 V, (d) 0.0 V, (e) 0.2 V, (f) 0.4 V, (g) 0.6 V	131

Figure A 11. TGA thermogram of P(HABTE/Th).....131

LIST OF TABLES

Tables

Table 3.1 Conductivities of the films (S/cm)	69
Table 3.2. Conductivities of DATE Polymers (S/cm)	79
Table 3.3 Electrochromic Properties of HABTE Polymers.....	87
Table 3.4 Electrochemical, Electronic, and Electrochromic Properties of POTE,..	89
Table 3.5 Electrochromic Properties of Conducting Polymers of DATE,.....	90
Table3.6 Colorimetry Data for PHABTE/PEDOT and P(HABTE-co-Th)/PEDOT ECDS	102
Table 3.7 Colorimetry Data for PDATE/PEDOT and POTE/PEDOT ECDs.....	110

ABBREVIATIONS

HABTE	Hexanedioic acid bis-(2-thiophen-3-yl-ethyl) ester
OTE	Octanoic acid 2-thiophen-3-yl-ethyl ester
DATE	Decanedioic acid bis-(2-thiophen-3-yl-ethyl) ester
PHABTE	Poly(hexanedioic acid bis-(2-thiophen-3-yl-ethyl) ester)
POTE	Poly(octanoic acid 2-thiophen-3-yl-ethyl ester)
PDATE	Poly(decanedioic acid bis-(2-thiophen-3-yl-ethyl) ester)
P(HABTE-co-Th)	Poly(hexanedioic acid bis-(2-thiophen-3-yl-ethyl) ester-co-thiophene)
P(OTE-co-MeTh)	Poly(octanoic acid 2-thiophen-3-yl-ethyl ester-co-3-methyl thiophene)
P(DATE-co-Th)	Poly(decanedioic acid bis-(2-thiophen-3-yl-ethyl) ester-co-thiophene)
EDOT	3,4-Ethylenedioxythiophene
Th	Thiophene
MeTh	3-Methylthiophene
Py	Pyrrole
PEDOT	Poly(3,4-ethylenedioxythiophene)
PXDOT	Poly(3,4-alkylenedioxythiophene)s
PXDOP	Poly(3,4-alkylenedioxy pyrrole)s
TEA	Triethylamine
TBAFB	Tetrabutylammonium tetrafluoroborate
ACN	Acetonitrile
BFEE	Borontrifluoride diethyletherate
PMMA	Poly(methylmethacrylate)
PC	Propylene carbonate

NMR	Nuclear Magnetic Resonance
FTIR	Fourier Transform Infrared Spectrometer
CV	Cyclic Voltammetry
SEM	Scanning Electron Microscopy
ESR	Electron Spin Resonance Spectroscopy
ECD	Electrochromic Device
HOMO	Highest Occupied Molecular Orbital
LUMO	Lowest Unoccupied Molecular Orbital
CB	Conduction Band
VB	Valence Band
E_g	Band Gap Energy
CIE	La Commission Internationale de l'Eclairage
L a b	Luminance, hue, saturation
ITO	Indium Tin Oxide
CP	Conducting Polymer
LED	Light Emitting Diode
OFET	Organic Field Effect Transistor
PTh	Polythiophene
PPy	Polypyrrole
PAT	Poly(3-alkylthiophene)
SCE	Standard Calomel Electrode

CHAPTER I

INTRODUCTION

1.1. Conducting Polymers

Conducting polymers are available since the two decades of the last century. Actually, more than a decade ago many of the nowadays 'new' conducting polymers are prepared by synthetic routes but they were discarded at the time of their original discovery because they were considered as only black, intractable powders. The term conjugated polymer defines a backbone chain that is unsaturated and therefore has alternating double and single bonds along the chain, all carbon atoms are singly bonded to neighboring carbon atoms and remaining valence electrons are bound to hydrogen atoms. Pure conjugated polymers are semiconductors. Conjugated polymers can be converted in to metals by doping and therefore form new a class of materials referred as synthetic metals, conducting polymers [1]. The field of conducting polymers aroused almost 30 years ago with the discovery of p-doped polyacetylene revealing near metallic electrical conductivity levels. This breakthrough caused an explosion of interdisciplinary research which continues up to date. The fact that the 2000 Nobel Prize in Chemistry went to Alan J. Heeger, Alan G. MacDiarmid and Hideki Shirakawa "*for the discovery and development of conductive polymers*" also reflects both research and practical importance of conducting polymers and their applications in modern science and daily life. Polyacetylene is the simplest form of conducting polymer that has the characteristic structure of a conjugated π system extending over a large number of chain linked monomer units. Conducting polymers based on aromatic systems and heteroaromatic compounds such as aniline, pyrrole and thiophene which posses higher

environmental stability and structural versatility [2]. The electronic and electrochemical properties of these polymers can be altered by modification of the monomer structure. Although the initial interest in conducting polymers was entirely due to their ability to conduct electricity, the current technology around these materials is more than that. Some of these materials have practical and potential applications including rechargeable batteries, sensors, light emitting diodes, microwave absorbing materials, smart windows, solar cells and field effect transistors.

1.2. Band Theory

Band theory has been used to describe the properties of insulators, metals, and semiconductors. Metals are materials that possess partially filled bands, where movement of charge carriers can occur freely leading to conduction. In a semiconductor, there is a filled valence band and an empty conduction band separated by a band gap (E_g) where no energy levels are present. The conduction band can be populated at the expense of the valence band by exciting electrons across the band gap either thermally or photochemically. Semiconductors can be doped which increases the conductivity of the material, and depending on the type of dopant used either holes (p-type) or electrons (n-type) are the charge carriers [3]. Insulators have a band structure similar to semiconductors except they have very large band gaps that are inaccessible under normal environmental conditions (Figure 1.1).

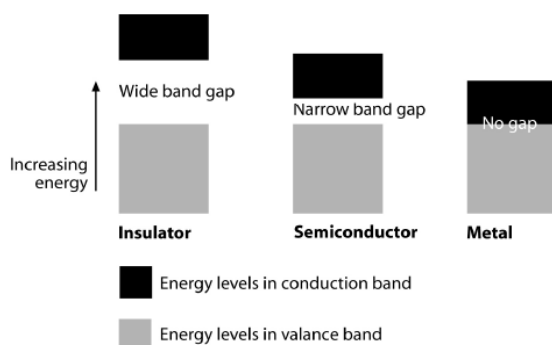


Figure 1.1 Simple band picture explaining the difference between an insulator, a semiconductor and a metal

Neutral conjugated polymers are usually treated as semiconductors and band theory can be used to describe their electronic energy levels. Figure 1.2 shows the formation of a band structure as conjugation increases from ethylene to polyacetylene. Since π conjugated polymers have regular alternation of single and double bond in their polymeric backbone, the π orbitals of the repeating units can overlap throughout the chain as in polyacetylene [4].As the number of repeating unit increases, the electronic levels no longer have discrete energies but rather, they display continuum of the states and formation of band structures. The energy difference between the highest occupied molecular orbital (also named as Valence Band) and the lowest unoccupied molecular orbital (also named as Conduction band) decreases as the conjugation length increases along with an increase in the number of energy levels. Since conjugated polymers have completely occupied valence band and a completely empty conduction band, they can not transport charge. According to band theory, for a polymer to be conductive an electron must be moved from the highest occupied state to the next lowest unoccupied state. The region between the VB and CB represents the band gap, E_g [5] Typically, a semiconductor has a band gap in the range of 0.5 to 3.0 eV, while insulators have gaps greater than 3.0 eV. Diamond for example, is an excellent insulator and has a band gap of 6.0 eV.

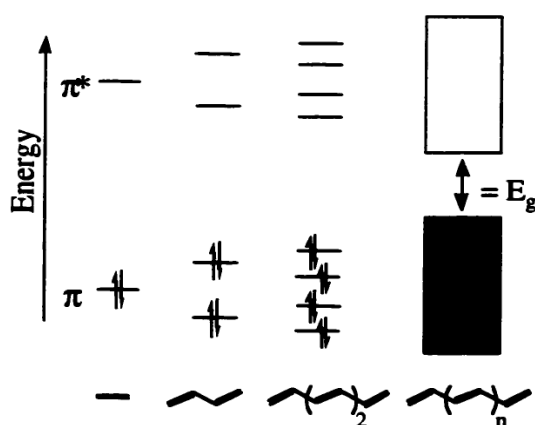


Figure 1.2 Generation of bands in polyacetylene

1.3. Conduction in Conducting Polymers

Conjugated polymers can become highly conductive upon doping. This term is borrowed from semiconductors, but the physics of conjugated polymer differs markedly from that of inorganic semiconductors such as Si or GaAs. Generally speaking inorganic semiconductors are three dimensionally bonded materials, the fourfold (or sixfold, etc.) coordination of each atom to its neighbors through covalent bonds. They are generally in rigid structure, and this rigidity of their lattice ensures that charge carriers added to the system are accommodated in the conduction and valence bands with negligible rearrangement of the bonding. For inorganic semiconducting materials, the amount of dopant added is in the order of thousandth of a percent and the material structure's show no significant change upon doping. Therefore, a partially filled valence band is formed and this can allow charge transport.

However, conjugated polymers have two-fold coordination which makes these systems generally more susceptible to structural distortion. As a result, the dominant electronic excitations are inherently coupled to chain distortions. Since it is energetically more favorable for conjugated polymers to localize these charges, new energy levels are formed within the otherwise forbidden band gap. The specific types of charged defects formed on the polymer backbone during doping depend on the structure of the polymer chain: those with degenerate ground state structures such as polyacetylene and those with nondegenerate ground state structures such as polypyrrole. Dopant in conducting polymers is in the order of 10-20 % [6] and the doped structures are different from that of the undoped species. The doped structures of conducting polymers can be *solitons*, *polarons* and *bipolarons* having higher energies than the neutral polymer.

1.3.1. Solitons, Polarons, Bipolarons

In a degenerate ground state, like trans-polyacetylene, the system has two isoenergetic regions (Figure 1.3). For a neutral chain soliton can be thought as a $2p_z$ un-hybridized orbital of a sp^2 hybridized carbon atom, which is a non bonding orbital occupied by a single electron. This excitation has $\frac{1}{2}$ spin with zero charge,

which can move along the chain without distortion. The non bonding orbital corresponds to a soliton level at the middle of the forbidden band gap. It may contain zero, one or two electrons. The addition or removal of an electron to the neutral state corresponds to a negative or positive soliton with zero spin. Further oxidation of the polymer creates dication. However, because of the two-fold degeneracy of polyacetylene, these cations are not bound to each other by any lattice distortion and can freely separate along the chain [7].

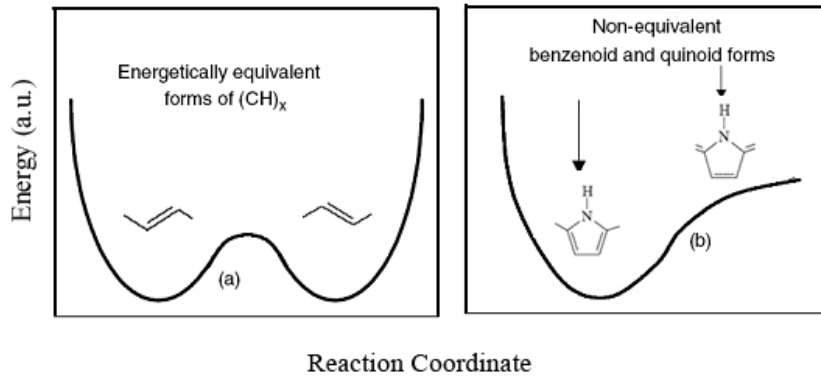


Figure 1.3 (a) Degenerate polyacetylene; and (b) non-degenerate polypyrrole

In the case of polypyrrole (Figure 1.4), when an electron is removed from the π -system of its backbone (chemical oxidation), an unpaired electron with spin $\frac{1}{2}$ (a free radical) and a spinless positive charge (cation) are created. The radical and cation are coupled to each other via a local bond rearrangement (as the polymer chain passes from the neutral benzenoid form to a partially-quinoid structure), creating a polaron which appears in the band structure as a single unpaired electron possessing charge and spin. This deformation causes the formation of two new electronic states which appear within the valence and conduction band of the polymer. The polaron is characterized by ESR signal and three electronic absorptions from partially oxidized polymers [8].

Further oxidation of the polymer creates dications in the polymer. An electron can be removed either from the polaron or from the remaining neutral portion of the chain. In the former case, the free radical of the polaron is removed and a dication is created comprised of two positive charges coupled through the lattice distortion, creating a new spinless defect bipolaron. Removal of an additional electron from a

neutral portion of the chain would create two polarons. Since the formation of a bipolaron produces a larger decrease in ionization energy compared to the formation of two polarons, formation of bipolaron is thermodynamically favorable [9]. These new empty bipolaron states are also located symmetrically within the band gap. Further doping creates additional localized bipolaron states, which eventually overlap to form continuous bipolaron bands at high enough doping levels.

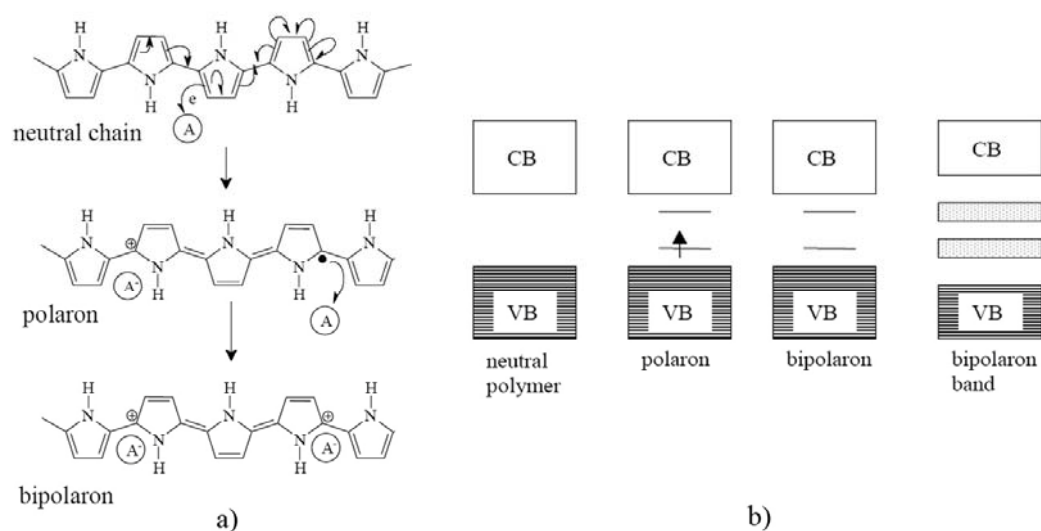


Figure 1.4 Charge carries in PPy and its corresponding energy bands in the mid gap

1.3.2. Doping Types in Conducting Polymers

Charge injection into conjugated, semiconducting macromolecular chains, “doping”, leads to the wide variety of interesting and important phenomena that define the field. According to the classification of A. J. Heeger, as summarized in Figure 1.5, reversible charge injection by “doping” can be accomplished by chemical, photochemical, interfacial or electrochemical means which could be exploited in various possible applications, some of which will be detailed in the following sections [10].

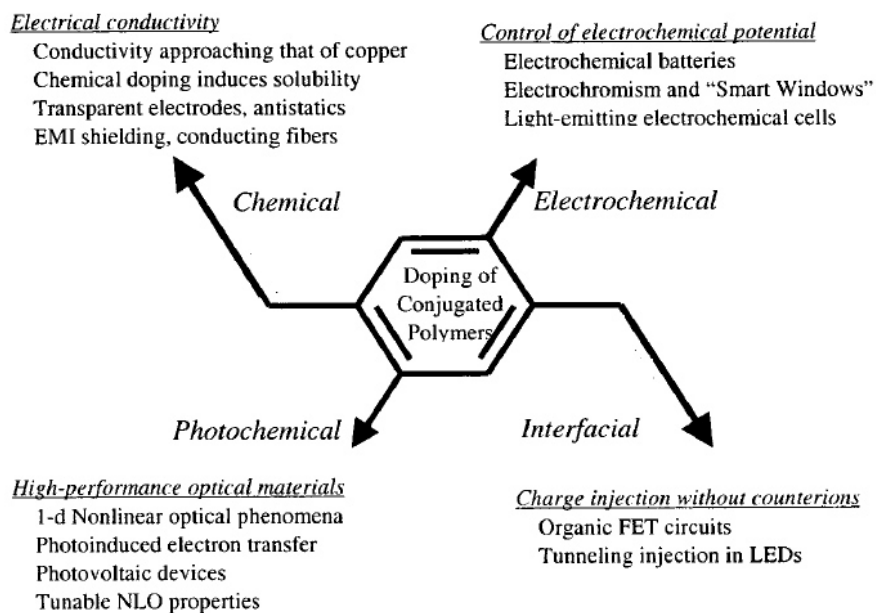


Figure 1.5 Doping mechanisms and related applications [10]

Chemical pathway, one of the first that was applied, doping is performed by the reaction of the polymer with suitable oxidizing or reducing agents. Chemical doping can be performed either by reaction with gaseous species, such as, AsF_3 , PF_3 , I_2 , or in solution by reaction with LiBH_4 in THF [11]. Although chemical (charge transfer) doping is an efficient and straightforward process, it is typically difficult to control. Complete doping to the highest concentrations yields reasonably high quality materials. However, attempts to obtain intermediate doping levels often result in inhomogeneous doping. Electrochemical doping eliminates such problems.

Electrochemical doping is performed by biasing the polymer film with appropriate potential in a suitable solution. Figure 1.6 shows a schematic illustration of the band diagrams for the p-doping (a) and n-doping (b) of a conducting polymer [12]. If the Fermi level of the electrode that is in contact with the conducting polymer film is lowered below the valence band of the polymer, a flow of electrons from the polymer to electrode will occur. This is termed as p-doping and it involves the extraction of the delocalized electrons from the p_x -orbital of the polymer. Likewise, if the Fermi level is raised above the conduction band of conducting polymer, then

electrons flow in to the film. This is termed as n-doping and it involves the injection of the electrons into delocalized p_z -orbital of the polymer

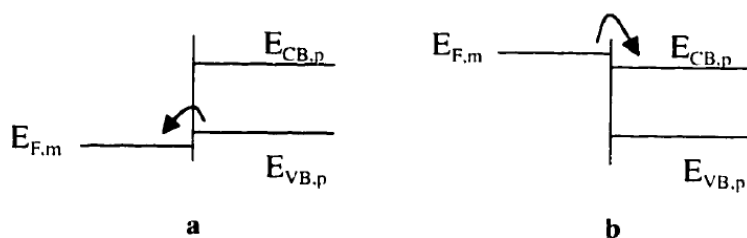


Figure 1.6 Schematic representation of doping a) p-doping and b) n-doping of conducting polymer

During p-doping, the π -conjugated film undergoes partial oxidation along with insertion of anions from the solution to maintain charge neutrality (Figure 1.7). During the neutralization the oxidized polymer is electrochemically reduces along with either counter ion repulsion from the polymer or cation insertion from the solution in order to maintain the charge neutrality. It should be noted that for the heteroatomic structures such as thiophene, the insertion and extraction of electrons is accompanied by a structural change from benzoid in character in the neutral form to quinoid in character for the doped form [13]. The term reversibility is used to describe the efficiency of switching a polymer between doped and undoped states.

1.4. Polythiophenes

Due to their structural versatility and good environmental stability, polythiophene and its derivatives are well established in the field of conducting polymers and much research has been devoted to them. The high conductivity, relatively low band gap and the ease of introduction of side groups on to the β -positions of the polymer backbone make polythiophene an ideal parent polymer for electronic and optoelectronic applications. Due to its electron rich character of thiophene ring, PThs can be easily and reversibly oxidized by chemical or electrochemical means to form p-doped, usually highly conducting materials. The first electronic

transition of undoped PTh (which strongly depends on the structure) lies between 300-500 nm. Upon doping, it undergoes a dramatic bathochromic shift transforming in to the conducting band, which tails from the visible to IR region [14].

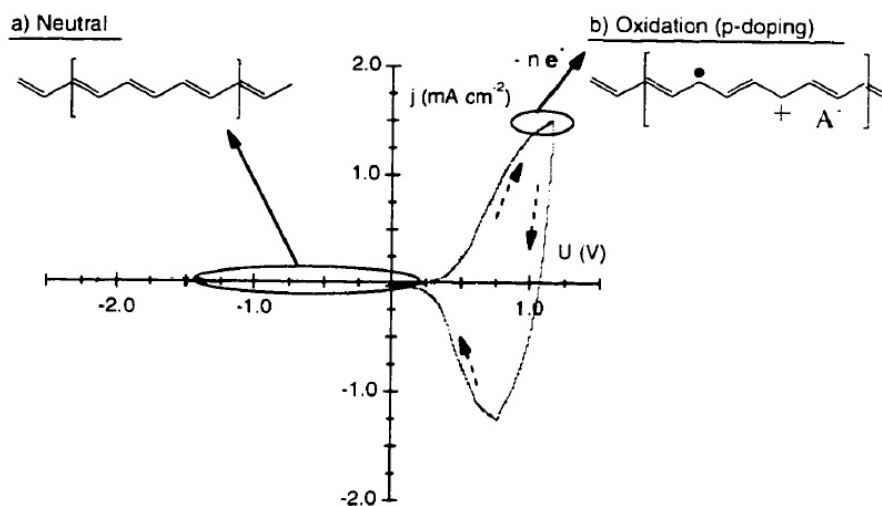


Figure 1.7 Typical cyclic voltammogram for a conducting polymer exhibiting p-doping, the structure of polyacetylene is shown only for illustrational purpose

1.4.1. Chemical polymerization

In 1980 Yamamoto et al. [15] reported the Ni-catalyzed polycondensation of 2,5-dibromothiophene (Figure 1.8a). The same year, Lin and Dudek described another example of metal catalyzed route by using acetylacetonates of Ni, Pd, Co and Fe as catalysts [16]. PTh synthesized by these methods is although a low molecular weight material, it is insoluble and precipitates from THF. FeCl_3 mediated polymerization of thiophene in chloroform was described by Yoshino et al [17] and currently is the most widely exploited oxidative route for polythiophenes. It produces rather high molecular weight polymers with polydispersities ranging from 1.3 to 5.

Unsubstituted PTh is an insoluble and infusible material. Once the polymer is prepared it is difficult to process further as a material for electronic applications. The solubility can be greatly enhanced by introduction of side chains at position 3, most widely with n-alkyl substituents. However, polymerization of these substituted thiophenes can lead to three different types of coupling of thiophene ring along the polymer main chain, namely, head to tail (HT), head to head (HH) and tail to tail (TT). The presence of HH coupling in irregular polythiophenes causes an increased twist of the thiophene units (due to steric repulsion) with a loss in conjugation. This results in increased band gap (blue shift in absorption) and decreased conductivity [14].

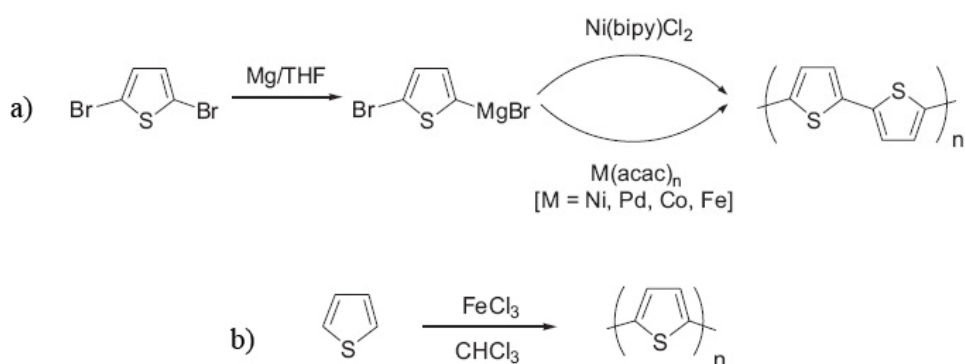


Figure 1.8 Synthesis of polythiophene via a) metal catalyzed coupling and b) chemical oxidation

Generally both oxidative and metal catalyzed polycondensation afford all three possible types of isomers. Amou et al. showed that regioregularity of FeCl_3 synthesized poly(3-hexylthiophene) depends on the temperature of reaction and the concentration and in dilute solutions at -45°C the regioregularity approaches to 90% [18]. Several approaches leading to selective formation of less sterically hindered HT regioregular polythiophenes have been developed. The McCullough [19] method was the first synthetic approach for this type of polymer yielding almost 100% HT coupling (Figure 1.19)

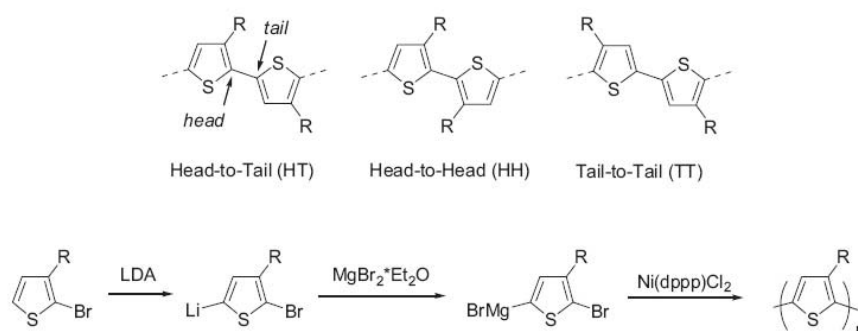


Figure 1.9 McCullough method for the synthesis of regioregular poly(alkylthiophenes)

1.4.2. Electrochemical Polymerization

Despite the fact that electropolymerization of heteroaromatics will most probably not be the technique to be used in industrial production, this technique is of utmost importance for fundamental studies regarding synthesis and properties of the corresponding polymers [20]. There are several advantages of this technique:

- 1- A small amount of material is required for the synthesis, as little as 10-50 mg of material.
- 2- It provides rapid analysis; the possibility to perform in-situ growing process of the polymer and further analysis by electrochemical and spectroscopic techniques.
- 3- This technique is rather simple and has high accuracy and precision.
- 4- It provides direct grafting of the conducting polymer onto electrode surface and control of the film thickness by checking the deposition charge.
- 5- During the electrochemical polymerization, doping of the polymer and processing take place simultaneously while in conventional method, first polymer synthesis is carried out first which is subsequently followed by doping and processing.

The general drawback of this technique is; rather small amounts of polymer is produced which is generally insoluble. Thus, characterization of these products with conventional methods like NMR, GPC is very difficult.

1.4.2.1. Mechanism of Electropolymerization

Figure 1.10a represents the mechanism proposed for the polymerization of heterocycles, where X can be S, O or N-R. An important aspect of the electrochemical polymerization is that, it proceeds with electrochemical stoichiometry. The oxidation of the monomer requires one electron while the excess of charge corresponds to reversible oxidation or doping of the polymer. The first electrochemical step (E) consists of the oxidation of the monomer into radical cation. Since the electron transfer reaction is much faster than the diffusion of the monomer from the bulk solution, high concentration of radicals is continuously maintained near the electrode surface. This provides the necessary conditions for the second reaction which involves the coupling of the two radicals to produce dihydro dimer cation. Consecutively, the chemical step (C) occurs which leads to dimer, with the loss of two protons and rearomatization. Actually, this rearomatization is the driving force of the chemical step. Due to extended conjugation over two rings, the dimer has a lower oxidation potential than the monomer itself, and therefore it oxidizes easily to form the radical cation and undergoes coupling with a monomeric radical or less likely, through coupling of a radical cation with a neutral monomer. Electropolymerization proceeds through successive electrochemical and chemical steps until the oligomers become insoluble in the electrolytic medium and precipitate onto the electrode surface [21]. Since conjugated oligomers are oxidized at less positive potentials than their corresponding monomers, polymer oxidation occurs concurrently during electrodeposition. Typically, one electron is removed from the polymeric backbone for every three to four monomer units to form polar structures, responsible for inherent conductivity. Anions, termed 'dopants', are thus incorporated into the film to maintain electrical neutrality.

Heterocycles such as thiophene and pyrrole have two possible reaction pathways, as shown in Figure 1.10b. Waltman *et al.* have shown using theoretical

calculations that the ability to distinguish between the α - and β - positions decreases as the conjugation increases for pyrrole oligomers. Polymerization proceeding exclusively through α - α couplings affords polymers with a linear backbone and enhanced electrical properties. The occurrence of a α - β linkage in a given chain changes its electronic distribution and could result in branching. As the polymerization proceeds the number of the α - β linkage increase with respect to α - α couplings, which consequently leads to a decrease in the effective mean conjugation length [22]. In a classical electropolymerization, monomers are continually oxidized while the electroactive polymer film grows at the electrode surface. Since the oxidation of the monomer occurs at a higher potential than that of the redox processes of the polymer, side reactions including overoxidation of the polymer could take place especially in the presence of water.

1.4.2.2. Factors Affecting Electropolymerization

Since the first electropolymerization of pyrrole by Diaz in 1979 [23], many scientists have investigated the influence of experimental parameters like solvent, temperature and pH on the mechanical, morphological and electrical properties of conducting polymer films.

The electropolymerization is generally achieved by potentiostatic (constant potential) or galvanostatic (constant current) methods. These techniques have been therefore, commonly utilized to investigate the nucleation mechanism and the macroscopic growth. Potentiodynamic techniques such as cyclic voltammetry correspond to a repetitive triangular potential waveform applied at the surface of the electrode. The latter, CV, has been mainly used to obtain qualitative information about the redox processes involved in the early stages of the polymerization reaction, and to examine the electrochemical behavior of the polymer film after electrodeposition. It was shown that electrochemical methods have an influence on the morphology, appearance and adhesion of the polymer. Especially use of potentiodynamic method was shown to be effective with the proper choice of supporting electrolyte.

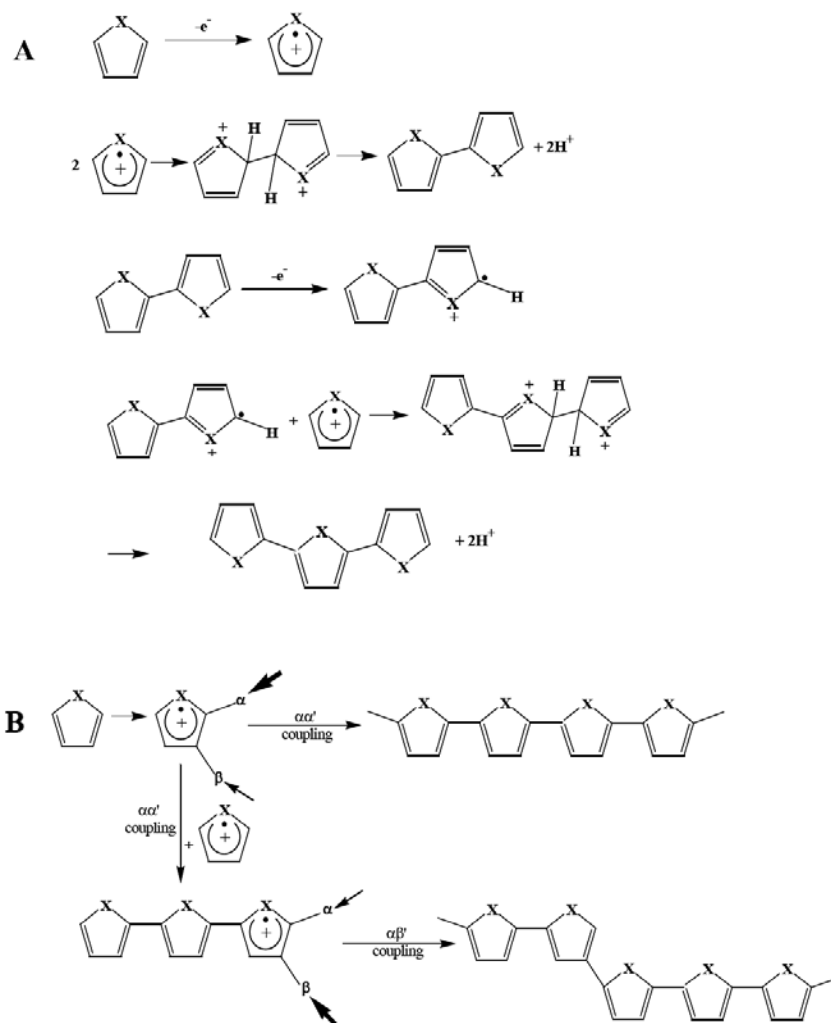


Figure 1.10 Electropolymerization mechanism. a) Polymerization of heterocycles (X = S, O, NH), b) Competitive reaction pathways in unsubstituted poly(heterocycles)

The type of solvent used during the electrochemical synthesis has a strong effect on both the physical and electrical properties of the resultant polymer. For a solvent to be utilized in electrochemical polymerization it should possess high dielectric constant to ensure ionic conductivity of the electrolytic medium and it should have high resistance against decomposition upon applied potential. Acetonitrile, benzonitrile, propylene carbonate, nitrobenzene are aprotic solvents which possess high dielectric constant and low nucleophilicity. The electrode used

during the synthesis affects both the polymerization process and properties of the resultant polymer. Conducting polymers are generally grown onto noble metals such as platinum, gold, indium tin oxide coated glass, titanium and stainless steel. Platinum is the one of most widely used since it adsorbs thiophene efficiently and provides a large number of active sites. This leads to high density of initial nucleation sites and more compact materials.

Supporting electrolyte used in electrochemical polymerization serves to achieve electrical conductivity in solution and meanwhile it dopes the polymer by allowing one of its ions to couple with a monomer unit. Conducting polymers are synthesized in the presence of small anions derived from strong acids such as ClO_4^- , PF_6^- , BF_4^- and AsF_6^- associated with lithium or tetraalkylammonium cations, while HSO_4^- and SO_4^- lead to poorly conducting materials [24]. The electrochemical behavior, morphology of conducting polymers depend significantly on the nature of the anion and cation in electrolytic solution. The type of counterion used can greatly affect the conductivity of the film. For example, for equal degrees of tetrafluoroborate doping, polypyrrole typically has conductivities in the range of $30\text{-}100\text{ S cm}^{-1}$, whereas with perchlorate anions, conductivities of $60\text{-}200\text{ S cm}^{-1}$ can be achieved [25]. It is generally assumed that polymer growth occurs via a nucleation process similar to that of metal deposition. Studies showed that anion affects primarily the electrodeposition process and polymer structure, whereas the nature of cation affects essentially the charge-discharge process for the polymer [26]. Actually it was shown that discharging of polymer not only involves the anion expulsion, but sometimes also the transient incorporation of cations [21]. Electrochemical cation doping (n-type doping) is not very common since the stability of polymer is reduced, especially in the presence of trace amount of water or oxygen. Electrochemical n-doping of polythiophenes has been achieved in the presence of tetraalkylammonium cations. The electrolyte concentration is also important although the effect is not entirely understood. Some studies declared that, the polymers of the high conductivity are produced when elevated concentrations of electrolyte are used [27]. Also, electropolymerization temperature has a substantial influence on the kinetics of polymerization as well as on the conductivity, redox properties and mechanical characteristics of the films. It should be noted that a decrease in the redox

properties is observed as the temperature increases. In general, higher conductivities are obtained at lower temperatures [28].

1.4.2.3. Polythiophene Paradox

Most conductive polythiophene films prepared by electrochemical polymerization of thiophene in an organic solvent, in which the electro-oxidation of thiophene is achieved at potentials above 1.6 V vs SCE. It is reported that at potentials higher than 1.4 V polythiophene degrades due to side reactions [26]. This phenomenon is called as polythiophene paradox [29] which signifies the presence of competition between electrodeposition and degradation, especially at high potentials or very low monomer concentrations [30]. It was concluded that, in order to obtain high quality electrochemically synthesized polythiophene, the oxidation potential of thiophene must be lowered.

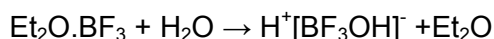
There are several approaches to overcome this problem. One of them is the polymerization of thiophene from its oligomers such as 2,2'-bithiophene or 2,2'-5,2''-terthiophene. Although thiophene oligomers can be electrochemically polymerized at lower potentials than the parent monomer, it was found that the resulting polymers exhibit lower average conjugation lengths and poor mechanical properties [31]. Another approach is the synthesis of β -substituted thiophenes with electron donating groups which has the ability to reduce greatly the oxidation potential. One of the simplest examples is 3-methylthiophene which has oxidation potential 0.2 V lower than the unsubstituted thiophene [32].

Xue et al. reported the low potential electrochemical synthesis of polythiophene in freshly distilled borontrifluoride diethyletherate (BFEE) [33]. It was found out that the resultant polymer has higher effective mean conjugation length with remarkable mechanical strength exceeding the aluminum sheets. Linear sweep voltammetry studies showed that the oxidation potential of thiophene was reduced to 1.3 V vs SCE [34], which is lower than the over-oxidation potential (1.4-1.5 V vs SCE) of the polymer. Thus, polythiophene with high mechanical quality was achieved. Other studies utilizing bithiophene [35], terthiophene [36], pyrrole in isopropyl alcohol [37] were performed which took the advantage of the decrease

in the oxidation potential of the monomers. Due to the decrease in the oxidation potential of thiophene, reactive metals such aluminum, nickel [38] and copper oxide [39] was shown to be useful as the working electrodes for electropolymerization of thiophene. Also composite electrolyte system made up of trifluoroacetic acid (TFA), BFEE and acetonitrile was used for electrochemical polymerization of benzene [40] and 3-chlorothiophene [41].

In an aromatic ring, the difference in bond length between the C=C and C-C is reduced due to conjugation and the force constant of a bond is related to its bond strength. Thus, Jin and Xue employed the frequency difference between the $\nu_{C=C}$ and ν_{C-C} , to evaluate the aromaticity of a thiophene ring by studying the Fourier Transform Raman (FT-Raman) spectra [34]. It was seen that the aromaticity of a thiophene ring was reduced in the presence of a Lewis acid. The strength of interaction between thiophene and the solution increases in the order of CH₃CN, AlCl₃/CH₃CN, and BFEE, which accords with their acidity order. With the increased interaction strength and decreased aromaticity, the oxidation potentials of thiophene in solvated Lewis acid are markedly lowered.

Up to date, the role of the BFEE in doping process is not fully established. It has been proposed that it facilitates electrochemical polymerization by lowering the aromatic resonance energy and promoting the abstraction of an electron from the α -position of the heterocyclic ring [34]. It is known that BFEE exists in diethylether as a polar adduct and the presence of small amount of water results in the formation of H⁺[BF₃OH]⁻ [42]. This complex is thought to provide a conducting medium and speculated previously that [BF₃OH]⁻ ion serves as the dopant during electrochemical polymerization [43].



1.4.2.4. Effect of Substitution on Thiophene

The other possible ways to overcome the adverse effect of thiophene paradox and to achieve solubility in the final product is the substitution of monomer. Up to

date, the electrochemical behavior of a wide-range of β -substituted thiophenes has been investigated. The electrochemical and physical properties of the polymers synthesized from electro-oxidation of substituted thiophenes are highly dependent on the type of substituent. This has been attributed to electronic and steric factors [25]. Quantitative relationships between structure and reactivity have been developed. One such relationship is given by the Hammett equation [44, 45]. The Hammett constant is an electronic substituent descriptor reflecting the electron-donating or accepting properties of a substituent. Hammett constant (ρ) is characteristic of the substituent and represents the ability of the group to withdraw or donate electron density by a combination of its inductive (I) and resonance (R) effects. Substituents with positive ρ values are more electron-withdrawing than hydrogen, and those with negative values are less electron withdrawing than hydrogen. A linear correlation has been found between monomer oxidation potential and Hammett constant for a series of β -substituted thiophenes (Figure 1.11), suggesting electronic effects dramatically affect the electronic density and hence, reactivity of the thiophene ring [46].

The radical cation formed at the electrode has three possible reaction pathways: polymerization reaction (k_p), diffusion into the solution (k_d) for stable cations, and reaction with solvent or electrolyte anions (k_n) for highly reactive species. The fraction of radical cations, which undergoes polymerization, could be given by the following equation:

$$f_p = k_p / (k_p + k_d + k_n)$$

Polymerization occurs when k_p is much higher than $(k_d + k_n)$. Highly electron withdrawing substituents, such as nitro and nitrile groups, coupled directly to thiophenes at the β -position cause the monomer oxidation process shift to much higher anodic potentials than the thiophene itself and as a result, electropolymerization does not occur. Similarly, highly electron donating species such as amino groups, increase the electron density at the thiophene ring thus, allows the monomer oxidation to occur at less anodic potentials relative to that of thiophene itself. However, such a high degree of stabilization of the radical cation results in diffusion of the species away from the electrode interface into the bulk

electrolyte before eventually being attacked by the electrolyte or other nucleophilic species in solution. It was found out that, the type of substituent also affects the redox behavior of the polymer, where polymer oxidation potentials are also found to vary linearly with Hammett constant [46].

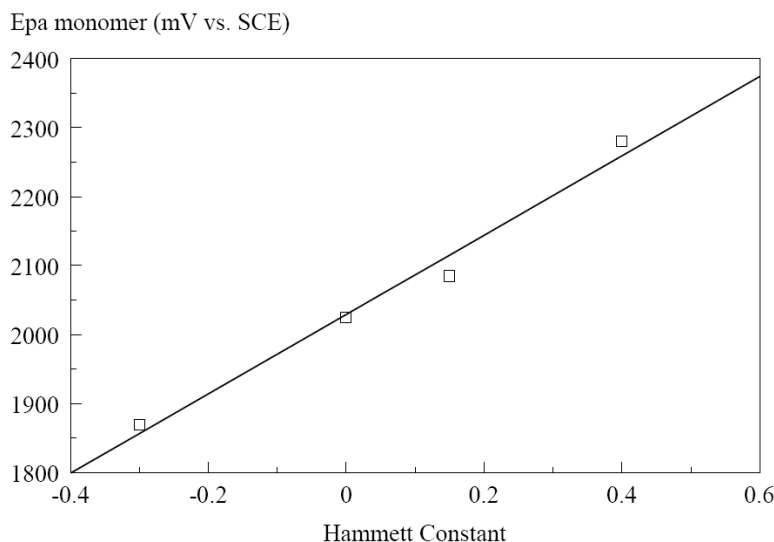


Figure 1.11 Variation of monomer oxidation potential with Hammett constant for β - substituted thiophene monomers; where β = Me, H, Br and COOH from left to right, respectively

In addition to electronic effects, steric factors also influence the electropolymerization reaction and properties of conducting polymers. Steric effects have little influence on the oxidation potential of the monomers, but do affect greatly the polymer structure and hence, the properties of the resulting polymer. Steric effects do not significantly hinder the formation of the radical cation but appear to become important in the subsequent coupling reaction [21]. For example, 3-methylthiophene undergoes electropolymerization at a potential of 200 mV less anodic than that of thiophene, as might be expected from Hammett constant considerations. However, a polymer of higher conductivity than polythiophene (σ : 450-510 S cm⁻¹ compared to 270 S cm⁻¹) is produced [47] and this can be explained by blocking one of the β -positions of the thiophene ring by a methyl substituent which reduces α,β' - and β,β' -linkages. It might, therefore, be expected that 3,4-dimethylthiophene would produce a polymer of even higher conductivity than poly(3-methylthiophene). However, a polymer of significantly

reduced conductivity (σ : 0.5 S cm^{-1}) was produced and this may be explained by steric interactions between methyl substituents grafted on consecutive thiophene rings which distort the π -system and thus decrease the degree of conjugation. Thus, in principle, a substituent may be chosen to produce the desired electrochemical properties in resulting polymer with careful choice of substituent.

1.5. Application Areas of Conducting Polymers

Electronic technology has rapidly evolved during the past decades. The emphasis is to make better, faster and smaller electronic devices for application in modern life. Almost all electronic devices are fabricated from semiconductor silicon. However, there is a practical limit to the density of stored information in a chip. One of the possible ways to overcome the present limitation is to use organic materials such as proteins, pigments, conducting polymers (CP) etc. to carry out the same functions that are presently being performed by conventional semiconductors. Among organic materials, CPs (or conjugated polymers) have attracted most attention owing to the unique electronic, electrical and optical properties, several potential, technological and commercial applications which can be splitted in to three categories. The first category takes advantage of conjugated polymers for their semi-conducting and luminescent properties when used in their neutral form. Examples of these applications are; light emitting diodes, solar cells and field effect transistors. The second category of applications involves using these polymers in their doped or conducting form, and some representative applications in this category are electrostatic charge dispersal and EMI shielding. The third category uses the ability of the polymer to reversibly switch between its conducting and reduced forms. Upon switching between these two states, the polymer undergoes color, conductivity, and volume changes. Applications that use these properties include battery electrodes, sensors, artificial muscles and electrochromic devices. Some of these applications are briefly described below.

1.5.1. Light Emitting Diodes

The first organic light-emitting diode (OLED) was fabricated with anthracene crystals in 1965 but failed to attract attention because of poor performance [48]. The interest was revived in 1987 when a light emitting diode (LED) fabricated with 8-hydroxyquinoline aluminum (Alq_3) emitted light with a green color upon application of a positive bias potential [49]. Polymeric light emitting diodes (PLED) have aroused much interest worldwide since the discovery of electroluminescence (EL) in a thin poly(p-phenylenevinylene) (PPV) layer by Friend and coworkers in 1990 [50].

The current interest in exploring the luminescent properties of CPs is their possible use in flat-panel displays. They, however, have limitations in size and power consumption. CPs on the other hand offer the potential applications in many battery operated devices, such as laptop computers, cellular telephones, small hand-held devices, large panel displays, notebook computer screens etc. The main advantages of these materials over conventional luminescent materials are the tuning of wavelength emitted by chemical modification, low operating voltage, flexibility, easy processing, low cost, possibility of making large area device and output colors in whole visible spectrum. Due to these unique features, a number of CPs have been synthesized that emit light across whole visible spectrum and have moderate quantum efficiencies.

A typical PLED consists of a thin layer of undoped conjugated polymer sandwiched between two electrodes deposited on top of a glass substrate. The polymer is spin-coated on top of a patterned indium-tin-oxide (ITO) electrode which forms the anode. The cathode on top of the polymer consists of an evaporated metal layer for which Ca, Mg, Al could be used. The device operation of a PLED under forward bias is schematically indicated in Figure 1.12. Electrons and holes are injected from the cathode and the anode respectively, into the polymer. Driven by the applied electric field, the charge carriers move through the polymer over a certain distance and couple to generate excitons. A radiative recombination of the excitons in the polymeric layer gives light. The device operation of a PLED is thus determined by four processes: charge injection,

charge transport, exciton generation and radiative recombination. The color of the emitted light is controlled by the band gap energy (E_g), while the charge injection process is controlled by the energy differences between the work functions of the respective electrodes and the electron affinity (E_a) (cathode injection) and ionization potential (I_a) (anode injection) of the polymer. There are still problems to be solved in this field regarding the durability of the device under drive and storage conditions, degradation at the polymer-metal interface and the formation of dark spots etc. Nevertheless, recent advances in technologies promise to overcome these problems and achieve commercialization of polymer electroluminescent devices.[52]

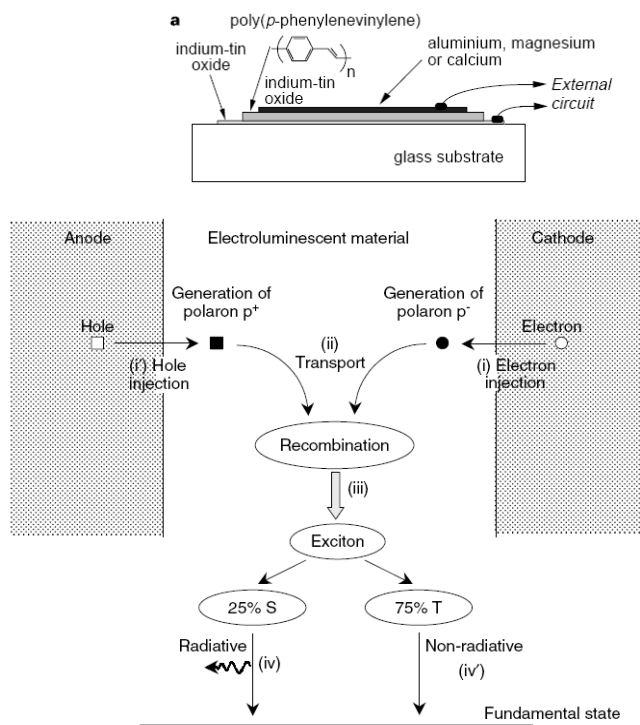


Figure 1.12 a) Schematic representation of a single-layer polymer electroluminescent diode b) Successive steps to electroluminescence [51], [52]

1.5.2. Solar Cells

The basic mechanism behind the solar cell is similar to PLEDs. When the light is incident upon the device, photons whose energies are matching the band gap of the polymer are absorbed. This absorption creates excitons (bound electron-hole pairs) in the bulk material. In order to generate current, the exciton must be dissociated into free charges which could be collected from the device. Otherwise, it will result in recombination and relaxation of the electron and hole pair either radiatively, with photoluminescence, or non-radiatively. Under illumination an intrinsic internal electric field is created in the photoactive layer due to the difference of the work-functions of the electrodes. The Fermi levels of the two metal electrodes are equalized through charge transfer when the device is connected to an external circuit. However, this simple approach generally results in an inefficient charge generation. To overcome this limitation of photoinduced charge carrier generation, a donor/acceptor (dual molecule) approach has been suggested [53] consisting of a composite thin film with a conjugated polymer/fullerene mixture. In such single composite photoactive films (PPV or P3HT), a bulk heterojunction is formed between the electron donors and acceptors (Figure. 1.13), and it was found that the efficiency of photogeneration of charges is near 100 percent.

A great deal of useful information on photovoltaic performance can be extracted from current - voltage behavior of the device in the dark and light. Short circuit current, I_{sc} , is measured at zero applied bias. The open circuit voltage V_{oc} is the voltage at which the current collected from the device is zero when the intrinsic voltage of the device is balanced by the applied potential. The maximum power delivery by the solar cell, normalized by I_{sc} and V_{oc} is represented by "fill factor", which is also related to quantum efficiency of the device. Up to now within polymer based solar cells, fill factor of 65% [54]. has been reported. However, even this value is lower than conventional silicon solar cells. One of the limiting parameters in plastic solar cells is their mismatch to the solar spectrum. The use of low band gap polymers $E_g < 1.8$ eV to expand the spectral region of bulk heterojunction solar cells was shown to enhance the spectral photon harvesting [55].

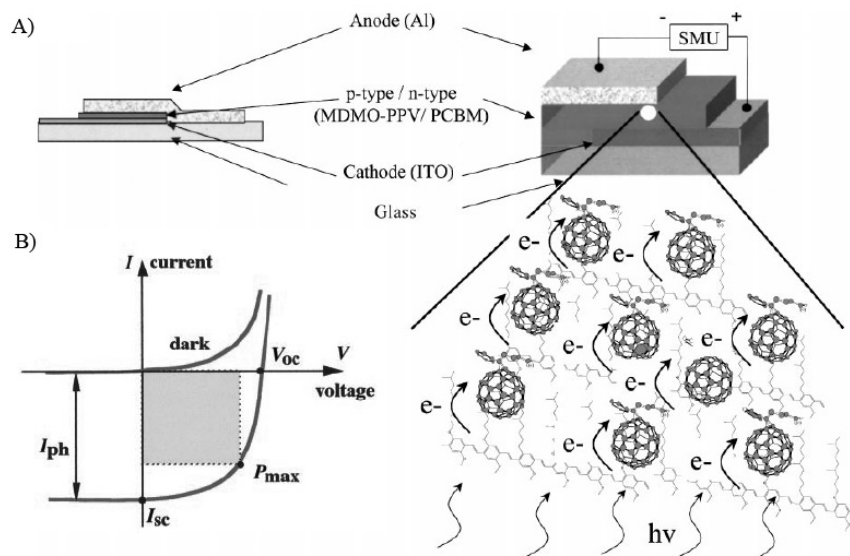


Figure 1.13 a) Formation of a bulk heterojunction and subsequent photoinduced electron transfer inside a composite formed from the interpenetrating donor/acceptor network plotted with the device structure for such a kind of junction [56] b) Typical I-V characteristics of a solar cell, with the three characteristic parameters: short circuit current I_{sc} , open-circuit voltage V_{oc} , and Fill factor $FF = P_{max}/(V_{oc} * I_{sc})$; P_{max} is the electrical power delivered by the cell at the maximum power point MPP [57]

1.5.3. Organic Field Effect Transistors

Organic Field Effect Transistor (OFET) is essentially a voltage- controlled device. It can operate as a basic “on” and “off” switch, depending on whether a voltage bias is applied at the gate electrode or not. Therefore, it can realize logic functionalities of either “1” or “0”. A typical FET is constructed with basic components as (Figure 1.14a) source, drain, gate electrodes, organic semiconductor layer, and the insulating layer. This architecture is proven to be well adapted for low conductivity materials. In an OFET, the current flow between the drain and source electrode is modulated by the applied gate voltage. When no gate voltage (V_g) is applied, the drain current (I_D) is very low and the transistor is considered to be “off”. With an increase in the applied gate voltage, a layer of mobile charges can accumulate at the interface (formation of n or p-type channel,

depending on the major charge carriers being electrons or holes respectively) between the semiconductor and insulator. Thus, the intensity of the drain current is increased due to increase in the charge carriers and the transistor is switched to “on” state [58].

Figure 1.14b illustrates a typical output characteristics of OFET, which corresponds to regioregular poly(3-hexylthiophene) (P3HT) with bottom contact architecture. There are several parameters in characterizing an OFET, such as field effect mobility, on/off ratio. The field effect mobility quantifies the average charge carrier drift velocity per unit electric field, whereas the on/off ratio is defined as the drain current ratio between the on and off states. Traditionally organic semiconductors used for OFETs commonly should have high mobility and low intrinsic conductivity. High mobility can enhance the performance of the devices and low intrinsic conductivity can deduce the drain current, improving the on/off ratio.

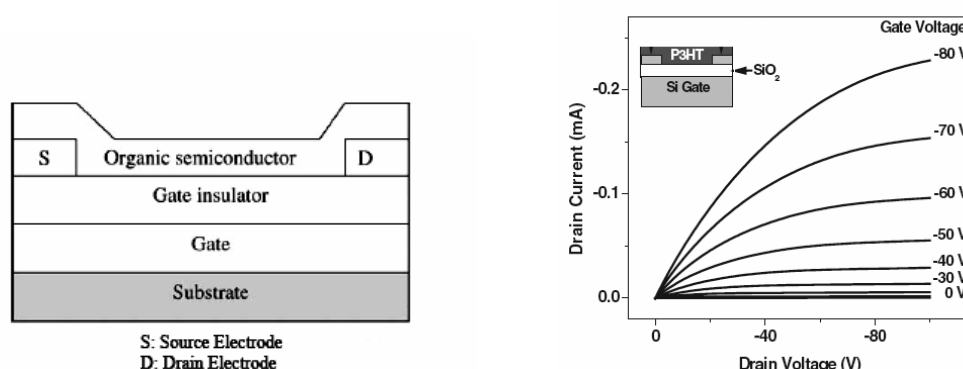


Figure 1.14 Typical a) bottom contact OFET architecture b) Current-Voltage curves of an OFET with different gate voltages [58]

One of the main obstacles to all-polymer optoelectronic circuits is the lack of a polymer FET with sufficiently high mobility and on-off ratio to achieve reasonable switching speeds in logic circuits, which is mainly attributed to the poor molecular ordering and low crystallinity of the polymers obtained by the solution techniques. Conjugated polymer FETs [59] typically show field-effect mobilities of $\mu_{\text{FET}} 5 \times 10^{-6}$ to $10^{-4} \text{ cm}^2 \text{ V}^{-1} \text{ s}^{-1}$, limited by variable range hopping between disordered polymer

chains and on-off current ratios of 10^4 [60]. This is much too low for logic and display applications. To achieve high field effect mobility, the semiconducting molecules should have an orientation in which π - π^* stacking direction between the molecules is arranged in the same direction as that of the current flow. Moreover, large grain size and smooth grains tend to give better mobilities. Recently, a polymer FET with a mobility of 0.01 to 0.04 $\text{cm}^2 \text{V}^{-1} \text{s}^{-1}$ and an on-off ratio of 10^2 to 10^4 using regioregular poly(3-hexylthiophene) (P3HT) was described [61]. The high mobility was attributed to the structural order in the polymer film induced by the regioregular head-to-tail (HT) coupling of the hexyl side chains. However, there are still some critical issues to be addressed before organic transistors can be used for commercial purposes

1.5.4. Sensors

Sensor is referred to a device, which provides direct information about the chemical composition of its environment. It consists of a physical transducer and a selective layer. In any sensor the sensing process can be divided into two parts, recognition which results in selectivity and amplification which increases the power of the usually weak signals to the level at which it can be conveniently manipulated by electronics [62] (Figure 1.15).

Sensors based on CPs have also been demonstrated to act successfully as gas and solution sensors. Real time monitoring of gases, such as carbon dioxide, oxygen and ammonia, is of great importance in many practical environmental and industrial situations. PPys and PThs show conductivity changes upon exposure to both oxidizing gases (e.g. NO_2) and reducing ones (e.g. NH_3) and there is a reproducible response in solution to the sensing of the anion used as dopant [63]. Gas sensing electrodes are highly selective device for measuring dissolved gases. They are reliable and simple but tend to have relatively slow response times.

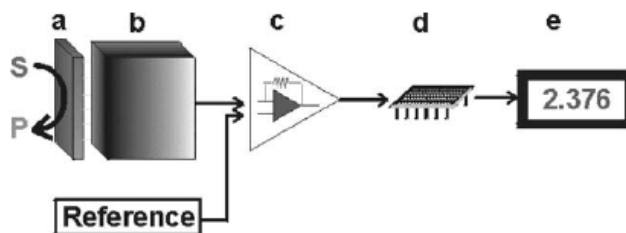


Figure 1.15 Schematic diagram showing the main components of a biosensor. The biocatalyst (a) converts the substrate to product. This reaction is determined by the transducer (b), which converts it to an electrical signal. The output from the transducer is amplified (c), processed (d) and displayed (e)[62]

1.5.4.1. Biosensors

CPs have a compatible chemical nature and they can be synthesized easily in conditions that permit immobilization of biomolecules on the electrode surface. The biomolecules used as sensors of the corresponding substrates can be entrapped in one step during the polymer formation process or attached to a functional group of the resultant polymer. Polymerization is frequently carried out with oxidizing potentials (electropolymerization), which permits anions to enter the polymer structure and simple entrapment of various moieties. The final porous structure, which allows the passage of electrons, and the organic chemical nature of these conductors, which facilitates interactions with biological macromolecules and provides a final configuration suited to the requirements of the biosensor.

The electronic properties of CPs allow us to obtain information about biomolecular events occurring on or in the active polymer to be relayed back to the electronic interface to produce analytical signals. The electronic information relayed back may be due to direct oxidation / reduction of the analyte or a product from an enzymatic reaction involving the analyte [62]. Measuring amperometric current is a simple and sensitive transduction that relates to the analyte concentration, even if the analyte is not electroactive [64].

1.6. Chromism

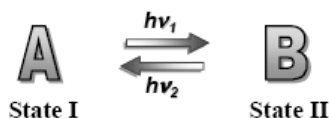
Chromism is a reversible change in a substance's color resulting from a process caused by some form of stimulus. Many materials are chromic, including inorganic and organic compounds and conducting polymers, and the property can result from many different mechanisms. There are also several types of chromism, like thermochromism, photochromism, halochromism, solvatochromism, piezochromism and electrochromism which are detailed below.

1.6.1. Thermochromism

Thermochromism is the reversible color change of a substance induced by temperature change. A large variety of substances, organic, inorganic, organometallic, supramolecular and polymeric systems exhibit this phenomenon. Some polythiophenes bearing relatively long alkyl or alkoxy side chains are known to exhibit thermochromism, both in solid state and in solution. Basically heat treatment of conducting polymers can cause color change. It is believed that the thermochromism observed in PAT films originates from the thermal movement of the side chains, shifting the planar structure of chains at low temperatures to a random conformation when the temperature is increased, thus forcing the polymer backbone out of planarity. This leads to decreased overlap and shorter effective conjugation, resulting in a band gap increase and blue shifted polymer absorbances. The long side chains induce mobility upon heating which causes a twisting of the conjugated backbone. This process is completely reversible and upon cooling the initial color is restored [14]. However, it is still unclear whether this conformational transition is related to an intrachain or interchain mechanism[65].

1.6.2. Photochromism

Photochromism can be defined as a reversible change of a single chemical species between two states having distinguishable absorption spectra, such change being induced in at least one direction by the action of electromagnetic radiation [66]. This can be represented by the following equation given below.



The inducing radiation is normally in the ultraviolet or visible regions, and the changes in their spectra are in the visible or near infrared. "A" may be a molecule or ion whereas "B" may be one or more ions or molecules. Commonly, state "B" is thermodynamically less stable than "A" and is more colored, though some exceptions exist. The reverse reaction often occurs thermally, though it can sometimes occur photochemically. Most photochromes change to state B upon radiation and slowly revert thermally back to state "A" when removed from the radiation. A wide variety of chemicals exhibit photochromism, including both organic and inorganic compounds [66]. Most organic electrochromes are activated by ultraviolet light in the range of 200 to 400 nm, and change by a number of processes including *cis-trans* isomerism, tautomerism, heterolytic cleavage and homolytic cleavage (Figure 1.16). This effect is reported in a thiophene based polymer containing azobenzene moieties [67]. It was assumed that the *trans-cis* isomerization of the side chain could interfere with assemblies of polythiophene by altering the order in the side chains. They measured the effect of light on polymer in solution.

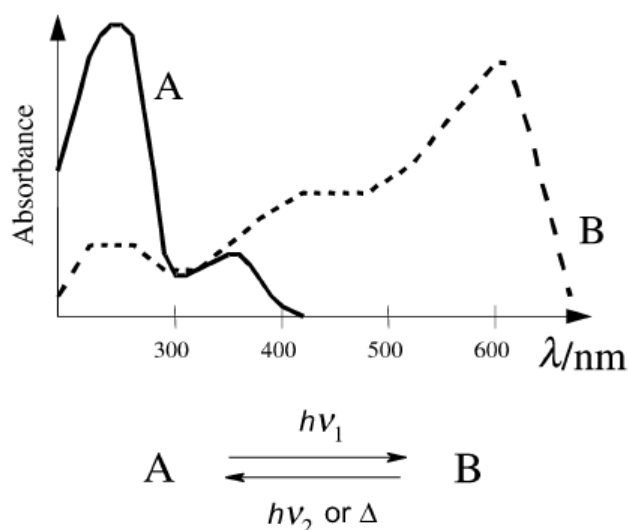


Figure 1.16 Schematic representation of photochromism

1.6.3. Halochromism

Halochromism is the reversible color change due to a change in pH of a solution. Halochromic compounds include phenolphthalein and titanium dioxide. The compounds themselves are weak acids or bases and become involved in acid-base reactions. A change in the pH causes a change in the ratio of ionized and non-ionized states, and, since these two states have different colors, the color of the solution changes. This color change can be used in acid-base titrations where the color change of the halochrome corresponds to the end-point of the reaction.

1.6.4. Piezochromism

Piezochromism is the reversible color change caused by mechanical grinding. This induced color change reverts back to its original color if the material is left in the dark over time. This type of effect was also observed in various polythiophene derivatives. For instance, the non planar (high temperature) form of poly(3-dodecylthiophene) is red shifted with increasing pressure. These results seem to indicate that the conformational change of the polymer and the increase in the band gap induced by heating can be compensated by the applied pressure [68].

1.6.5. Solvatochromism

Solvatochromism is the reversible color change induced by solvents. This often derives from changes in polarity of various solvents. This affects charge transfer mechanisms in solvatochromic compounds, causing color changes. Poly(3-alkylthiophenes) are known to be solvatochromic. The effect on the polymers' color of increasing the solvent polarity is very similar to decreasing temperature of the polymer i.e. the absorption maxima is red-shifted. This is due to the solvent being less able to intermingle with the alkyl chains and so the polymer becomes more planar, causing a decrease in the band gap. The color of poly(3-hexylthiophene) solution was changed by the addition of a poor solvent. [69, 70].

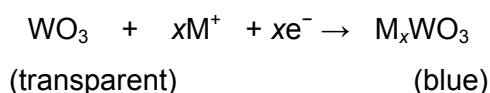
1.6.6. Electrochromism

Electrochromism is the reversible and visible change in transmittance and/or reflectance that is associated with an electrochemically induced oxidation–reduction reaction. It results from the generation of different visible region electronic absorption bands on switching between redox states. The color change is commonly between a transparent (“bleached”) state and a colored state, or between two colored states. The electrochromic materials may exhibit several colors and termed as polyelectrochromic and the possess is called to be multicolor electrochromism [71].

Electrochromic materials have been known since 1968 [72]. Starting from the first discovery in inorganic materials, this phenomenon has been investigated by many scientists. Electrochromism is the most commercially utilized type of chromism which might have some potential applications, including displays, smart mirrors and windows, active optical filters and computer data storage. Especially electrochromic rear-view mirrors have been recently commercialized in the automotive industry with an extraordinary success [73]. The important characteristics of electrochromic materials are the switching times, the contrast ratios, coloration efficiency, electrochromic memory and long term stability. The contrast ratio is defined as the difference in transmittance in the visible spectrum between the two different colored states. The electrochromic memory is the ability of the material to remember its color without applied current. The long term stability is the ability of the material to retain its electrochromic properties over a large number of switching cycles.

Basically three classes of electrochromic materials are known; metal oxide films, molecular dyes and conducting polymers. A typical and most widely studied example of metal oxides is the tungsten trioxide (WO_3) system. Tungsten oxide has a nearly cubic structure which may be simply described as an “empty-perovskite” type formed by WO_6 octahedra that share corners. The empty space inside the cubes is considerable and this provides the availability of a large number of interstitial sites where the guest ions can be inserted. Tungsten

trioxide, with all tungsten sites have the oxidation state W_{VI} , is a transparent thin film. On electrochemical reduction, W_V sites are generated to give the electrochromic (blue coloration to the film) effect. Although, there is still controversy about the detailed coloration mechanism, it is generally accepted that the injection and extraction of electrons and metal cations (Li^+ , H^+ , etc.) play an important role [74]. WO_3 is a cathodically ion insertion material. The blue coloration in the thin film of WO_3 can be erased by the electrochemical oxidation. The generalized equation can be written as follows:



Another type of material that shows electrochromism are small molecules that are produced by diquatization of 4,4'-bipyridyl, 1,1'-disubstituted-4,4'-bipyridilium salts, commonly known as viologens' [75] Of the three common viologen redox states (Figure 1.17), the dication is the most stable and is colorless. Reductive electron transfer to viologen dications forms radical cations. Generally the viologen radical cations are intensely colored, with high molar absorption coefficients, owing to optical charge transfer between the (formally) +1 and zero valent nitrogens. A suitable choice of nitrogen substituents in viologens to attain the appropriate molecular orbital energy levels allows the color choice of the radical cation.

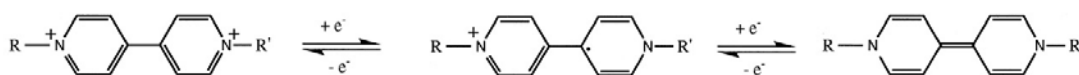


Figure 1.17 The three common viologen redox states, dication, radical cation, neutral species from left to right respectively

1.7. Electrochromism in Conducting Polymers

Electrochromism can be exploited in a series of optical devices with potential use in various applications, such as in information display and storage, in the

automotive industry (as rear-view mirrors and visors), and in architecture (as smart windows to control luminosity and save energy through the control of sunlight transmission [76]). Among organic molecules, conducting polymers have attracted significant interest in the field of electrochromism, since they offer additional advantages, such as, low processing cost, enhanced mechanical properties, no dependence with angle of vision, good UV stability high coloration efficiency, fast switching ability and fine-tuning of the band gap through the modification of polymer's chemical structure. By adjusting the electronic character of the π system along the neutral polymer backbone, the $\pi - \pi^*$ transition can be adjusted across the electromagnetic spectrum from the UV, through the visible and into the near-infrared [77].

The redox switching of conjugated polymers is accompanied by changes in electronic transitions. Figure 1.18 shows the expected transitions in a conjugated polymer according to literature [78]. In the neutral state the polymer exhibits single broad transition from the valence band to the conduction band (π to π^*). The energy difference between these two levels is the band gap (EG), and it is measured as the onset of the π to π^* absorption in the neutral state of the polymer. Upon oxidation, removal of an electron from the valence band, leads to the formation of polaron. This results in state with an unpaired electron whose energy state is higher than the valence band. Accordingly, there occurs the lowering of the corresponding antibonding level in the conduction band; leading to formation of new two intragap states. This should lead to possible four new transitions. However, since the oscillator strength of transitions **a** and **b** (Figure 1.18a) are much greater than transitions **c** or **d**, two low energy transitions are expected as the signature for a polaron. Upon oxidation, the absorbance of the main inter-band peak (π to π^*) decreases along with a formation a new peak at lower energy region of the spectrum. Further oxidation of the polymer will create more polarons by the removal of electrons from the valence band. The unpaired electron of the polaron will be removed to form a dication. Thus, bipolaron will be formed (Figure 1.18 c). Since the bipolaron levels are unoccupied, only transitions from valence band are possible. The signature of a bipolaron is one broad low energy transition. This is because of the stronger nature of the transition **e** with

respect to transition **f**. Yet, basically conducting polymers change color by the creation and destruction of polarons and bipolarons.

Among the conducting polymers, polypyrrole is the one of the first to be investigated both in terms of electropolymerization mechanism and optical properties. Doped (oxidized) polypyrrole film is blue-violet ($\lambda_{\max} = 670 \text{ nm}$). Electrochemical reduction yields the yellow-green ($\lambda_{\max} = 420 \text{ nm}$) “undoped” form. Removal of all dopant anions from polypyrrole yields a pale-yellow film. However, complete dedoping is only achieved if the PPy films are extremely thin. This means that thick films of polypyrrole (this is necessary to achieve high optical contrast) can not be used in device construction. This material is also highly susceptible to degradation upon color switching. CPs with improved electrochromic properties are, however, formed by electrochemical polymerization of 3,4-disubstituted pyrrole.

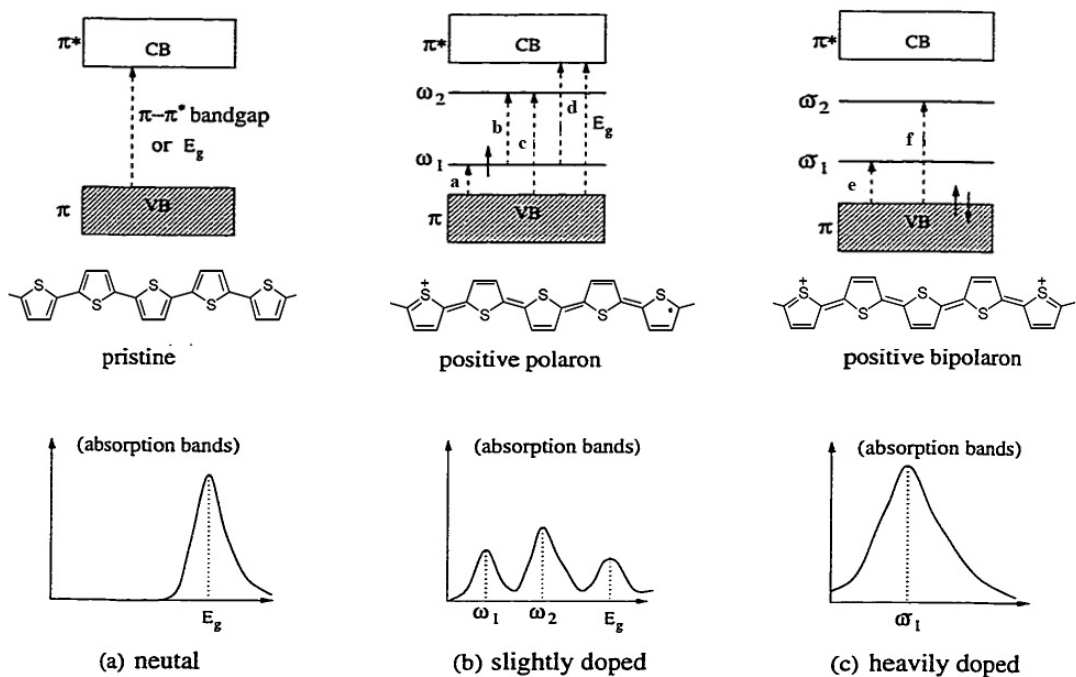
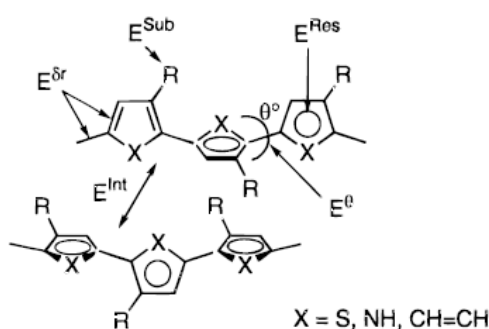


Figure 1.18 Polaron and bipolarons in non-degenerate ground state polymers: band diagrams for neutral (left), positive polaron (center) and positive bipolaron (right); B) neutral (left), lightly doped (center) and heavily doped (right)

Color changes involve the movement of counter ions in and out of the electrochromic matrix. The charged species enters the polymer matrix and migrates slowly through the film. The speed of the color change depends on the speed at which the dopant ions can migrate in and out of the polymer matrix. As the response time is dependent on the movement of charge compensating counter ions, open polymer morphology often results in a reduced response time [79]. The ideal electrochromic polymer should have a high contrast between its extreme states, having short switching time. Stability and maintenance of color after the current has been switched off are also among the expected features to be fulfilled.

1.7.1. Factors Affecting the Band Gap and Color of Conducting Polymer

In its neutral state, the color of the polymer depends on the energy gap between the valence and conduction band. The energy gap between bipolaron band and conduction band determines the color in oxidized state. These are all dependent on the conjugation of the polymer, the electrochemical nature of side groups and their effects on the polymer backbone. There are basically five documented contributors that influence the band gap of the conjugated polymer. Energy related to the bond alternation ($E^{\Delta r}$), the mean deviation from planarity (E^{θ}), the aromatic resonance energy (E^{Res}), the inductive and mesomeric electronic effects of substituents (E^{Sub}) and interchain interactions (E^{Int}) [80].



$$E_g = E^{\Delta r} + E^{\theta} + E^{\text{Res}} + E^{\text{Sub}} + E^{\text{Int}}$$

Figure 1.19 Schematic representation of parameters that play a determining role on E_g [80]

According to the definition of Bredas et al. [81] bond alternation is defined as the maximum difference between the length of a C-C bond inclined relative to the chain axis and a C-C bond parallel to the chain axis. Poly(aromatics) such as polythiophene have non degenerate ground state. Aromatic and quinoid structures are energetically not equivalent. Up to a certain extent, the band gap is known to decrease as the contribution of the aromatic geometry decreases or the quinoid geometry increases. The classical example of aromaticity control in conjugated polyheterocycles is polyisothianaphthene, a polythiophene with a benzene ring fused at the 3- and 4-positions along the polymer backbone [82].

The existence of single bonds between the aromatic cycles causes interannular rotations in conjugated polymers. The overlap of the orbitals varies with this twist angle, which causes the departure from co-planarity. The decline in the extent of overlap results in an increase of E_g by a quantity of E^Q . Up to date several studies has been conducted especially on polythiophenes. Results implied that introduction of flexible side chains cause steric interactions with sulphur groups of neighboring monomeric units and with each other which increases the rotational distortions [83]. Regioregular poly(3-alkylthiophene)s has shown to have much lower band gaps and better electrochemical properties due to the ordering of the polymer films. Especially, head-to-head regiochemical defects are found to cause large twist around the bonds, leading to lowering of π electron configuration. Other than control of regioregularity, several methods, including synthesis of ladder-type polymers like polyquinoxalines was applied [84].

Aromaticity in poly(aromatics) results in a competition between π -electron confinement within the rings and delocalization along the chain. It was shown that the band gap of conjugated polymer generally decreases with decrease in the resonance energy per electron. Such an example is polyisothianaphthene [82]. Benzene, with an energy of aromatization of 1.56 eV, is more aromatic than thiophene (1.26 eV). This forces PITN to be more energetically stable in the quinoidal state, which provides the lowered band gap, 1.1 eV, compared to polythiophene with a band gap of 2.0 eV.

The introduction of electron-donating substituents onto a conjugated chain is a commonly used approach to decrease the polymer's oxidation potential by raising the energy of the valence band electrons ("HOMO" of the conjugated chain) and thereby band gap decreases by E^{Sub} . Electron releasing or withdrawing substituents are known to increase the HOMO and lower the LUMO respectively. Among the electrochromic materials, polythiophene derivatives gained special interest owing to their facile switching properties, processibility, ease of color tunability and their comparatively low cost [85]. Polythiophene thin films are blue ($\lambda_{\text{max}} \approx 800 \text{ nm}$) in their doped (oxidized) state and red ($\lambda_{\text{max}} = 490 \text{ nm}$) in their 'undoped' form. Tuning of color states is possible by suitable choice of thiophene monomer, and this represents a major advantage of using conducting polymers for electrochromic applications.

Poly(alkoxythiophenes) have been extensively studied in this regard. Introduction of strong electron donating groups like alkoxy side chains leads to polymers with low oxidation potentials and good stability in oxidized form since this allows the electrosynthesis to proceed under milder conditions and eliminate overoxidation during synthesis [21]. In addition, the presence of alkoxy side chains lowers the steric hindrance in the surroundings of the main chain, due to smaller van der Waals radius of oxygen in comparison to methylene group. This results in more planar, highly conjugated structures with low band gaps.

In principle, di-substitution at the β, β positions should provide the synthetic basis to perfectly stereoregular polymers since di-substitution eliminates the possibility of β coupling and reduces the likelihood of cross-linking. However, this approach is severely limited by the steric interactions between substituents, which lead to a decrease in polymer conjugation length. In fact, poly(3,4-dialkylthiophenes) have higher oxidation potentials, higher optical band gaps and lower conductivities than poly(3-alkylthiophenes) [21]. This problem was solved by fusing the ring onto the heterocycle, effectively pinning the substituents back from the main chain, like in the case of poly(3,4-ethylenedioxythiophene). Cyclization between the 3 and 4 positions relieves steric hindrance in thiophenes.

Materials based on poly(3,4-ethylenedioxythiophene) (PEDOT) have developed into one of the most successful electrochromic material, owing to its low oxidation potential and band gap with good stability in their oxidized states [20]. The presence of the two electron-donating oxygen atoms adjacent to the thiophene unit lowers the oxidation potential and blocks the β -position of the heterocyclic ring. This results in a more ordered structure and longer conjugation lengths due to elimination of α - β and β - β linkages during polymerization. Jonas et al. [86] were the first to anodically polymerize EDOT and they found out that, relative to other substituted polythiophenes, this material exhibits an exceptional stability in the doped state associated with its high conductivity. Doped PEDOT is almost transparent in the visible region (with a sky-blue tint) and the neutral polymer is dark blue. To date, a large family of poly(3,4-alkylenedioxythiophene)s has been synthesized to investigate the structure-property relationships. Appropriate substitution leads to soluble polymers allowing for processing by common methods including spin- or spray-coating which are important for industrial applications. For instance, the presence of alkyl side chains is known to increase the polymers' processibility. Alkyl substituted PXDOT derivatives also exhibits faster redox switching times [87] and higher degree of electrochromic contrast [88] than unsubstituted parent polymer.

Similar to PXDOT, poly(3,4-alkylenedioxy pyrrole)s has been extensively studied in recent years. PEDOP has both high HOMO (higher than PEDOT) and LUMO level, which resulted in an increase in the band gap up to 2.0 eV revealing red color in reduced state and sky blue-transparent in oxidized state. Change in the size of the alkylenedioxy bridge induces slight steric interaction that serves to decrease the π overlap along the backbone very slightly. This results in an increase in the band gap without affecting the redox properties [89].

In the literature there are series of studies that acknowledge the combination of heterocycles, phenylenes and/ or vinylenes in extended conjugation monomers. Several polymers containing both EDOT and arylene moieties are synthesized. Indeed a series of electron rich, low oxidation potential bis(EDOT) arylenes, including benzene [90] and carbazole [91], has been reported. Also use of vinylenes in a similar approach resulted polymers with even lower band

gaps. [91]. These are basically donor-acceptor or so called push-pull substituted polymers. By this approach both electron donating and withdrawing groups are combined in a 1:1 ratio alternating across the polymer backbone. The resultant polymer has the valence band of the donor and the conduction band of the acceptor.

1.8. Electrochromic Devices

In recent years, a lot of attention is paid in understanding the physical and chemical properties of various electrochromic materials and particularly on CPs not only from basic research point of view but also from the commercial view [71]. It has brought various electrochromic materials and devices actually in the market, such as, in automobile sector rear view mirrors and several others like sunroofs and visors are under prototype production (Figure 1.20). Widespread applications of ECDs, particularly, for architectural applications depend on reducing costs, increasing device lifetime and overcoming the problem of ECD degradation.

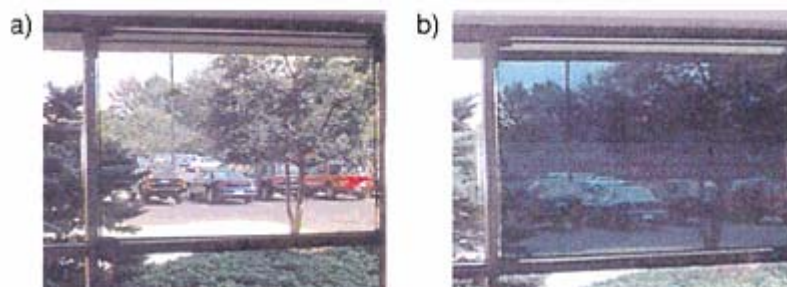


Figure 1.20 Some examples of commercial applications of ECDs

An electrochromic device (ECD) is essentially a battery in which the electrochromic electrode is separated by a suitable solid or liquid electrolyte from a charge balancing counter electrode, and the color changes occur by charging and discharging the electrochemical cell with the application of few volts [71]. The arrangement of these layers depend on the operation mode. [76]

1.8.1. Types of Electrochromic Devices

The smart window is only one of the interesting application areas for electrochromism and not necessarily the one where electrochromism will first be introduced on a large scale. In fact, there are four different fields within which electrochromic devices offer distinct advantages over alternative technologies; all are schematically represented in Figure 1.21. The smart windows in Figure 1.20 are likely to have important applications in innovative and energy-efficient architecture where they would adjust the inflow of luminous radiation and solar energy through glazing in buildings.

As shown in Figure 1.21a the dual type ECDs are constructed in a sandwich cell device configuration with electrochromically complimentary high and low band gap polymers on top of the transparent ITO coated glass electrodes. These electrodes are separated by a thin layer of gel electrolyte to allow switching. These devices provide highly transparent and colored states which could be useful in controlling the light intensity in offices etc. By replacing one of the transparent electrodes of the smart window with a metallic reflector, one reaches the variable reflectance device of Figure 1.21b. Its possible applications include anti dazzling rear view mirrors for cars. If one integrates a white pigment in electrochromic device, it can serve for information display purposes like, signs and labels, as depicted in Figure 1.21c. Another possible device concerns surfaces with variable thermal emittance as sketched in Figure 1.21d. Such surfaces are of interest for temperature stabilization or camouflage applications [92].

1.8.2. Dual Type Transmissive /Absorptive Type Electrochromic Devices

As shown in Figure 1.22 the dual type polymer ECDs are constructed in a sandwich cell device configuration. The electrochromically complimentary polymers were deposited on top of the transparent ITO coated glass electrodes. These electrodes are separated by a thin layer of gel electrolyte to allow switching. In order to prepare an ECD that can undergo a distinct switch from a

highly transmissive state to a deeply absorptive state, material choice is extremely important.

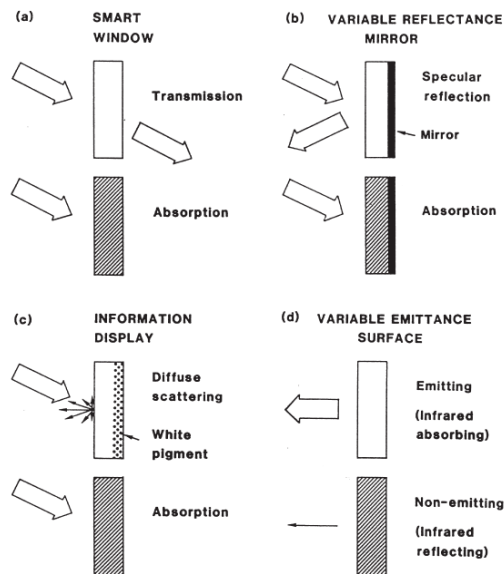


Figure 1.21 The principles of four different applications of electrochromic devices

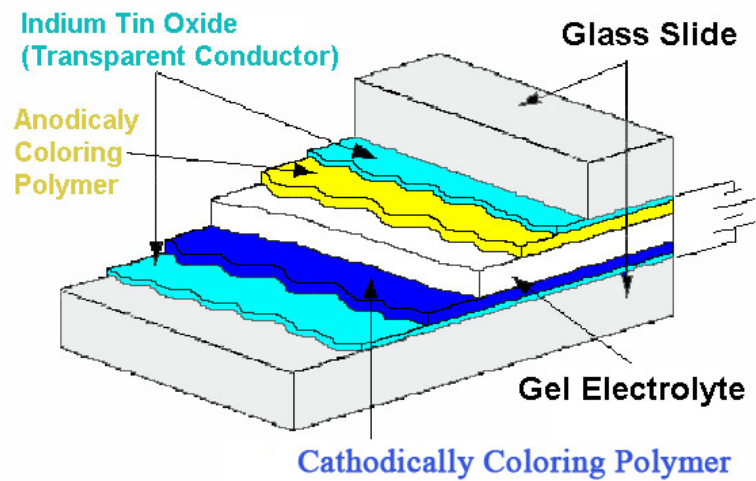


Figure 1.22 Schematic illustration of Dual Type Transmissive /Absorptive Type Electrochromic Device configurations

Change in the color of the device is achieved by the change in the electronic properties of the polymers due to applied potential across the device. Since this is a two-electrode electrochemical cell, during functioning of the device, one of the polymers should be oxidized while the other is reduced (Figure 1.23). A change in applied voltage results in the neutralization of the doped polymer with simultaneous oxidation of the complementary polymer, generating color change in the device.

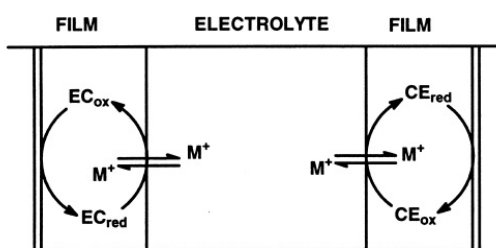


Figure 1.23 Schematic illustration of electrochemistry in ECDs

Color of a device could be estimated from the summation of the two polymers (Figure 1.24). For this reason, to construct an electrochromic device, one of the active electrochromic materials must possess anodic coloration (colored when oxidized) and the other must possess cathodic coloration (colored when reduced). By this way the resulting device would have a transparent and a colored state which is important for applications like office windows etc. Figure 1.24 represents the schematic representation of visible spectra for both anodically and cathodically coloring polymers and demonstrates the concept of dual polymer ECDs. As seen, the ideal device represents no significant absorption within the visible region in one of its states (Figure 1.24 a), yet the other extreme state reveals high coloration (Figure 1.24 b). At bleached state high band gap polymer is in neutral and low band gap polymer is in oxidized state where both of which do not reveal any absorption within the visible region. Upon applied potential high band gap polymer oxidizes and low band gap polymer is reduced to its neutral state and device reveals to colored state.

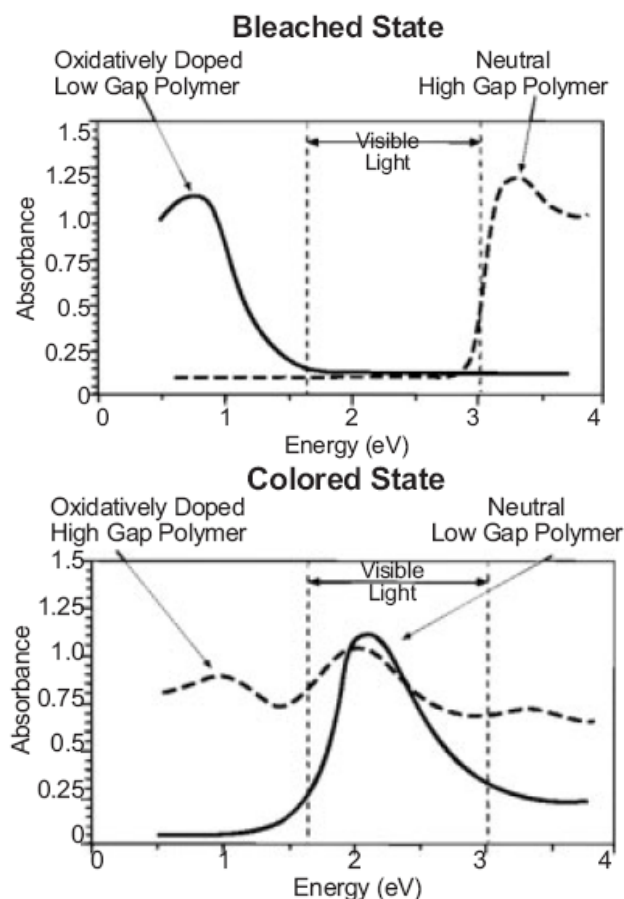


Figure 1.24 Schematic representation of the visible spectra for both anodically and cathodically coloring polymer demonstrating the concept of dual polymer ECDs for absorptive/ transmissive windows [20]

An ideal cathodically coloring material is the one that has highly colored neutral state and highly transparent oxidized state. For this, a material should have a band gap around 1.8-2.2 eV revealing $\pi-\pi^*$ transition within the range of 550-650 nm, where the human eye is highly sensitive. On the contrary, an anodically coloring polymer is chosen to have a high band gap (E_g) > 3.0 eV (π to π^* transition onset < 410nm) with all of the absorption lying in the ultraviolet region of the spectrum. However, most of the high band gap conjugated polymers synthesized to date (e.g. poly(p-phenylene vinylene) (PPV), poly(p-phenylene) (PPP), etc.) have high oxidation potentials which could have negative effect on the life time of the device. Some of the most promising conducting polymers for

use in ECDs are based on PEDOT (as cathodically coloring material), PEDOP (as anodically coloring material) and their derivatives, which exhibit high electrochromic contrasts, low oxidation potentials and high conductivity, as well as good electrochemical and thermal stability. Up to now PProDOT-Me₂ as the cathodically and N-alkylated PProDOP as the anodically coloring resulted in the best optical contrast [93].

Basic requirements for high performance electrochromic devices are: a) short response time; b) good stability; c) optical memory, defined as the color stability under open circuit potential conditions; d) optical contrast, also called write-erase efficiency, and e) color uniformity [76].

CHAPTER II

EXPERIMENTAL

2.1. Materials

Acetonitrile (ACN) (Merck), and tetrabutylammonium tetrafluoroborate (TBAFB) and borontrifluoride diethyletherate (BFEE) (Sigma) were used without further purification. Thiophene (Th) (Aldrich) was distilled before use, 3-Thiophene ethanol (Aldrich), adipoyl chloride (Aldrich), octanoyl chloride (Aldrich), sebacoylchloride, triethylamine (TEA) (Aldrich) and MgSO_4 (Aldrich) were used without further purification. The gel electrolyte used in this study was prepared by mixing poly(methyl methacrylate), TBAFB, ACN and propylene carbonate with 7:3:20:70 ratio by weight.

2.2. Equipment

The cyclic voltammograms were recorded in ACN / TBAFB solvent-electrolyte couple using a system consisting of a potentiostat (Wenking POS 73), an X-Y recorder and a CV cell containing Pt foil working and counter electrodes, and a Ag/Ag^+ reference electrode. Measurements were carried out at room temperature under nitrogen atmosphere. Spectroelectrochemical studies were carried out on a HP8453A UV-Vis Spectrophotometer. Colorimetry measurements were obtained by a Coloreye XTH Spectrophotometer (GretagMacbeth). Thermal behavior of the samples was investigated via a Du Pont 2000 Thermal Gravimetry Analyzer and Differential Scanning Calorimetry. Scanning electron microscopy (SEM) studies were performed by JEOL JSM-6400. NMR spectra of the monomers were recorded on a Bruker-Instrument-NMR Spectrometer (DPX-400) with CDCl_3 as

the solvent and chemical shifts (δ / ppm) are given relative to tetramethylsilane as the internal standard. The IR spectrum was recorded on a VARIAN 1000 FTIR spectrometer.

2.3. Procedure

2.3.1. Synthesis of monomers

In the first part of the study, three different thiophene functionalized monomers were synthesized and characterized via $^1\text{H-NMR}$, $^{13}\text{C-NMR}$, FTIR, DSC, TGA techniques.

Stoichiometric amount of 3-thiophene ethanol and triethylamine (TEA) were dissolved in 20 mL dichloromethane. Adipoyl chloride, octanoyl chloride or sebacoylchloride was added drop wise to this mixture at 0°C under inert atmosphere for the synthesis of Hexanedioic acid bis-(2-thiophen-3-yl-ethyl ester (HABTE), Octanoic acid 2-thiophen-3-yl-ethyl ester (OTE) and Decanedioic acid bis-(2-thiophen-3-yl-ethyl) ester (DATE) respectively. The resulting monomers were purified with successive extractions and dried by anhydrous MgSO_4 .

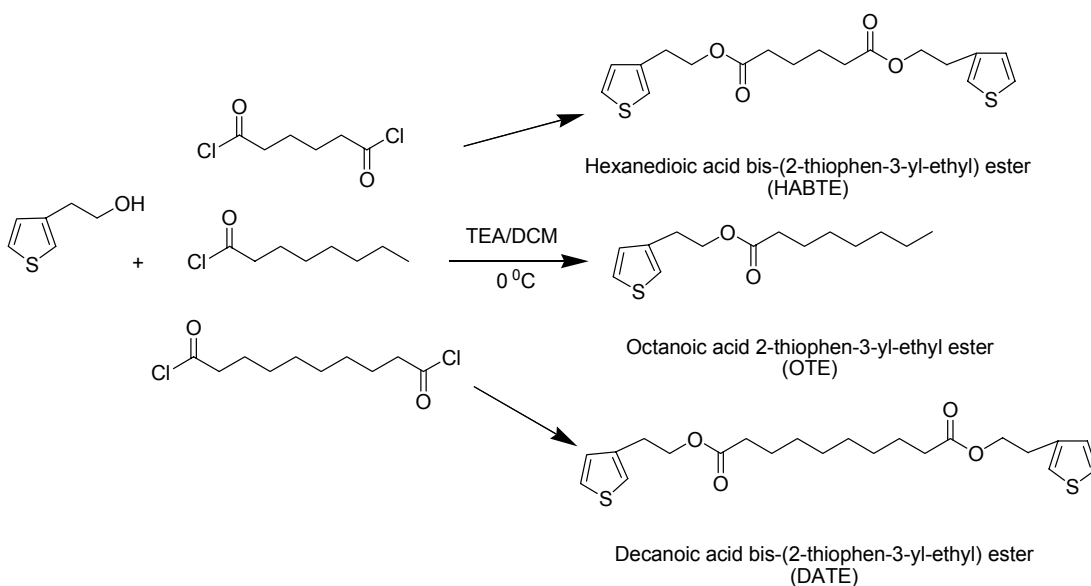


Figure 2.1 Synthesis route of monomers

2.4. Synthesis of Conducting Polymers

2.4.1. Electrochemical Polymerization

2.4.1.1. Homopolymerization

Electrochemical polymerizations of the monomers were achieved under constant potential electrolysis. Throughout this study tetrabutylammonium tetrafluoroborate (TBAFB) was used as the supporting electrolyte. Acetonitrile, borontrifluoride diethyletherate (BFEE) were the solvents for these systems. Homopolymerization of monomers were achieved via constant potential electrolysis in a single compartment cell, in the presence of 50 mg monomer, 0.1 M TBAFB in ACN/BFEE (8:2) at 1.5V, equipped with Pt working and counter electrodes and a Ag/Ag⁺ reference electrode. The free standing homopolymers were washed with ACN in order to remove excess TBAFB and unreacted monomer after the electrolysis.

2.4.1.2. Copolymerization

2.4.1.2.1. Copolymers of HABTE

Conducting copolymer of HABTE was achieved in the presence of thiophene under constant potential electrolysis. 50 mg of monomer was dissolved in 15 mL acetonitrile, and 15 μ L of thiophene was introduced into a single compartment electrolysis cell. During these studies TBAFB was used as the supporting electrolyte. Constant potential electrolysis was run at 1.9 V for 30 min at room temperature under inert atmosphere. The resultant polymer was abbreviated as P(HABTE/Th).

A second type of copolymer was synthesized via procedure where electrolysis was performed in the presence TBAFB, in ACN / BFEE solvent system (8:2, v/v) at 1.5 V. The free standing polymer was washed with ACN in order to remove excess TBAFB and unreacted monomer after the electrolysis. The resultant polymer was coded as P(HABTE-co-Th).

2.4.1.2.2. Copolymer of DATE: P(DATE-co-Th)

Conducting copolymer of DATE was synthesized in the presence of thiophene under constant potential electrolysis at 1.5V. 50 mg of monomer were dissolved in 15 mL acetonitrile/ BFEE solvent system (8:2, v/v) containing 0.1M TBAFB, and 15 μ L of thiophene was introduced into a single compartment electrolysis cell. The free standing polymer was washed with ACN in order to remove excess TBAFB and unreacted monomer after the electrolysis.

2.4.1.2.3. Copolymer of OTE with 3-methyl thiophene : P(OTE-co-MeTh)

40 mg of OTE was dissolved in 15 ml acetonitrile, and 15 μ l of 3-methyl thiophene 0.1 M tetrabutylammonium tetrafluoroborate were introduced into a single compartment electrolysis cell. The electrolysis was run for 30 min at 1.9 V at room temperature under inert atmosphere. The resulting copolymer films were washed with acetonitrile to remove tetrabutylammonium tetrafluoroborate and unreacted monomers after the electrolysis.

2.4.2. Chemical Polymerization

50 mg of monomer was dissolved in 5 mL carbon tetrachloride. FeCl_3 (1.1×10^{-3} mol) was dissolved in 15 mL nitromethane and placed in three-necked flask. Monomer solution was added drop wise to the solution of FeCl_3 at 0°C . The reaction was carried out for 24 h with constant stirring. Then methanol was added for precipitation and the black solid was obtained by filtration. It was washed with methanol and ACN several times to remove excess ferric chloride and monomer.

2.5. Characterization of Conducting Polymers

2.5.1. Cyclic Voltammetry (CV)

Cyclic voltammetry (CV) is the most widely used technique for acquiring qualitative information about electrochemical reactions. CV is often used as the first experiment for electroanalytical study. In particular, it offers a rapid location of

redox potentials of the active species. CV consists of scanning linearly the potential of a stationary working electrode using a triangular potential waveform (Figure 2.2a). During the potential sweep, the potentiostat measures the current resulting from the applied potential. Figure 2.2b illustrates the expected response of a reversible redox couple during a single potential cycle. Typically, as the applied potential approaches the characteristic E^0 for the redox process the current begins to increase, until a peak is reached. Then the direction of the potential sweep is reversed. During the reverse scan, the molecules generated in the forward half cycle, accumulated near the surface are re-oxidized. [94]

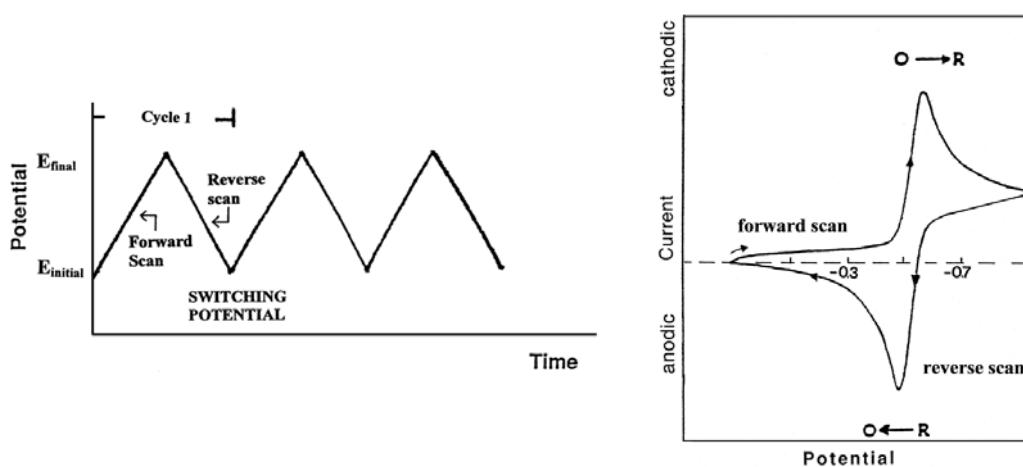


Figure 2.2 Typical (a) Potential–time excitation signal in CV (b) cyclic voltammogram of a reversible $O + ne^- \leftrightarrow R$ redox process [94]

The characteristic peaks in the CV are caused by the presence of the diffusion layer near the electrode surface. Figure 2.3 illustrates three concentration gradients for the reactant and product at different times corresponding to (a) the initial potential value (b) the formal potential of the couple, during forward scan and (c) the achievement of a zero reactant surface concentration. The resulting current peak thus reflects the continuous change of concentration gradient with time. Hence, the increase in the current corresponds to the achievement of diffusion control, while current drop (beyond the peak) exhibits independence to the applied potential.

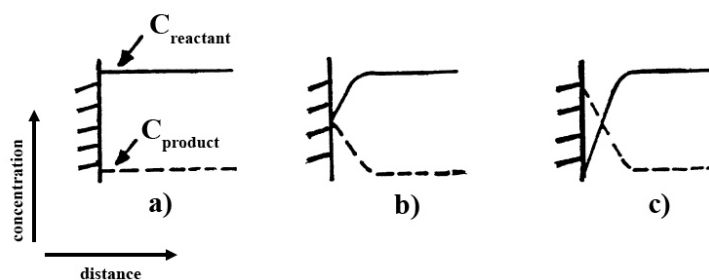


Figure 2.3 Concentration distribution of the oxidized and reduced forms of the redox couple at different times during cyclic voltammetric experiment correspond to a) the initial potential, b) the formal potential during the forward scan and c) zero reactant concentration at the surface [94]

The peak current for a reversible couple is given by Randles & Sevcik equation:

$$i_p = (2.69 \times 10^5) n^{3/2} A D^{1/2} C v^{1/2}$$

where n is the number of electrons, A is the electrode area (in cm^2), C is the concentration (in mol cm^{-3}), D is the diffusion coefficient (in $\text{cm}^2 \text{s}^{-1}$), and v is the scan rate (in Vs^{-1}). Accordingly, the current is directly proportional to concentration and increases with the square root of the scan rate. For these processes, it was assumed that the reactants and products are soluble in solution and the surface processes (adsorption of reactants and products) can be neglected.

In case of the electroactive polymer electrochemistry, the process is somewhat different. Polymerization of electroactive monomer is an irreversible process, where the monomer is irreversibly oxidized and a film of electroactive polymer is formed. Thus, in this situation there are two electroactive species in the system, one of which being the monomer and the other is polymer deposited on the electrode. A typical CV investigation generally starts at low potentials where no redox reactions occur in anodic direction. Anodic current starts to increase in the vicinity of the potential where the electrode has reached sufficient potentials at

which the monomer starts to oxidize to its radical cation. The anodic current increases rapidly until the concentration of the monomer at the electrode surface approaches zero, which is signified by the formation of a peak. The intensity of the current starts to decay since the solution in the vicinity of the electrode has almost zero monomer concentration. Monomer oxidation is immediately followed by chemical coupling which results in the formation of firstly the dimer and the oligomers. However, in some cases like pyrrole, the oxidation of monomer could not be observed in the form of a peak due to immediate formation of dimers and oligomers all of which are highly electroactive. This results in an infinitely high concentration of electroactive species at the electrode surface which prevents the observation of monomer in terms of a peak. Indeed, only a dramatic increase in the cathodic current could be observed. Once these oligomers reach a certain length, they precipitate onto the electrode surface where the chains can continue to grow in length. In the cathodic run the reduction of the deposited polymer is observed. Upon consecutive cycle formation of a new oxidation peak is appears due to the re-oxidation of the polymer which is followed by the monomer oxidation peak again. It should be noted that as the number of cycle increases there is an increase in the intensity of the current. This is due to increase in the active area of the working electrode owing to coating of already electroactive polymer on the metal electrode (Figure 2.4) [95].

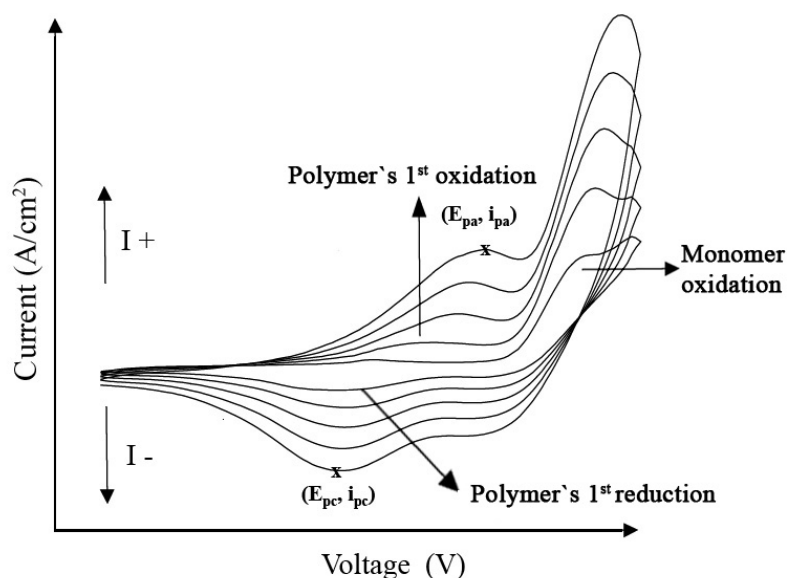


Figure 2.4 Cyclic Voltammogram of a representative type of electroactive monomer [95]

To study the electrochemistry of a polymer, a monomer free system should be used. The polymer redox process is quasi-reversible and since the polymer is immobilized at the electrode surface, the redox process is not diffusion controlled. Thus under these circumstances Randles & Sevcik equation is no longer valid. Instead, according to the theory of immobilized redox centers, the peak current is given by ;

$$i_p = n^2 F^2 \Gamma v / 4RT$$

where Γ is the total amount of reactant initially present at the electrode surface. According to this equation the current peak depends linearly on scan rate. Thus investigation of peak current intensity with respect to scan rate will indicate the nature of electrochemical process being diffusion controlled or the polymer is well adhered to the electrode surface [96,97].

2.5.2. Conductivity

The Four Probe Method is one of the standard and most widely used method for the measurement of conductivity. The four osmium probes aligned in a colinear geometry. The error due to contact resistance, which is significant in the electrical measurement on semiconductors, is avoided by the use of two extra contacts (probes) between the current contacts. In this arrangement the contact resistance may all be high compare to the sample resistance, but as long as the resistance of the sample and contact resistance's are small compared with the effective resistance of the voltage measuring device (potentiometer, electrometer or electronic voltmeter), the measured value will remain unaffected. Because of equal pressure contacts, the arrangement is also especially useful for quick measurement on different samples or sampling different parts of the sample. Figure 2.5 demonstrates a simple four-probe measurement setup. Four equally spaced osmium tips touch the surface of polymer film taped on an insulating substrate. A known steady current is passed through the electrodes 1 and 4 and measured while the potential drop (ΔV) between contacts 2 and 3 assessed.

Conductivity is calculated from the following equation,

$$\sigma = \frac{\ln 2}{\pi R t}$$

where R is the resistance of the sample, and t is the thickness.

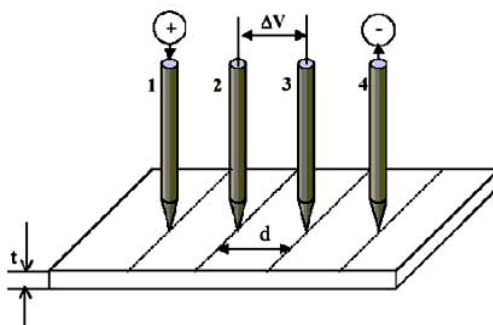


Figure 2.5 Four-probe conductivity measurement setup [95]

2.5.3. Electrochromic Properties of the Conducting Polymers

2.5.3.1. Spectroelectrochemistry

Spectroelectrochemistry combines electrochemical and spectroscopic techniques that can be operated at the same time. Compared to common electrochemical methods, it can provide information on both electrochemical response and accompanying optical characteristics of all states of the electrochemical reaction. It is essential to gather information in-situ, during electrochemical process. Ex-situ measurements, outside the electrochemical cell, may not yield the true picture of the electrode process because of the transformations that can occur after the loss of electrode potential control. Spectroelectrochemistry is a powerful tool to probe unique species that are generated in-situ during redox reactions at electrode surfaces.

The redox switching of conjugated polymers is accompanied by changes in electronic transitions. These absorption change is the property that makes

conjugated polymers useful in electrochromic applications such as smart windows, mirrors, etc. The electronic transitions of conjugated polymers have been the subject of many articles. These electronic transitions can be probed by the use of UV-Vis spectroscopy. Spectra are recorded while the polymer is oxidized by increasing the potential stepwise. This experiment is commonly referred as spectroelectrochemistry, and can be easily accomplished by constructing a three electrode cell inside a normal cuvette for conducting polymers. Spectroelectrochemistry experiments reveal key properties of conjugated polymers such as band gap (E_g), λ_{max} , the intergap states that appear upon doping and evolution of polaron and bipolaron bands. Similar studies were accomplished for electrochromic devices in order to investigate the spectral variations.

Spectroelectrochemical analyses of the homopolymer and copolymers were studied by depositing the samples as thin films on ITO-coated glass slides in ACN/BFEE mixture (8:2, v/v) solution consisting of 0.01 M monomer and 0.1 M TBAFB (also in presence of 0.01M Th in case of copolymers). Basically a UV cuvette was utilized as an electrolysis cell equipped with Pt counter and Ag/Ag⁺ reference electrodes (Figure 2.6). Different potentials from fully reduced states of polymer to fully oxidized states are applied to coated ITO slides in a monomer free (0.1 M) TBAFB/ACN/BFEE solvent electrolyte couple, while spectral series are recorded at the same time.

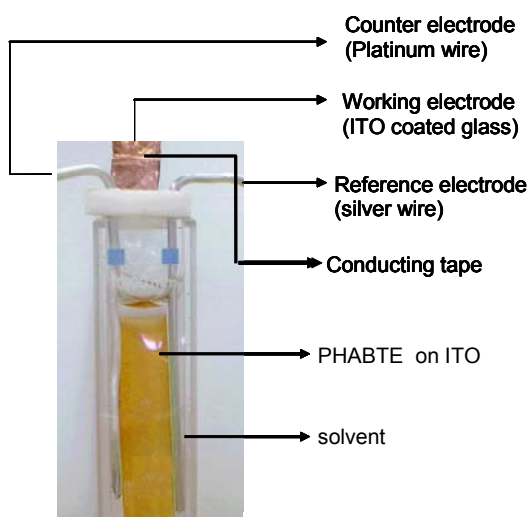


Figure 2.6 Schematic representation of electrochemical used in spectral studies

2.5.3.2. Switching Studies

For electrochromic applications, the ability of a polymer to switch rapidly and exhibit a striking color change is important. Electrochromic switching studies can monitor these types of properties. A square wave potential step method coupled with optical spectroscopy known as chronoabsorptometry was used to probe switching times and contrast in these polymers. In this double potential step experiment, the potential was set at an initial potential for a set period of time, and was stepped to a second potential for a set period of time, before being switched back to the initial potential again.

In order to study switching properties of polymers, homopolymers or copolymers were deposited on ITO-coated glass slides as in the form of thin films, via constant potential electrolysis in ACN/BFEE mixture (8:2, v/v) solution consisting of 0.01 M monomer and 0.1 M TBAFB. Square-wave potential was applied to coated ITO slides in a monomer free (0.1 M) TBAFB/ACN/BFEE solvent electrolyte couple, between fully reduced states of polymer to fully oxidized states with a residence time of 5 seconds, while simultaneously the percent transmittance change during doping and dedoping process was monitored at the maximum absorption wavelength.

2.5.3.3. Colorimetry

Colorimetric analysis is rapidly becoming a popular technique in the study of electrochromic polymers. This method allows for accurately reporting a quantitative measure of the color and graphically representing the track of doping-induced color changes of an electrochromic material or device. There are three attributes that are used to describe the color: hue, saturation and brightness. Hue represents the wavelength of maximum contrast (dominant wavelength) and is commonly referred to as color. Saturation takes into consideration the purity (intensity) of a certain color, whereas the third attribute, brightness, deals with the luminance of the material, which is the transmittance of light through a sample as seen by the human eye. It is important to note that color is a matter of perception and subjective interpretation. Several factors affect color perception, such as light

source differences, observer differences, size differences (color covering large areas tends to appear brighter and more vivid than color covering a smaller area), background differences (an object placed in front of a bright background looks duller than in front of a dark background). When studying the color, its hue will vary depending on the illumination and its surrounding. Color is the product of wavelengths that are either absorbed or reflected by the surface of an object being strongly illuminated. A commonly used scale that numerically defines colors has been established in 1931 by The Commission Internationale de l'Eclairage (CIE system) with $L^*a^*b^*$, CIE color spaces (Figure 2.7). Color measurements were performed via Coloreye XTH Spectrophotometer.

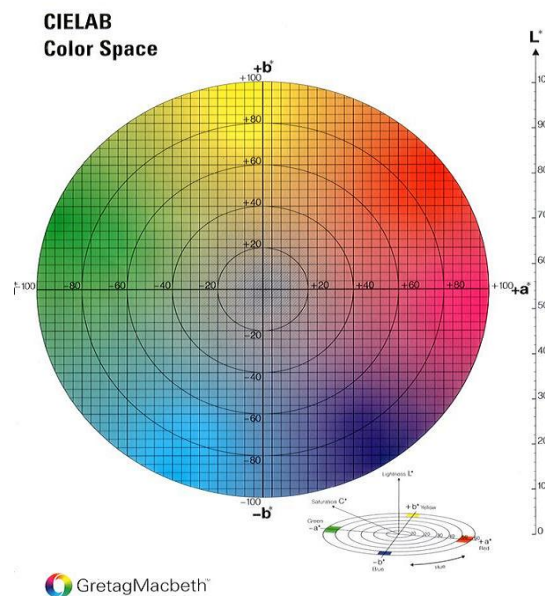


Figure 2.7 CIELAB color space

2.6. Device Construction

The construction of a transmissive type ECD consists of two thin polymer films deposited on transparent indium tin oxide coated glass (ITO), and separated by a viscous gel electrolyte (Figure 2.8). Polymer films used to assemble a device will be obtained by constant potential oxidative polymerization. Cathodically coloring polymer, poly(3,4-ethylenedioxythiophene) (PEDOT), was electrochemically deposited onto the ITO-coated glass from a 0.1 M solution of EDOT in 0.1M ACN

at +1.5 V versus Ag/Ag⁺. The anodically coloring polymers, the homo and copolymers were potentiostatically deposited onto the ITO-coated glass at 1.5 V in ACN/BFEE mixture (8:2, v/v) solution consisting of 0.01 M monomer and 0.1 M TBAFB (also in presence of 0.01 M Th in case of copolymers). Duration of polymerization was determined according to chronocoulometry studies.

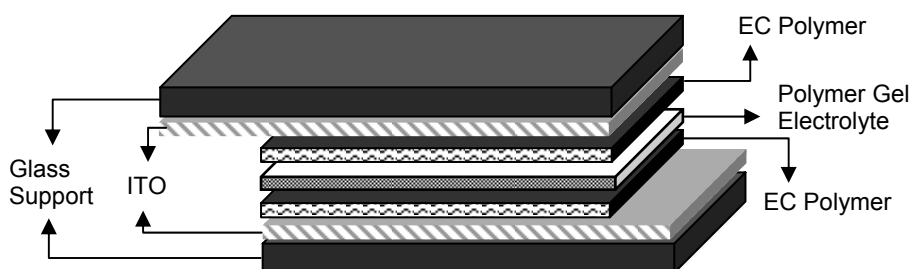


Figure 2.8 Schematic representation of the transmissive/absorptive type ECD

Before assembling the devices, it was important to balance the charge capacities of the electrochromic layers. Otherwise, it would result in incomplete electrochromic reaction and residual charges will remain during the coloring/bleaching processes, which would lead to residual coloration of the ECD in the bleached state. To minimize the effect of charge imbalances in EC device, we matched the redox charges of the two complementary polymer films by chronocoulometry and we provided a balanced number of redox sites for switching. Figure 2.9 reflects the redox site charge versus deposition charge of PEDOT which was synthesized at 1.5 V in 0.1M ACN, onto the ITO-coated glass at different time intervals. Actually in these studies control of deposition charge is considered as a reliable parameter that is bound to the film thickness. The redox site charges of the films were calculated according to potential square wave experiments where the ultimate oxidation and reduction potentials were applied in monomer free electrolytic medium. This quantity indicates the charge requirement of the film to have full cycle. Similar type of a correlation data has been prepared for the 3-ester substituted polymers. Thus, electrochromic layers of the devices were synthesized at predetermined conditions so as to have the same redox site charges.

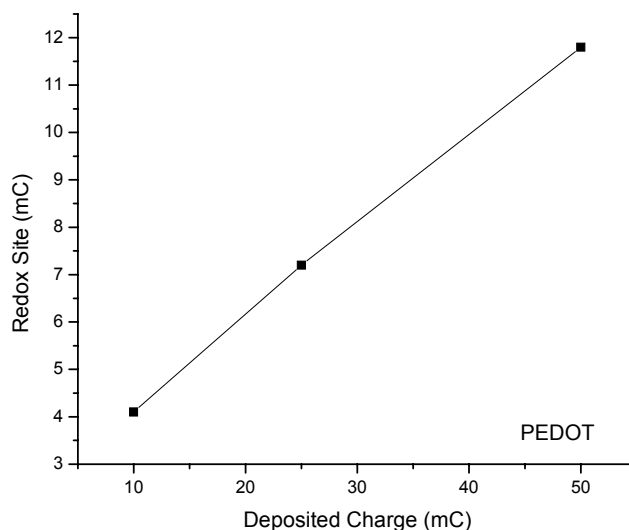


Figure 2.9 Redox site charge vs synthesis charge graph for PEDOT synthesized at 1.5 V

Prior to assembly, cathodically coloring films were fully oxidized and anodically coloring polymers were fully neutralized, to provide the ion exchange within the device. The films were then coated with gel electrolyte by the casting solution until the entire polymer surface is uniformly covered. The gel electrolyte forms a seal around the edges, the devices becomes self-encapsulated.

2.6.1. Preparation of Gel Electrolyte

The gel electrolyte was prepared from an acetonitrile solution containing poly(methyl methacrylate) and TBAFB. The acetonitrile was slowly evaporated via stirring and a few drops of propylene carbonate were added to decrease the vapor pressure of the gel electrolyte yielding a highly conducting transparent gel. The ratio of the composition of TBAFB-PMMA-PC-ACN was 3:7:20:70 by weight.

2.7. Characterization of the Electrochromic Devices

2.7.1. Spectroelectrochemistry Studies of Electrochromic Devices

Agilent 8453 UV-Vis spectrophotometer were used in order to characterize the optical properties of electrochromic devices (ECDs). During spectroscopic studies a device having no the active polymer layer, was used as the reference. Applied potentials were delivered via potentiostat where the counter and the reference electrodes were short cut and working electrode was connected to anodically coloring polymer layer. Spectroelectrochemical studies of electrochromic devices were recorded under sequential variation of applied potentials between ultimate operation conditions, while measuring the absorbance as a function of wavelength.

2.7.2 Switching Properties of Electrochromic Devices

Potential square wave technique, similar to described procedure in section 2.5.3.2 was applied to determine switching properties of ECDs, where the applied potentials and wavelength of inspection were determined according to spectroelectrochemistry studies.

2.7.3. Open Circuit Stability

The color persistence in the electrochromic devices is an important feature since it is directly related to aspects involved in its utilization and energy consumption during use. In order to explore this behavior, experiment will be performed by polarizing the electrochromic devices in its two extreme states by an applied pulse for 1 second and device would be kept at open circuit conditions for 200 s, simultaneously the optical spectrum at maximum optical contrast point as a function of time at open circuit conditions will be monitored.

2.7.4 Stability of the Electrochromic Devices

The stability of the devices was evaluated via CV studies by continuous sweeping of the applied potential across the device up to 1000 cycles.

CHAPTER III

RESULTS AND DISCUSSION

3.1. Conducting Polymers of HABTE

3.1.1. Synthesis and Characterization of HABTE

Hexanedioic acid bis-(2-thiophen-3-yl-ethyl) ester (HABTE), was synthesized via condensation reaction of 3-thiophene ethanol and adipoyl chloride in the presence of triethylamine (TEA). Figure 3.1 represents the $^1\text{H-NMR}$ of the monomer in CDCl_3 . The chemical shifts were assigned as follows,

$^1\text{H-NMR}$ (CDCl_3)-HABTE: δ : 7.17 (a, thiophene), 6.94 (b, thiophene), 6.91 ppm (c, thiophene) and 2.88 ppm (d, thiophene $-\text{CH}_2$), 4.23 ppm (e, $\text{CH}_2\text{-O}$), 2.23 ppm (f, CO-CH_2), 1.55 ppm (g, $-\text{CH}_2$), 7.2 ppm (s, CDCl_3).

$^{13}\text{C-NMR}$ (CDCl_3)-HABTE: (δ / ppm): 172.2 from CO, 120.5, 124.6, 127, 137 ppm (thiophene), 28.6 ppm (thiophene-C), 63.1 ppm (C-O), 32.8 ppm (CO-C), 23.3 ppm (C-C), 76 ppm (t, CDCl_3). $^{13}\text{C-NMR}$, FTIR of HABTE is given in appendix Figures A1 and A2.

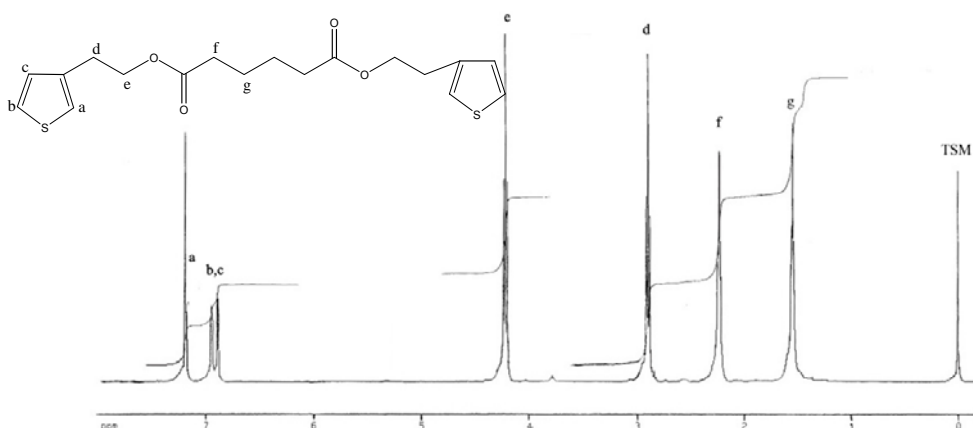


Figure 3.1 $^1\text{H-NMR}$ of HABTE

3.1.2. Cyclic Voltammetry

Cyclic voltammetry (CV) is the most widely used technique for acquiring qualitative information about electrochemical reactions. It is often the first experiment performed in an electroanalytical study, since it offers a rapid location of redox potentials of the electroactive species. Another very important aspect of this method, especially in the field of conducting polymers, is its ability to generate a new redox species during the first potential scan and then probe the fate of species on the second and subsequent scans. Therefore, CV allows to follow the growth of a conducting polymer film along with its further characterization during a single experiment.

In order to investigate the electrochemical behavior of HABTE, CV experiment was performed in TBAFB/ACN supporting electrolyte/solvent system. As reflected in the CV (Figure 3.2 a), voltammogram of the monomer exhibited an irreversible electroactivity at 1.95 V. However, current sharply decreased upon repetitive cycles. Continuous deposition of the polymer onto the WE was monitored by the increase in the polymer's anodic and cathodic peak currents which was achieved with the addition of borontrifluoride diethyletherate (BFEE) to the same system (Figure 3.2 b).

In 1995 Xue et al. reported the low potential electrochemical synthesis of polythiophene in freshly distilled borontrifluoride diethyletherate [33]. It was found out that the resultant polymer has higher effective mean conjugation length with remarkable mechanical strength. This improvement was attributed to the decrease in the aromatic resonance energy and promotion of the abstraction of an electron from the α -position of the heterocyclic ring. Yet oxidation potential of the monomer was decreased. [34,35]. Up to date, the role of the BFEE in doping process is not fully established. It is known that BFEE exists in diethylether as a polar adduct and the presence of small amount of water results in the formation of $H^+[BF_3OH]^-$. This complex is thought to provide a conducting medium and stated previously that $[BF_3OH]^-$ ion serves as the dopant during electrochemical polymerization [43].

As seen in Figure 3.2b, the homopolymer revealed an oxidation peak at 0.9 V and there was a slight increase in the oxidation potential and a decrease in the reduction potential respectively with the further cycling by the addition of BFEE. Free standing conducting polymer films were successfully synthesized. The free standing film was washed with ACN several times to remove unreacted monomer.

In order to synthesize and investigate the CV behavior of the copolymer, we performed CV studies in the presence of thiophene under the same experimental conditions. There was a drastic change in the voltammogram; both the increase in the increments between consecutive cycles and the oxidation potential of the material was different than those of both monomer and pure thiophene, which in fact could be interpreted as the formation of copolymer, which needs to be supported by other means of characterization (Figure 3.2c).

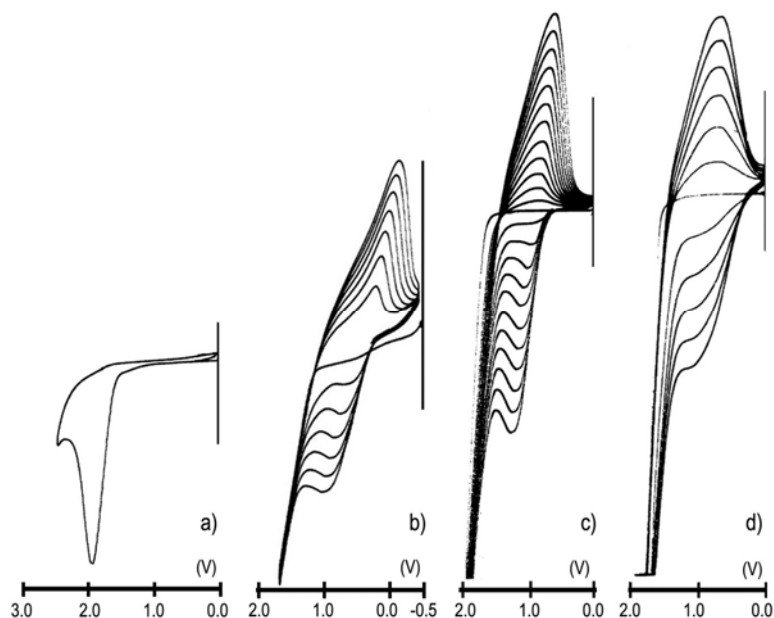


Figure 3.2 Cyclic voltammogram of (a) monomer (HABTE), (b) HABTE in the presence of BFEE, (c) HABTE in the presence of thiophene and BFEE, (d) thiophene in the presence of BFEE, with platinum working and counter electrodes and a Ag/Ag^+ reference electrode in 0.1 M TBAFB/ACN with 500mV/s scan rate

3.1.3. FTIR

Infrared (IR) spectroscopy is a chemical analytical technique, which measures the infrared intensity versus wavenumber of light. Infrared spectroscopy detects the vibration characteristics of chemical functional groups in a sample. When an infrared light interacts with the matter, chemical bonds stretch, contract or bend. As a result, a chemical functional group tends to adsorb infrared radiation in a specific wavenumber range regardless of the structure of the rest of the molecule. In this study we acknowledged the use of FTIR spectroscopy to investigate the presence of specific functional groups both in monomer and synthesized conducting polymers. FTIR spectrum of the HABTE monomer revealed the following absorptions at 3067 cm^{-1} (aromatic C-H), 2932-2900 cm^{-1} (aliphatic C-H), 1748 cm^{-1} (C=O stretching), 1260-1000 cm^{-1} (C-O-C symmetric and asymmetric stretching), 788 cm^{-1} (thienylene out of plane C-H $_{\alpha}$ stretching), 840 cm^{-1} (thienylene out of plane C-H $_{\beta}$ stretching), 1068,1050 cm^{-1} (in plane C-H deformations) , 1415, 1347 cm^{-1} (aromatic C=C, C-C ring stretching), 612 cm^{-1} (C-S-C stretching) [98].

In accordance with the CV studies, homopolymerization of HABTE was achieved via constant potential electrolysis in a single compartment cell, in the presence of 50 mg HABTE, 0.2 M TBAFB in ACN/BFEE (8:2) at 1.5V, equipped with Pt working and counter electrodes and a Ag/Ag⁺ reference electrode (Figure 3.3). Upon homopolymerization of HABTE, most of the characteristic peaks of monomer remained unperturbed. The band at 788 cm^{-1} indicating C-H $_{\alpha}$ stretching and the two bands at 1068 and 1050 cm^{-1} corresponding to the out of plain C-H vibration of the monomer disappeared completely, whereas evolution of a new absorption peak at 840 cm^{-1} (2,3,5-trisubstituted thiophene) was observed. The shoulder at 1644 cm^{-1} and the intense band at 1081 cm^{-1} were assigned to be due to the formation of polyconjugation, and presence dopant anion respectively (Figure 3.4). Similar type of FTIR spectrum was observed in the case of chemical polymerization of HABTE.

For the synthesis of conducting copolymer of HABTE, thiophene was used as the comonomer. 40 mg of HABTE was dissolved in acetonitrile/ BFEE solvent system

(8:2, v/v), and 15 μL of thiophene was introduced into a single compartment electrolysis cell. Polymerization was accomplished via application of 1.5 V (Figure 3.3). Resulting copolymer films were washed with solvent to remove TBAFB after the electrolysis. FTIR spectra of electrochemically synthesized copolymer, P(HABTE-co-Th) showed similar absorptions to homopolymer which were related to aromatic C-H, aliphatic C-H, C=O stretching, aromatic C=C, C-C ring stretchings. The peaks around 1080 and 1640 cm^{-1} indicated the presence of dopant anion and polyconjugation (Figure 3.4). Presence of the band at 1744 cm^{-1} , which was attributed to the carbonyl group originating from monomer, was considered as the proof of successive copolymerization.

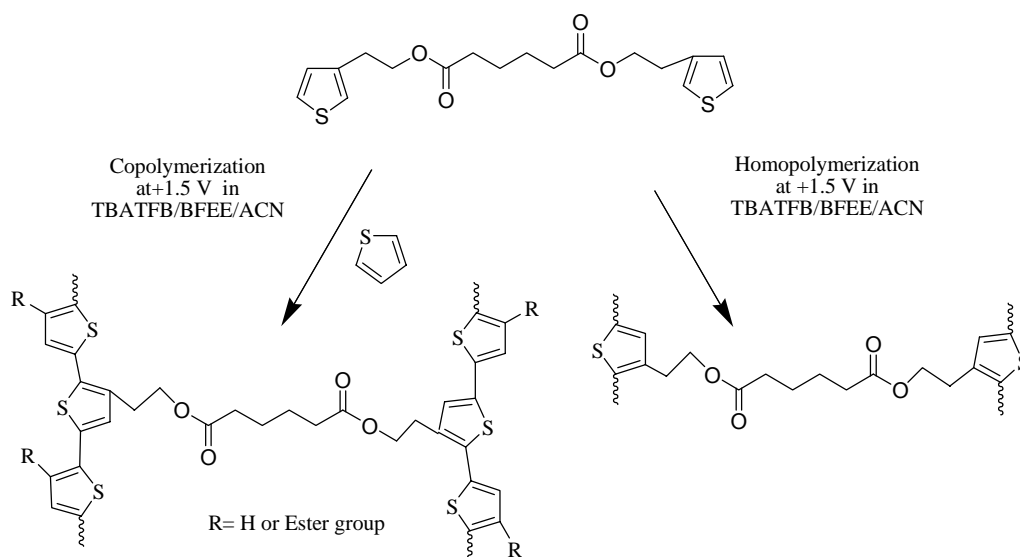


Figure 3.3 Electrochemical polymerization of HABTE

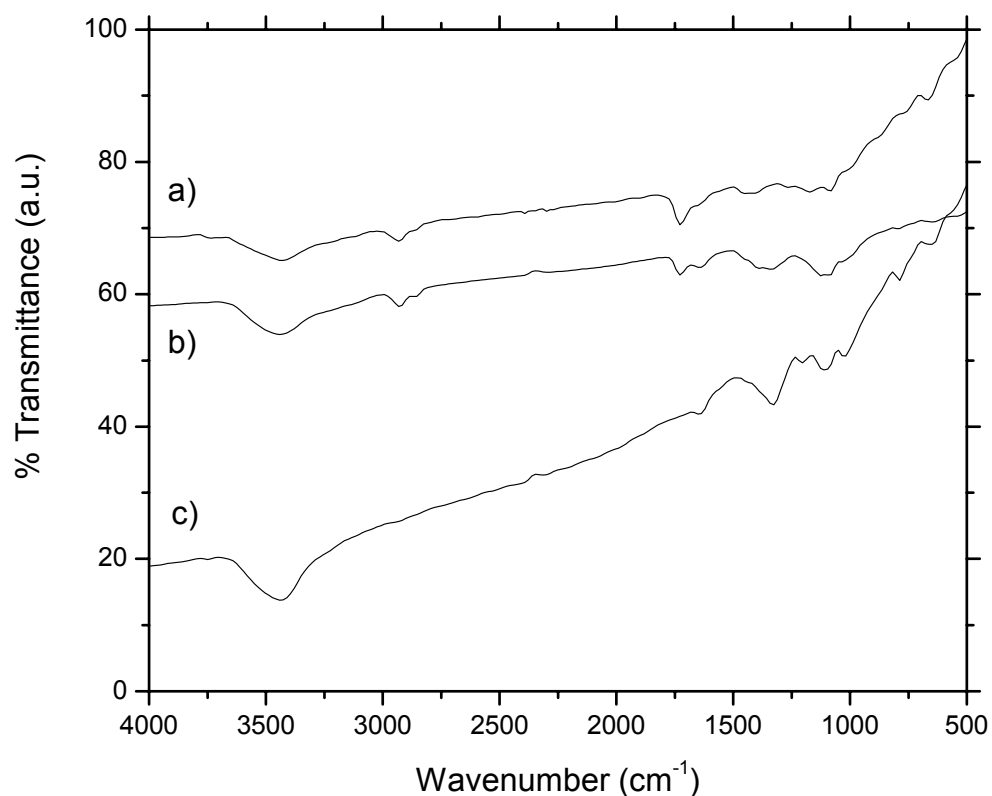


Figure 3.4 FTIR spectra of a) PHABTE b) P(HABTE-co-Th) c)PTh

3.1.4. Thermal Properties

DSC thermogram of HABTE showed a sharp melting point at 81.5 °C and onset of its decomposition was 291.9 °C. The thermogravimetry scan of the monomer showed single weight loss starting from 290 °C and reached its maximum at 384°C where the remaining residue was less than 0.6 % after 630 °C (Figure. 3.5). However, this behavior drastically altered in case of potentiostatically homopolymerized conducting polymer, where 44.2% of the polymer residue remained at the same temperature. In case of chemical polymerization (Figure. 3.6) both DSC and TGA studies revealed that homopolymer was stable up to 300°C and decomposition reached its maximum at around 368°C. However, TGA thermogram of the copolymer P(HABTE-co-Th), showed two weight losses at

232°C and 426°C leaving 36.74 % residue which is significantly different from pure PTh in terms of thermal behaviors (Figure A11).

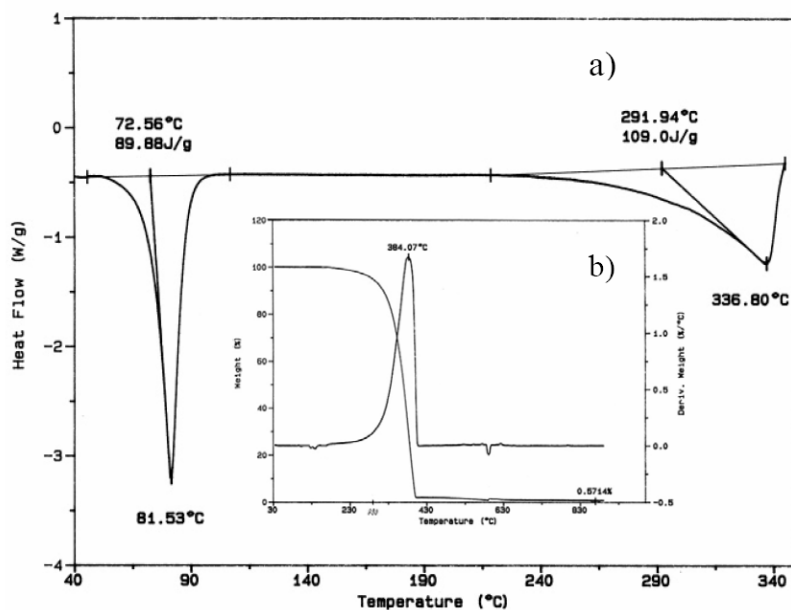


Figure 3.5 (a) DSC thermogram of HABTE (b) TGA thermogram of HABTE

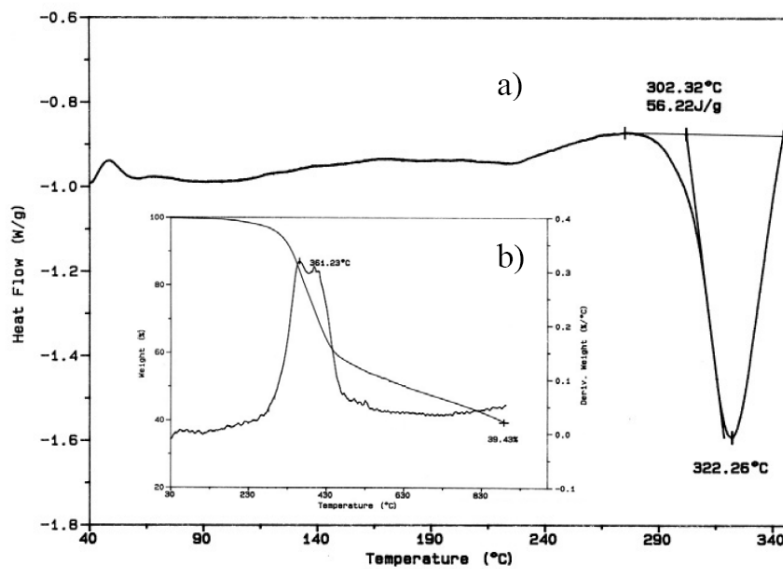


Figure 3.6 Chemically synthesized PHABTE (a) DSC thermogram (b) TGA thermogram

3.1.5. Morphologies of the Films

SEM micrographs of PHABTE imply that the synthesized monomer is good in film forming, exhibiting homogeneous and compact structure. The copolymer P(HABTE/Th) and P(HABTE-co-Th) reveal droplets on the surface which is different from the homopolymer and pure polythiophene cauliflower morphology (Figure. 3.7).

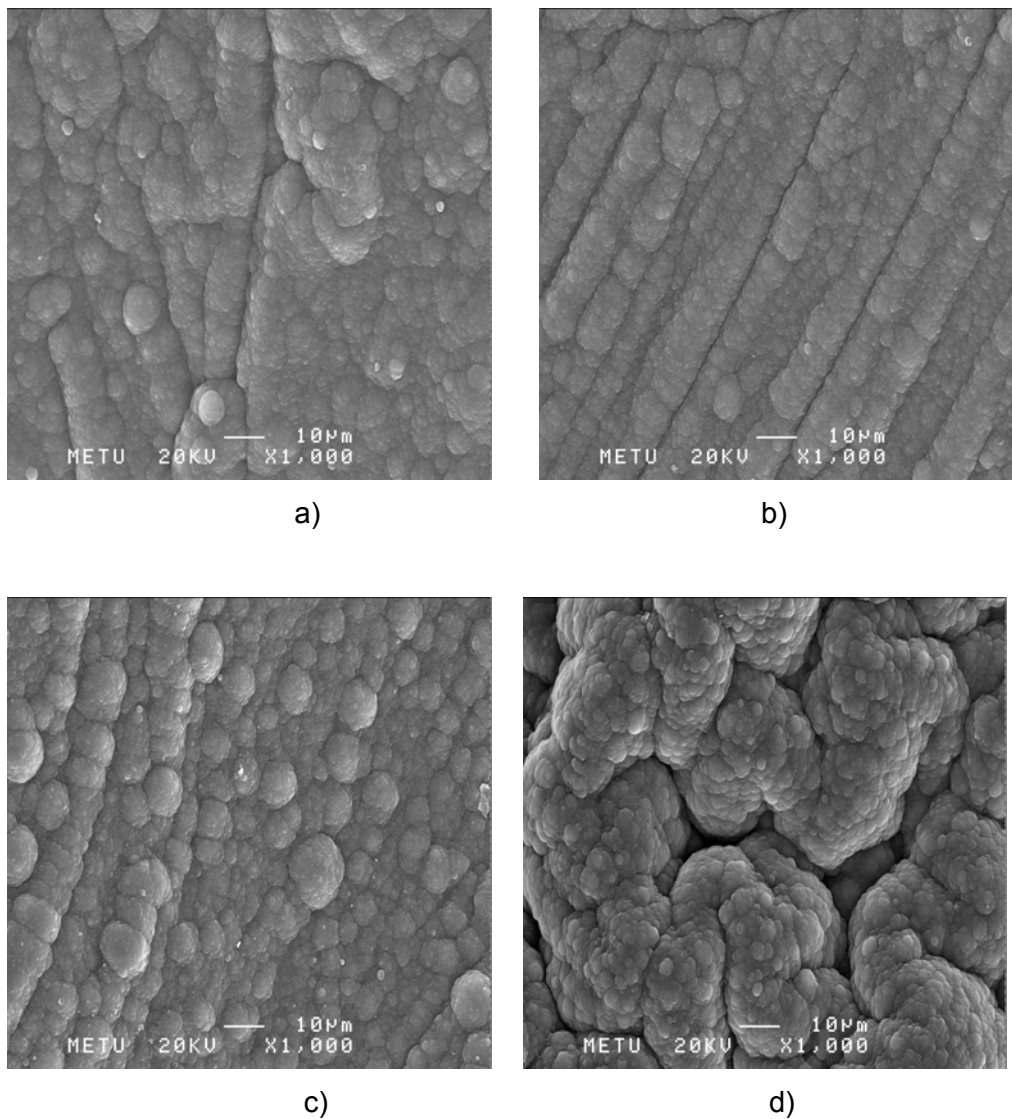


Figure 3.7 SEM micrographs of (a) PHABTE (b) P(HABTE/Th) c)P(HABTE-co-Th) d)PTh/BFEE

3.1.6. Conductivities of the Films

Although the conductivity of PHABTE is in the order of 10^{-4} S/cm, this value was enhanced by iodine doping up to 10^{-2} S/cm. I_2 doping seems to be a reasonable route to achieve higher conductivity. It is observed that the conductivity increased 100 and 1000 orders of magnitude upon copolymerization in the absence and presence of BFEE respectively. This could be related to the increase in degree of conjugation which is in accordance with the literature [33] (Table 3.1).

Table 3.1 Conductivities of the films (S/cm)

Polymer	Conductivity
PHABTE	3.2×10^{-4}
PHABTE - I_2 doped	2.3×10^{-2}
P(HABTE-co-Th)	1.7×10^{-1}
P(HABTE/Th)	9.1×10^{-2}

3.2. Conducting Polymers of OTE

3.2.1. Characterization of OTE

Octanoic acid 2-thiophen-3-yl-ethyl ester (OTE), was synthesized via condensation reaction of 3-thiophene ethanol and octanoyl chloride in the presence of triethylamine (TEA). Figure 3.8 represents the $^1\text{H-NMR}$ of the monomer in CDCl_3 . The chemical shifts were assigned as follows,

$^1\text{H-NMR}$ (CDCl_3)-OTE: (δ / ppm): 7.17 ppm (m, 11), 6.93 ppm (m, 10), 6.88 ppm (m, 12) and 2.88 ppm (t, 9), 4.19 ppm (t, 8), 2.20 ppm (t, 7), 1.53 ppm (m, 6), 1.23 ppm (shoulder, 2), 1.19 ppm (m, 5-3), 0.8 ppm (t, 1),

$^{13}\text{C-NMR}$ (CDCl_3)-OTE: (δ / ppm): 174.1 from CO, 138.4, 128.6, 125.9, 121.8 ppm (thiophene), 30.6 ppm (9), 64.4 ppm (8), 34.7 ppm (7), 25.4 ppm (6), 29.3 ppm (5,4), 32.0 ppm (3), 22.9 ppm (2), 14.4 ppm (1), 76 ppm (t, CDCl_3). $^{13}\text{C-NMR}$, FTIR of OTE is given in appendix Figure A3 and A4.

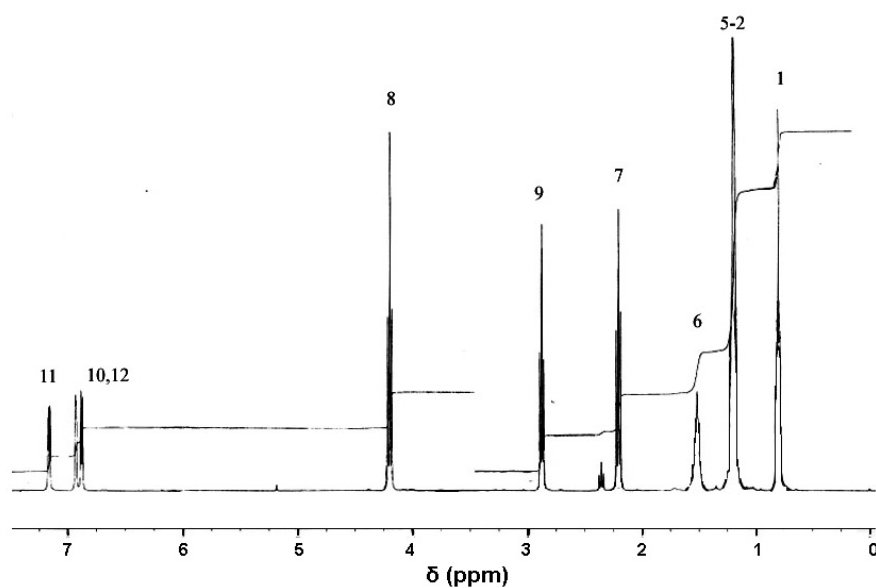


Figure 3.8 ¹H-NMR spectrum of OTE

3.2.2. Cyclic Voltammetry

Conducting polymers are an interesting class of materials that are able to exhibit very different properties depending on their redox state. Therefore, it is necessary to probe these states via cyclic voltammetry. With cyclic voltammetry electrochemical polymerization of a monomer, along with the accessibility of the redox sites of the polymer, can be investigated. For this purpose the electrochemical behavior of OTE, examined in TBAFB/ACN supporting electrolyte/solvent system where the potential was scanned between 0 and 2.5 V. As seen in Figure 3.9 a monomer revealed an irreversible oxidation peak at 2 V whose intensity decreases upon consecutive cycles along with the leakage of oligomers. Upon addition of BFEE to the same electrolytic system (in 4/1 ratio ACN/BFEE (v/v)), the oxidation potential of the monomer decreases and synthesis of homopolymer of OTE was achieved. POTE revealed an oxidation peak at 1.1 V and a reduction peak at 0.6 V (Figure 3.9 b). Upon consecutive cycles, there was a gradual increase in the current intensity, indicating the continuous film formation. Extended improvement was observed in case of using

pure BFEE during the CV studies. Monomer's oxidation potential was even more reduced, where the homopolymer could be synthesized via scanning of the potential between -0.2 to 1.2 V. The resultant polymer revealed a reversible redox behavior where the oxidation and reduction peaks appeared at 0.4 and 0.1V respectively. These signified the importance of use of BFEE, which provides the possibility to synthesize the homopolymers of high oxidation potential monomers.

It is known that, to ensure successful electrochemical copolymerization, both of the monomers used for the synthesis should oxidize and form their reactive radical cations in approximately the same potential range [99]. The electrochemical copolymerization behavior of OTE with MeTh was examined using the repeated potential scan method in 0.1M TBAFB ACN solution, to yield the electroactive copolymers. In comparison to CV of OTE in Figure 3.9a and MeTh in Figure 3.9d there was as an abrupt change in the voltammogram of the copolymer both in terms of oxidation and reduction potentials and the peak increments. This result is supported by the fact that MeTh and OTE are oxidized with in the same potential range and radical cations of both monomers would form at the working electrode surface where they can react with each other.

3.2.3. FTIR

The Fourier transform infrared (FTIR) spectrum of the monomer showed the usual features of ester functionalized thiophenes, revealing the peaks positioned at 3067 cm^{-1} (aromatic C-H), $2932\text{-}2900\text{ cm}^{-1}$ (aliphatic C-H stretching), 1748 cm^{-1} (C=O stretching), $1260\text{-}1000\text{ cm}^{-1}$ (C-O-C symmetric and asymmetric stretching), 788 cm^{-1} (thienylene out of plane C-H_α stretching), 840 cm^{-1} (thienylene out of plane C-H_β stretching), 1068 and 1050 cm^{-1} (in-plane C-H deformations), 1415 , 1347 cm^{-1} (aromatic C=C, C-C ring stretching), 612 cm^{-1} (C-S-C stretching). Homopolymerization of OTE was pursued by the variation in the several characteristic peaks of the monomer (Figure 3.10). Disappearance of the thienylene out-of-plane C-H_α stretching and in-plane C-H deformations, evolution of the new absorption peaks at 840 cm^{-1} (2,3,5-trisubstituted thiophene), at 1644 cm^{-1} (polyconjugation) and at 1081 cm^{-1} (dopant anion) was considered to be due to homopolymerization [100]. Moreover, unperturbed presence of the peaks due

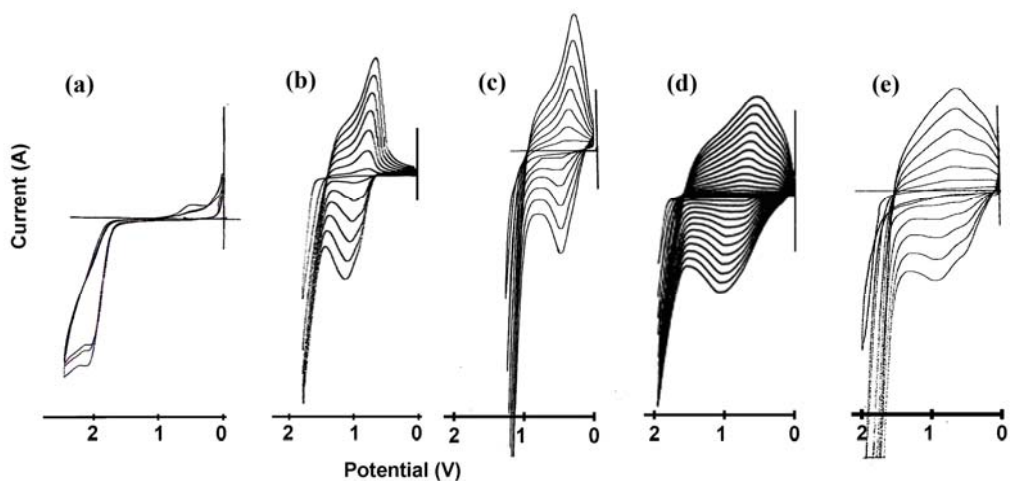


Figure 3.9 Cyclic voltammogram of (a) OTE in TBAFB/ACN and (b) OTE in TBAFB/ACN/BFEE (c) OTE in pure BFEE (d) OTE in the presence of 3-methyl thiophene and e) 3-methyl thiophene in TBAFB/ACN (Multi scans reveal the polymer chain growth)

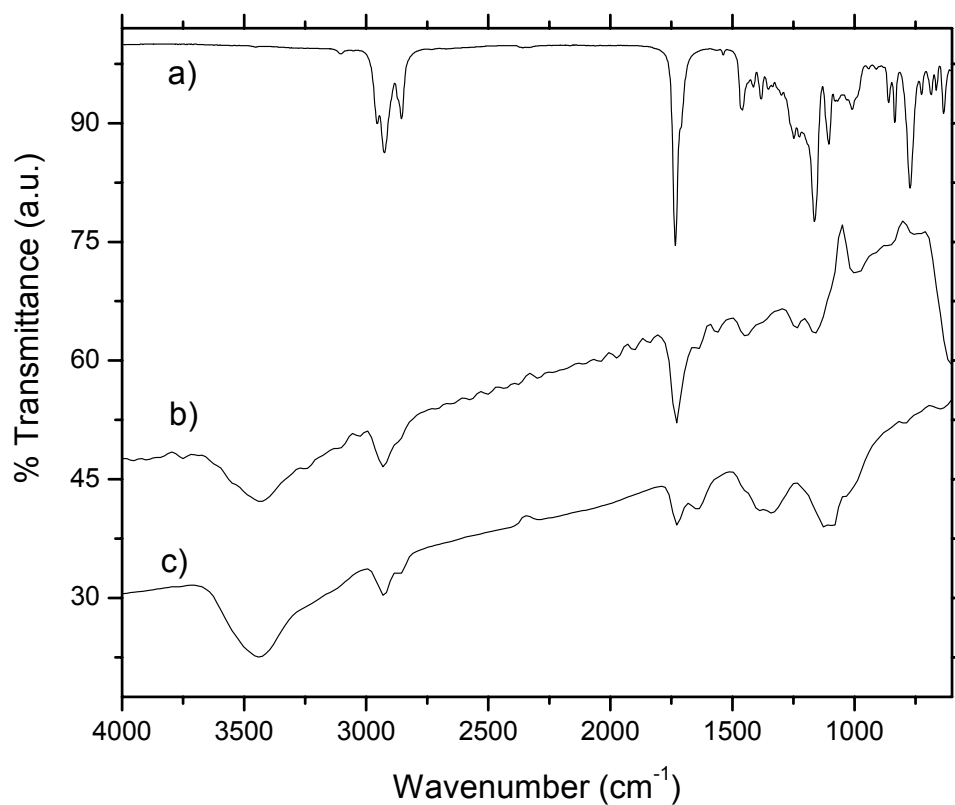


Figure 3.10 FTIR spectra of a) OTE b) POTE c) P(OTE-co-MeTh)

to C-H (aliphatic), C=O and C-O-C stretchings were observed. A similar type of spectrum was observed for the product obtained by oxidative polymerization of OTE. In this study, characteristic peaks of both poly(3-methyl thiophene) P(MeTh) and POTE were exploited as a proof of copolymer formation, especially the presence of the C=O stretching peak at 1750 cm^{-1} was quite indicative.

3.2.4. Thermal analysis

Both electrochemically and chemically synthesized homopolymer of OTE showed single-step decomposition at 415 and $425\text{ }^{\circ}\text{C}$, leaving 23.1 and 35.2% residue, respectively, regardless of the type of the dopant anion in the system. This type of behavior could be related with the low conductivity of the homopolymer. Since the degree of doping was too low, removal of the dopant anions from the matrix, leading to a significant weight loss, might not be observed. P(MeTh) showed a weight loss at around $230\text{ }^{\circ}\text{C}$ and started to decompose beyond $430\text{ }^{\circ}\text{C}$ until 24.6% of the initial material left at $800\text{ }^{\circ}\text{C}$. The thermogravimetry analysis of the copolymer P(OTE-co-MeTh) revealed two weight losses at 203 and $414\text{ }^{\circ}\text{C}$, which could be attributed to the removal of dopant anion from the matrix and decomposition of the polymer itself, respectively (Figure. 3.11a). Although both the P(MeTh) and P(OTE-co-MeTh) exhibited two-step decomposition, both the dopant removal and decomposition of the polymer matrix were very different from each other.

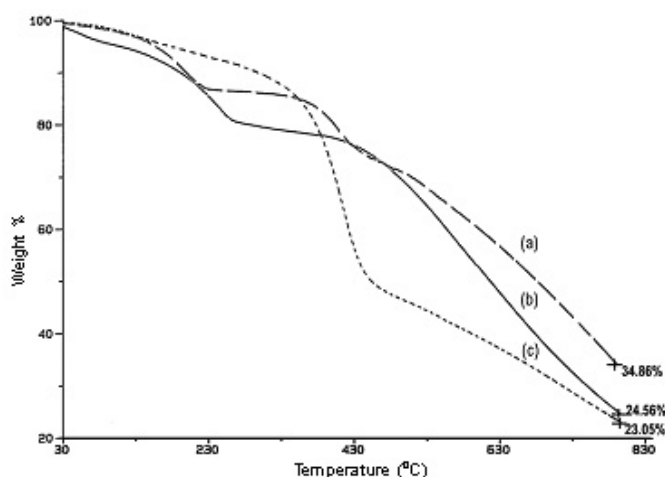


Figure 3.11 Thermogram of (a) P(OTE/MeTh), (b) P(MeTh) and (c) POTE

3.2.5. Morphology of the films

As seen in Figure. 3.12a the morphology of POTE presented a compact cauliflower-like structure, however, the copolymer was in globular form (Figure. 3.12b). Thus, besides other characterization techniques, SEM also reflected the formation of a copolymer, since the resulting morphology was both remarkably different from homopolymer and pure poly(3-methylthiophene).

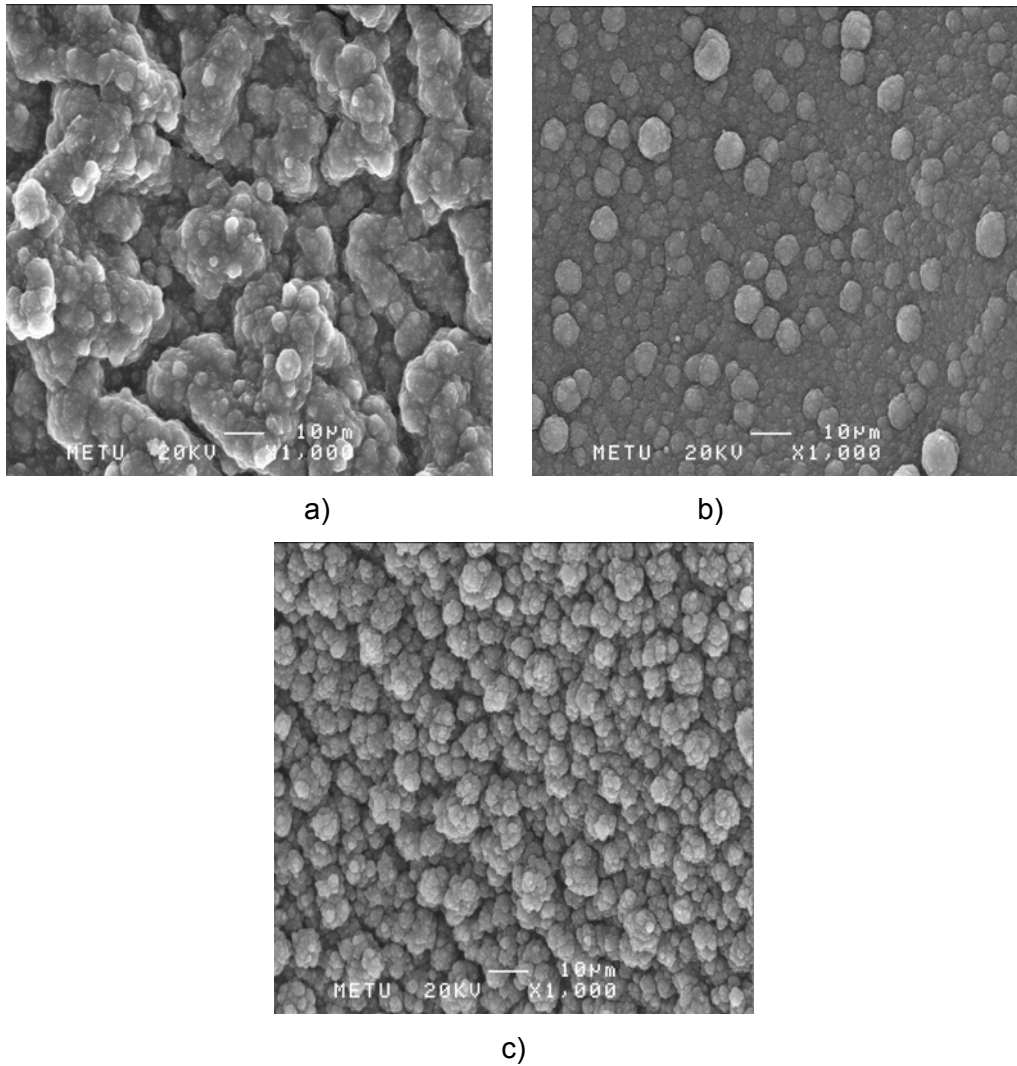


Figure 3.12 SEM images of (a) P(OTE), (b) P(OTE-co-MeTh) and (c)P(MeTh)

3.2.6. Conductivity Measurements

The conductivity of POTE and P(OTE-co-MeTh) was 3.2×10^{-4} and $9.1 \times 10^{-2} \text{ Scm}^{-1}$, respectively. Although the conductivity of the homopolymer was low, this value could be enhanced up to 10^{-2} Scm^{-1} via simple iodine doping or copolymerization, both being a reasonable approach to achieve a higher conductivity.

3.3. Conducting Polymers of DATE

3.3.1. Characterization of DATE

Decanedioic acid bis-(2-thiophen-3-yl-ethyl) ester (DATE), was synthesized via condensation reaction of 3-thiophene ethanol and octanoyl chloride in the presence of triethylamine (TEA). Figure 3.13 represents the $^1\text{H-NMR}$ of the monomer in CDCl_3 . The chemical shifts were assigned as follows,

$^1\text{H-NMR}$ (CDCl_3)-DATE ($\delta/\text{ ppm}$): 7.17 (2H, m, thiophene), 6.94 (2H, m, thiophene), 6.91 ppm (2H, m, thiophene) and 2.88 ppm (4H, t, thiophene- CH_2), 4.23 ppm (4H, t, $\text{CH}_2\text{-O}$), 2.23 ppm (4H, m, CO-CH_2), 1.55 ppm (4H, m, $-\text{CH}_2$), 1.20 ppm (8H, m, $-\text{CH}_2-$), 7.2 ppm (s, CDCl_3)

$^{13}\text{C-NMR}$ (CDCl_3) ($\delta/\text{ ppm}$) : 173.7 ppm from CO, 121.5, 125.6, 128, 138 from (thiophene), 34, 29, 24 ppm from aliphatic group, 64 ppm $-\text{OCH}_2$, 77 ppm (t, CDCl_3). $^{13}\text{C-NMR}$, FTIR of DATE is given in appendix Figure A5 and 6.

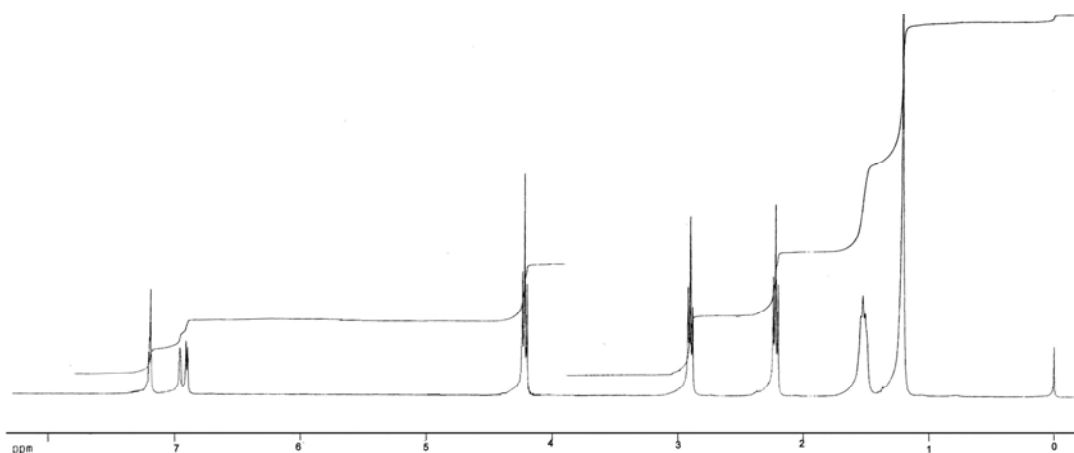


Figure 3.13 $^1\text{H-NMR}$ of DATE

3.3.2. Cyclic Voltammetry

The oxidation/reduction behavior of the DATE through homopolymerization and copolymerization in the presence of thiophene was investigated via cyclic voltammetry. CV experiments were carried out in ACN /TBAFB solvent-electrolyte couple under nitrogen atmosphere. As it was the case for the other 3-ester substituted thiophenes, DATE also revealed an irreversible oxidation peak at 2 V. Continuous electroactivity was achieved via addition of BFEE to the system. As seen in Figure. 3.14 a, P(DATE) revealed an oxidation at 0.83V and a reduction peak at 0.63V. Upon consecutive cycles there was a continuous film formation, indicated by the continuous increase of the current intensity. In the presence of thiophene within the same electrolyte system, it was observed that the oxidation and reduction potentials were shifted to 0.91 V and 0.53V, respectively (Figure. 3.14 b). When CV of P(DATE-co-Th) is compared with the voltammogram of pristine thiophene and P(DATE), the redox peaks are different. (pure PTh- $E_{p,a}$: +0.98 V, $E_{p,c}$: +0.70). This shift could be considered as an indirect indication for the reaction between thiophene and the thiophene moiety of the monomer, resulting copolymer formation.

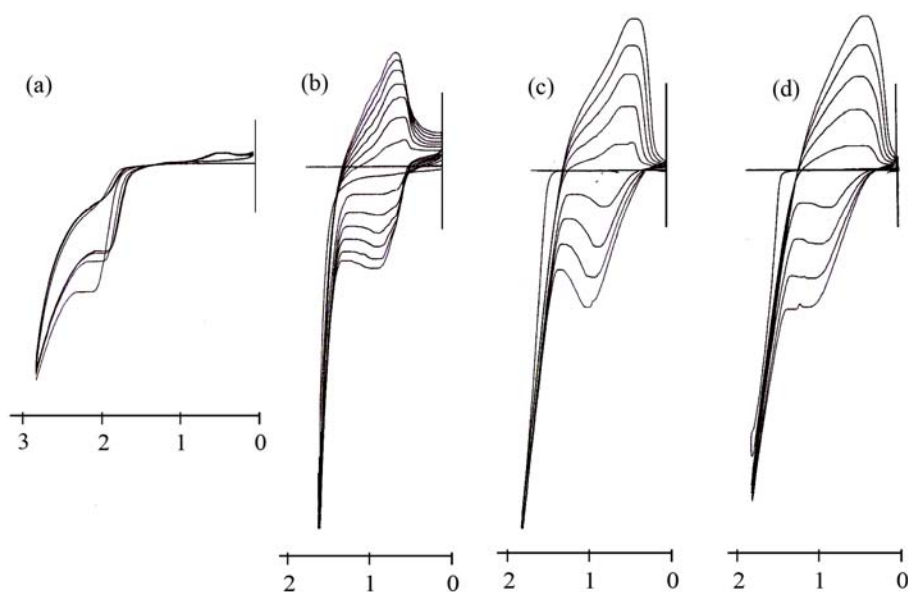


Figure 3.14 Cyclic Voltammogram of (a) DATE in 0.1M TBAFB in ACN (b)P(DATE) (c)P(DATE-co-Th) (d) PTh in 0.1M TBAFB in BFEE / ACN

3.3.3. FTIR Spectra

The identification of DATE was carried out by FT-IR spectroscopy. Figure. 3.15a shows the FT-IR spectrum of the DATE product in the range 4000-400 cm^{-1} . The absorption bands at 1544, 1408, 1053, 855, 789 and 688 cm^{-1} were due to the vibrations of C-H and C=C bonds of thiophene rings (Figure. 3.15 a). The sharp intense peak at 1731 cm^{-1} was attributed to C=O stretching vibrations and the bands in the region of 1100-1250 cm^{-1} was due to C-O-C symmetric and asymmetric stretching vibrations of spacing methyl chain [100].

After the potentiostatic homopolymerization of DATE, a new shoulder appeared at 1637 cm^{-1} indicating the polyconjugation upon polymerization. The band at 796 cm^{-1} indicating cis C-H wagging of the thiophene ring and the band at 686 cm^{-1} due to deformations of C-H out of plane of the thiophene ring disappeared completely upon polymerization. Also, evolution of new peak at 824 cm^{-1} indicated the formation of 2,3,5-trisubstituted thiophene structure. The peak appeared at 1083 cm^{-1} revealed the presence of the dopant ion (BF_4^-), due to homopolymerization. All of the above could be considered as an evidence of the polymerization at thiophene ring.

FTIR spectra of electrochemically synthesized copolymer of P(DATE-co-Th), Figure. 3.15 b shows a band at 1732 cm^{-1} indicating of carbonyl group due to monomer. The peaks indicating the polyconjugation were observed very clearly at 1672 cm^{-1} . FTIR spectra of P(DATE-co-Th) also contained the characteristic monomer peaks. The intense band at 1083 cm^{-1} was related to the dopant anion (Figure A.10). All of these peaks were a proof of copolymerization.

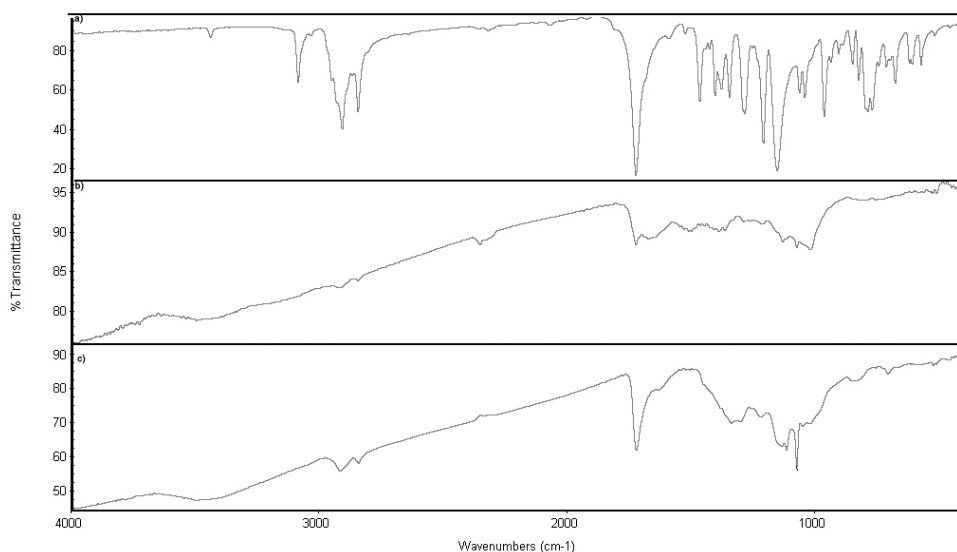


Figure 3.15 FTIR spectra of (a) DATE (b) P(DATE-co-Th) (c)P(DATE)

3.3.4. Thermal Behavior of Samples

DSC thermogram was obtained under nitrogen atmosphere, in the range of 25^oC to 450^oC at a heating rate of 10^oC/min. DSC thermogram of DATE showed a sharp melting point at 74^oC and it was stable up to 269^oC. According to TGA studies the onset point of the decomposition was 266^oC and it reached its maximum at 376 ^oC. Only 2.286 % of the monomer remained after 830 ^oC (Figure. 3.16 a). Thus, results of DSC and TGA are consistent with each other.

The TGA curve of homopolymer revealed two transitions at 232 ^oC and 433 ^oC (Figure. 5(c)). The former weight loss could be attributed to the removal of the solvent, later could be due to decomposition of the polymer matrix. The char residue of P(DATE) was 42.11% after 830 ^oC. TGA thermogram of P(DATE-co-Th) (Figure 3.16 b) revealed different behavior than both homopolymers of DATE and Th. Thus, besides the other techniques used, TGA also reflected the copolymer formation.

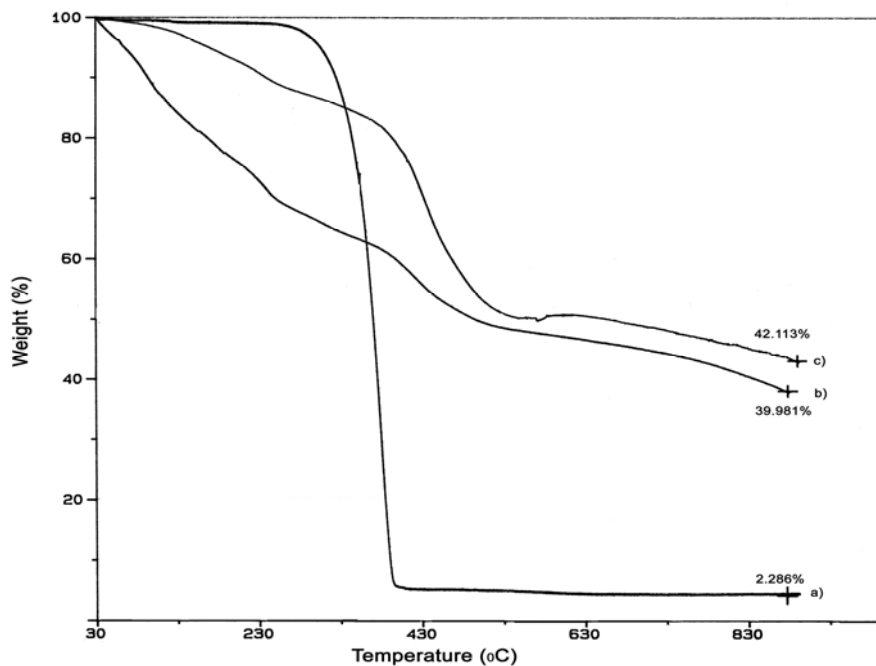


Figure 3.16 TGA thermogram (a) DATE (b) P(DATE-co-Th) (c)P(DATE)

3.3.5. Conductivity Measurements

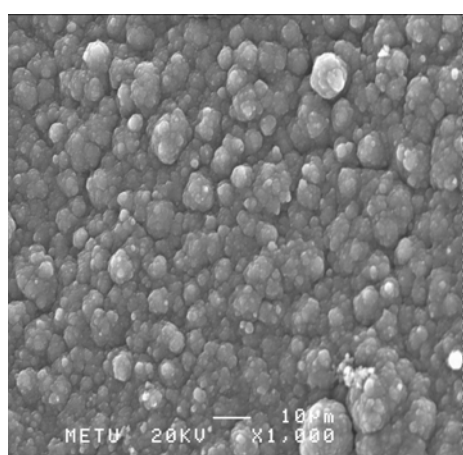
Standard four-probe technique was used to find out the conductivities of homopolymer and copolymer. Conductivities of the films, both solution and electrode sides, were measured and given in Table 3.2. Conductivity values of electrode and solution sides were found to be in the same order of magnitude in both homo and copolymer. This observation revealed the homogeneity of the films. In the view of conductivity data reported for PTh, we may conclude that a new product was obtained in a small expense of electrical conductivity.

Table 3.2. Conductivities of DATE Polymers (S/cm)

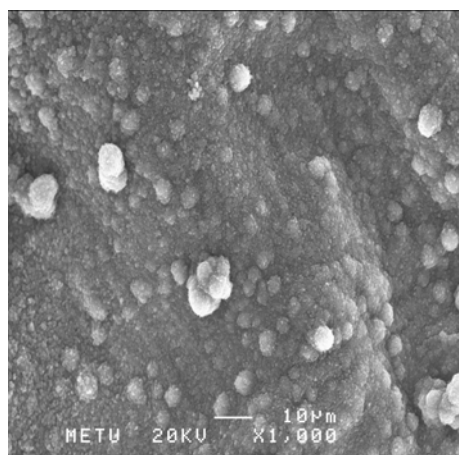
Polymer	Conductivity
P(DATE)	1.2×10^{-3}
P(DATE-co-Th)	8×10^{-2}
PTh	5

3.3.6. Morphologies of the films

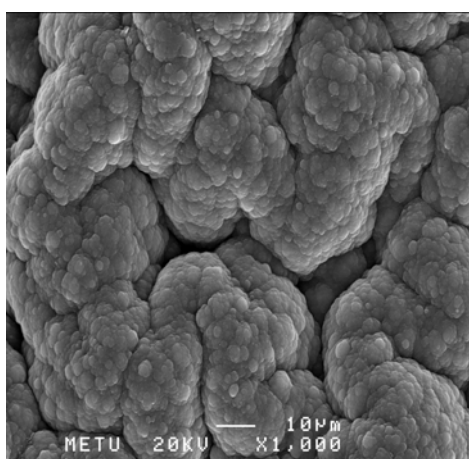
Analysis of the surface morphologies of films was done by using Scanning Electron Microscope. SEM micrograph of solution side of P(DATE) film showed uniform globular structure (Figure. 3.17 a). P(DATE-co-Th) revealed droplet like structure (Figure. 3.17 b) which was significantly different from both P(DATE) and PTh, all of which were deposited under the same experimental conditions. The abrupt change in the morphology could be due to incorporation of monomer units in to polythiophene matrices, revealing the existence of an interaction between monomer and polythiophene. This could be considered as another proof of copolymerization.



(a)



(b)



(c)

Figure 3.17 SEM micrographs of (a) P(DATE) (b) P(DATE-co-Th) (c)PTh

3.4. Electrochromic Properties of Polymers

The change in optical properties that accompany the redox switching of conjugated polymers can be examined through spectroelectrochemistry. Spectroelectrochemistry is important in understanding the electronic structure of conducting polymers and examining the optical changes upon doping. It provides information about the material's band gap and intraband states created upon doping. Also it gives some insight into a polymer color through the location of the absorption maxima and intensity of the peak on the main π - π^* transition. For this purpose in this part of the thesis spectroelectrochemical investigation of the synthesized polymers were performed.

3.4.1. Electrochromic Properties of Polymers of HABTE

In order to investigate the spectroelectrochemistry of the PHABTE, the polymer film was deposited on ITO via potentiostatic electrochemical polymerization of HABTE (0.01 M) in the presence of BFEE and TBAFB in ACN at 1.5V. PHABTE coated ITO was investigated by UV-Vis spectroscopy in the same but monomer free electrolytic system by switching between +1.0 V and -1.0 V with incremental increase in applied potential. Figure 3.18 shows the spectroelectrochemistry of PHABTE, monitored while the polymer was sequentially stepped between its fully oxidized and reduced forms. The electronic band gap, defined as the onset energy for the π - π^* transition, was found to be 1.92 eV and λ_{\max} was 385nm. Upon applied voltage, reduction in the intensity of the π - π^* transitions along with evolution of new bands located at 550 nm and 900 nm was observed. These transitions were attributed to polaron and bipolaron charge carrier band formation respectively, which are found to be in accordance with the expected transitions in a conjugated polymer as described by Fesser et al. (FBC Theory, [78] schematic representation is given in Figure 1.18).

In order to successively prove the formation of polaron and bipolarons during oxidation of the polymer, ESR studies were performed. For this purpose PHABTE was deposited on to the working electrode of the ESR cell and its redox behavior was investigated by CV in the same cell while scanning the potential between -1

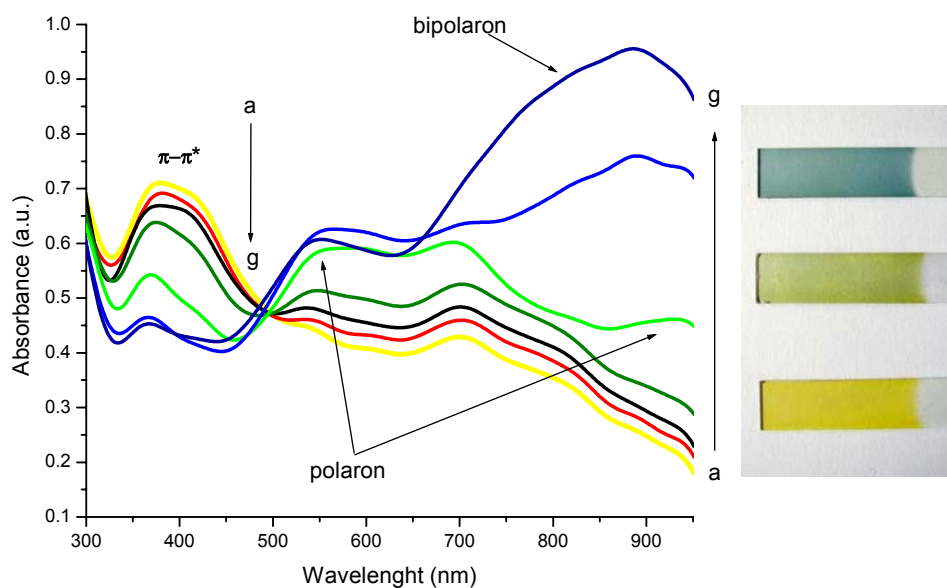


Figure 3.18 Optoelectrochemical spectrum of PHABTE as at applied potentials between -1.0 and +1.0 V in 0.1 M TBAFB/ACN in the presence of BFEE: (a) -1.0 V, (b) -0.4 V, (c) 0.0 V, (d) +0.2 V, (e) +0.4 V, (f) +0.6 V, (g) +1.0 V

and 2.5 V. Figure 3.19 reflects the ESR experiments of PHABTE, where the study was performed in situ in an electrochemical cell, while stepping the applied potential. In the neutral form (-1.2 V) the material did not reveal any significant ESR signal. Upon increase in applied potential, there was the formation of a well defined signal whose intensity increased along with the increase in potential and reached a maximum at 2.5 V. This behavior was found to be reversible, the signal did not seem to appear as a result of accidental defects, they were clearly connected to doping process. The signals were consistent with the widely described picture of polaron ($\text{spin} = \frac{1}{2}$). Starting from 3 V on, there was a gradual decline in the intensity with increasing duration of oxidation, which was associated with formation of bipolarons ($\text{spin}=0$) due to recombination of polarons. Thus, ESR and optical data seem to support the evidence of the formation of polarons and bipolarons.

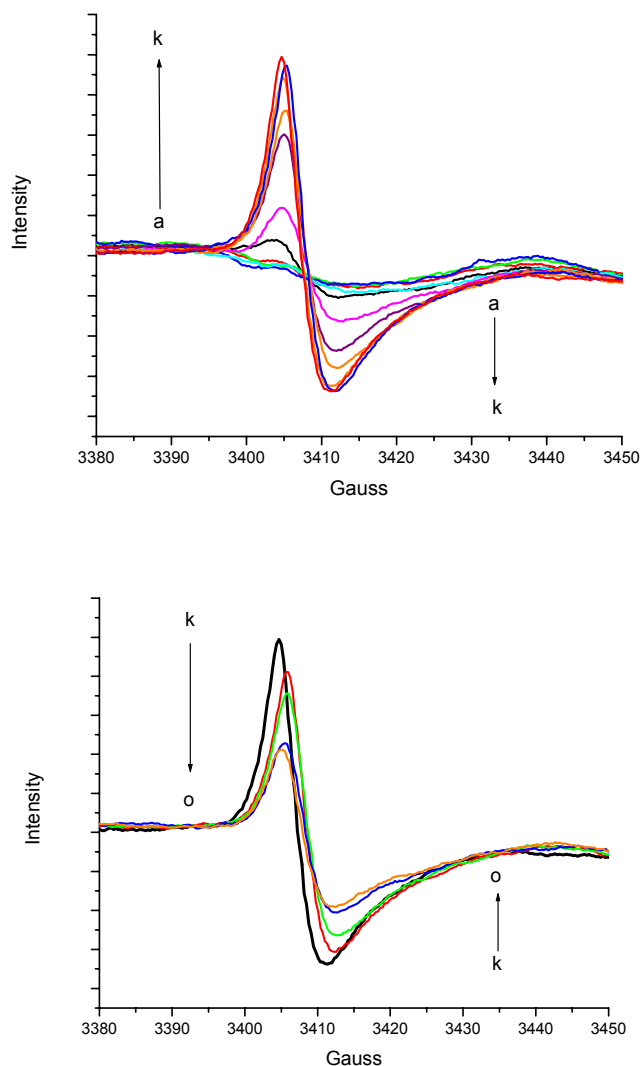


Figure 3.19 The ESR spectrum of PHABTE at a)-1.2, b)-1.0, c)-0.6, d)0.2, e)0.7, f) 1.0, g)1.3, h)1.5, i)2.0, j)2.3, k) 2.5 V (3 min) and at 3V with duration of l) 3, m) 12, n) 20, o)30 min

In order to investigate the spectroelectrochemical behavior of the copolymer of HABTE with Th, films were deposited onto ITO-coated glass slides in TBAFB/ACN/BFEE potentiostatically at 1.5 V. Spectroelectrochemical properties were studied in the same but monomer free solution. The λ_{\max} value for the π - π^* transitions in the neutral state of copolymer was found to be 470 nm, revealing orange color which is significantly different than pure polythiophene (λ_{\max} =497 nm,

red, given in appendix Figure A7) and PHABTE. The electronic band gap defined as the onset energy for the π - π^* transition was found to be 1.85 eV. Upon increase in the applied voltage, the evolution of a new absorption band at 800 nm was observed due to evolution of charge carriers, polarons (Figure 3.20), which was accompanied by gradual decrease in the intensity of the bands at λ_{max} . At this mid-stage copolymer displayed dark green color. At 1.0 V, the extreme oxidation was achieved, where the color of the copolymer was blue with an intensified absorption beyond 900 nm.

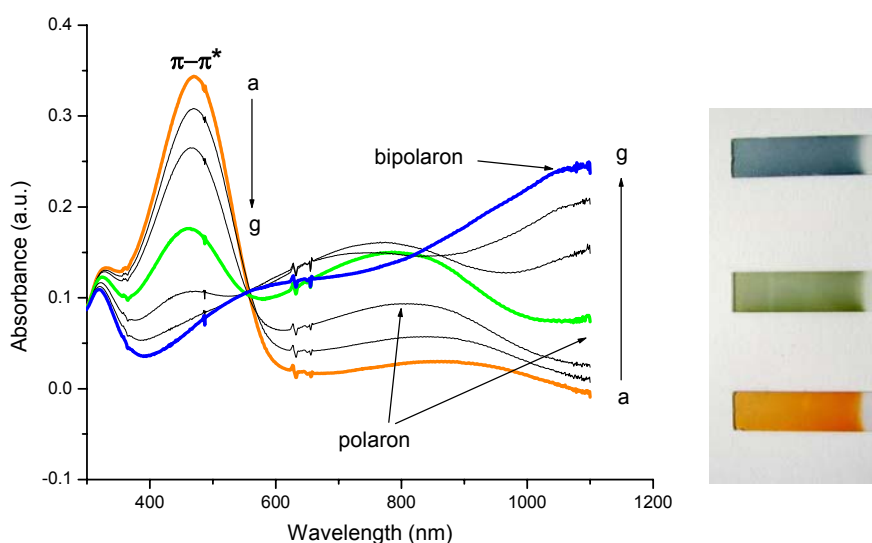


Figure 3.20 Optoelectrochemical spectrum of P(HABTE-co-Th) as at applied potentials between 0.4 and +1.0 V in 0.1 M TBAFB/ACN in the presence of BFEE: (a) 0.4 V, (b) 0.5 V, (c) 0.6 V, (d) 0.7 V, (e) 0.8 V, (f) +0.9 V, (g) +1.0 V

For electrochromic applications, the ability of a polymer to switch reversibly and rapidly between its extreme states, while exhibiting striking color change is of importance. Electrochromic switching studies can monitor these types of properties via kinetic experiments, allowing the measurement of switching time and percent transmittance of the polymer between the two extreme redox states. For this purpose a square wave potential step method coupled with optical spectroscopy known as chronoabsorptometry was applied. In this double potential

step experiment, the potential was set at an initial potential for a set period of time, and was stepped to a second potential for a set period of time (5 sec.), before being switched back to the initial potential again. Kinetic studies were proceeded within the light of spectroelectrochemistry, since it involves the information about the potentials to be applied for a full switch and wavelength of maximum contrast.

As seen in Figure 3.18, PHABTE displayed a full oxidation and neutralization at 1.0 V and -1.0 V respectively, where the λ_{\max} of π - π^* was located at 385 nm. According to these results, a potential square-wave experiment was performed as given in Figure 3.21a, where the variation in percent transmittance was monitored simultaneously by UV-Vis spectrophotometer at λ_{\max} . The optical contrast is measured as the difference between %T in the neutral and oxidized forms and noted as 26 %T. As seen in Figure 3.21b, homopolymer has good stability with a switching time of 1.5 s.

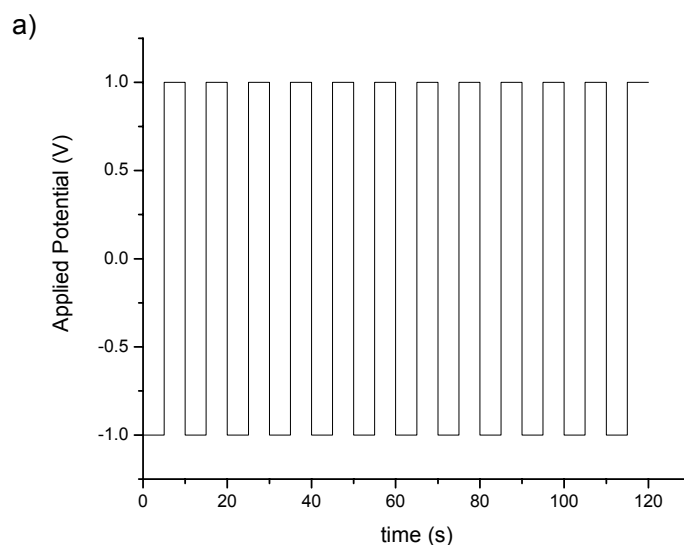


Figure 3.21 Electrochromic switching, a) applied potential for PHABTE in TBAFB/BFEE/ACN

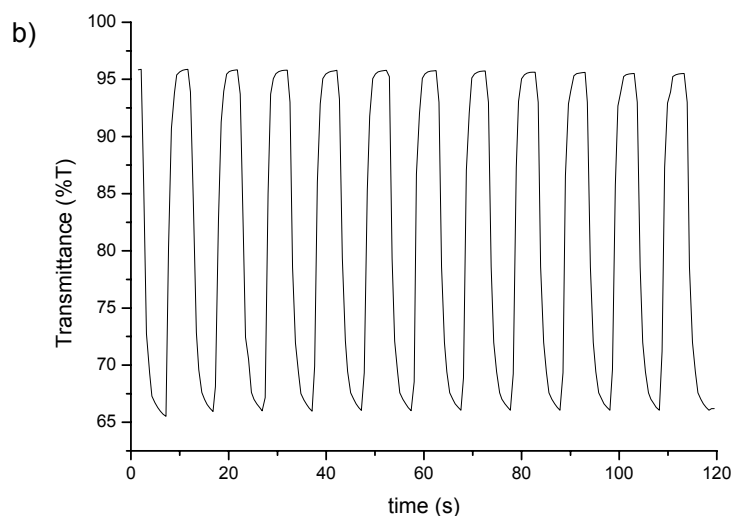


Figure 3.21 Electrochromic switching, b) optical absorbance change monitored at 385 nm for PHABTE in TBAFB/BFEE/ACN

The switching time of the copolymer was determined by monitoring the % T change at 470 nm through switching of the applied potential in a square wave form between 0.4 V and 1.0 V with a residence time of 5 s. Applied potentials, which correspond to the extreme states of the polymer were in accordance with the spectroelectrochemistry study. The optical contrast was measured as the difference between %T in the neutral and oxidized forms and noted as 24 %. Copolymer has good stability with 1.2 s of switching time (Figure 3.22).

Colorimetry is used to make the measurement of color in an objective and quantitative practice, which can allow for matching of colors in electrochromic devices. Color is made up of three attributes; hue, saturation, and luminance, and color systems such as the often-used CIE system are used as a quantitative scale to define and compare colors. Colorimetry measurements were performed in the same electrolyte system by using the Coloreye XTH Spectrophotometer. The relative luminance (L) and the a,b values (Table 3.3) were measured at the fully oxidized and reduced states.

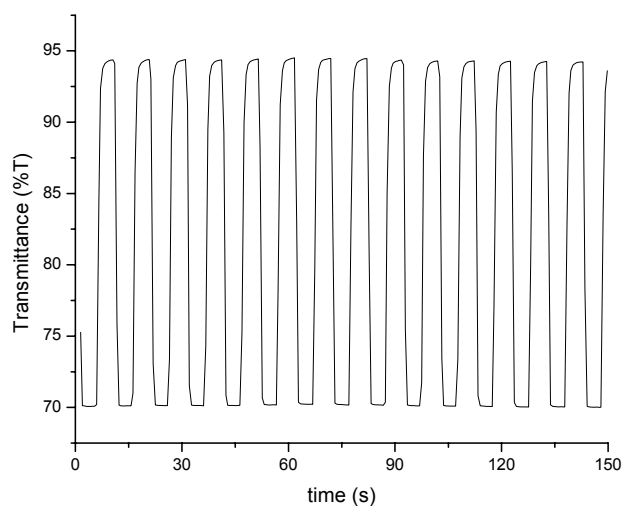


Figure 3.22 Electrochromic switching, optical absorbance change monitored at 470 nm for P(HABTE-co-Th) in TBAFB/BFEE/ACN

Table 3.3 Electrochromic Properties of HABTE Polymers

<i>Material</i>	$E_{p,a}$	$E_{p,c}$	λ_{max} (nm)	<i>Color</i> (Ox)	<i>Color</i> (Red)	<i>L</i>	<i>a</i>	<i>b</i>
PHABTE	0.75	-0.1	385	Blue	Yellow	(ox) 48	-4	-4
						(red) 68	-3	20
P(HABTE-co-Th)	1.04	0.71	470	Blue	Orange	(ox) 36	-15	-9
						(red) 63	25	69
PTh	1.14	0.85	495	Blue	Red	(ox) 47	-7	-2
						(red) 51	52	46

(ox) oxidized state, (red) reduced state

3.4.2. Electrochromic Properties of POTE

Neutral POTE exhibited an electronic band gap of approximately 1.96 eV and showed one well-defined peak at 434 nm in the visible region, causing the film to appear in brownish yellow (Figure 3.23). Upon stepwise increase in the applied potential, evolution of polaron charge carriers signaturred by the peaks at around 800 nm was observed, while the intensity of the $\pi-\pi^*$ transition decreased. Upon further oxidation, appearance of absorptions at longer wavelengths (> 1000 nm) was observed, due to formation of bipolaron charge carriers [101].

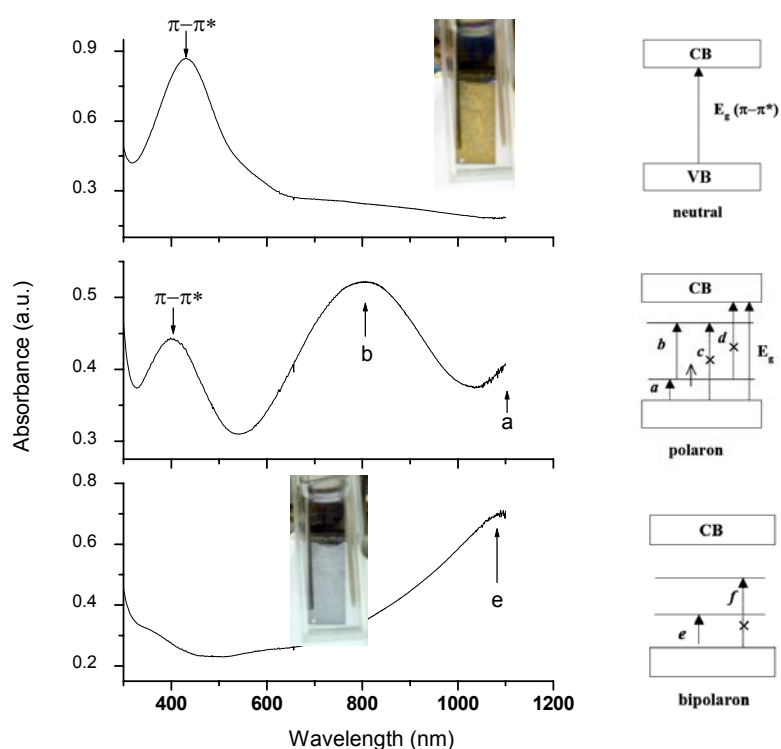


Figure 3.23 Optoelectrochemical spectrum of POTE at applied potentials between 0.4 ,0.7 and 1.2 V (from top to bottom) in 0.1 M TBAFB/ACN in the presence of BFEE

The electrochromic switching study of a polymer film of OTE was performed at a fixed wavelength (434 nm), switching between fully oxidized and reduced states by repeated potential steps and the transmittance, was followed as a function of

time (Figure 3.24). The results showed that the time required to reach 90 % of ultimate transmittance was less than 1 s.

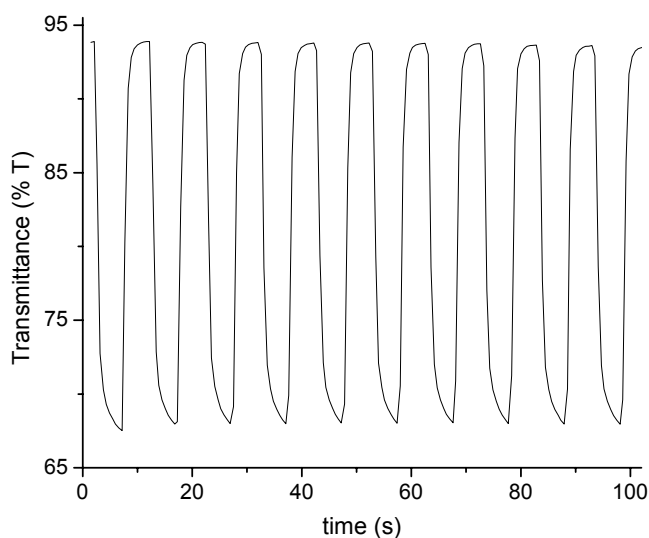


Figure 3.24 Electrochromic switching: Optical absorbance change monitored at 434 nm for POTE in TBAFB/ BFEE / ACN

Table 3.4 Electrochemical, Electronic, and Electrochromic Properties of POTE,

Material	$E_{p,a}$ [a]	$E_{p,c}$ [a]	λ_{max} (nm)	E_g (eV)	Color (Ox)	Color (Red)	L	a	b
POTE	1.1	0.6	434	1.96	Blue	Brownish Yellow	69 [c] 44 [b]	-4 -6	24 -2

E_{pa} = anodic potential E_{pc} = cathodic potential E_g = band gap, λ_{max} = maximum absorption wavelength, [a] Volts vs Ag/Ag⁺, [b] (ox) oxidized state, [c] (red) reduced state

3.4.3. Electrochromic Properties of Polymers of DATE

Figure. 3.25 and Figure. 3.26 show series of optoelectrochemical spectra of P(DATE) and P(DATE-co-Th) respectively. The observed band gap was found to be 2.87 eV and 2.06 eV and λ_{max} were 432 nm and 475 nm for P(DATE) and P(DATE-co-Th) respectively. Stepwise oxidation of polymers showed reduction in absorbance throughout the visible region as the color changes. Upon applied potential, reduction in the intensity of π - π^* transitions and formation of charge carrier band was observed. The absorptions observed at 734 nm and 768 nm were attributed to formation of polarons, absorptions at 1000 nm and 950 nm were attributed to bipolarons of P(DATE) and P(DATE-co-Th) respectively. Polymers change color between yellow (fully reduced state), green (mid stage) and blue (highly oxidized state) with the listed chromaticity values in Table 3.5.

Table 3.5 Electrochromic Properties of Conducting Polymers of DATE

<i>Material</i>	$E_{p,a}$	$E_{p,c}$	λ_{max} (nm)	<i>Color</i> (Ox)	<i>Color</i> (Red)	<i>L</i>	<i>a</i>	<i>b</i>
PDATE	0.75	0.5	432	Blue	Yellow	ox : 68 red: 61	-7 -4	-1 21
P(DATE-co-Th)	0.85	0.35	475	Blue	Orange	ox : 23 red: 48	-5 28	1 47
PTh	1.1	0.5	495	Blue	Red	ox : 57 red: 51	-7 52	-2 46

(ox) oxidized state, (red) reduced state

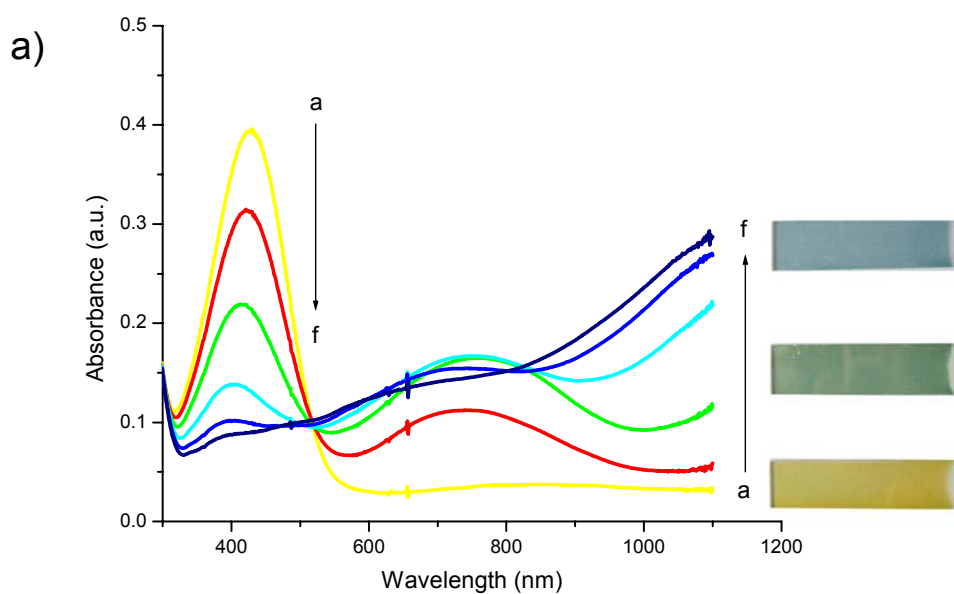


Figure 3.25 Optoelectrochemical spectrum of P(DATE) at applied potentials between 0.5 and +1.0 V in 0.1 M TBAFB/ACN in the presence of BFEE: (a) 0.5 V, (b) 0.6 V, (c) 0.7 V, (d) 0.8 V, (e) 0.9 V, (f) +1.0 V

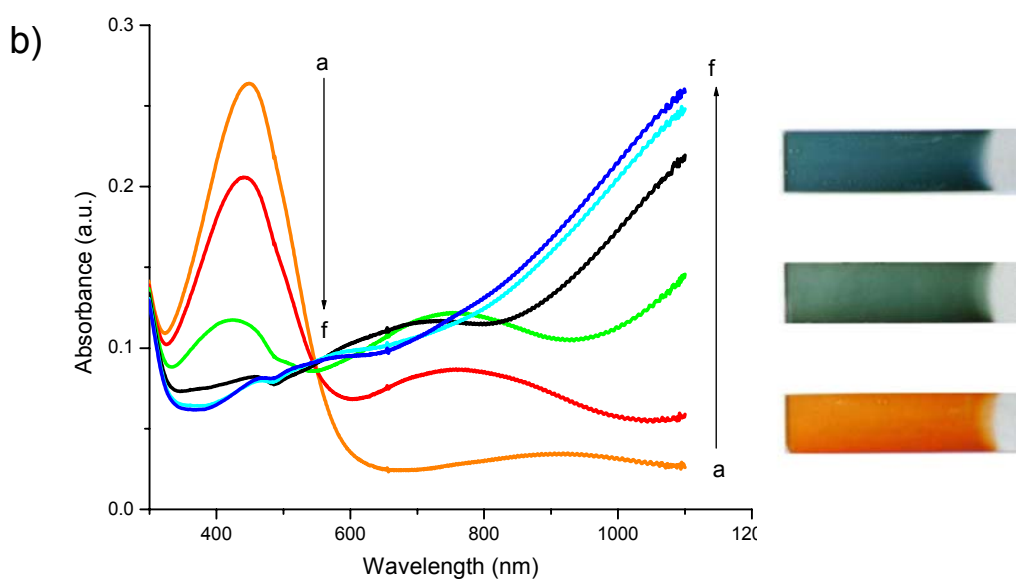


Figure 3.26 Optoelectrochemical spectrum of P(DATE-co-Th) at applied potentials between 0.4 and +1.0V in 0.1 M TBAFB/ACN in the presence of BFEE: (a) 0.4 V, (b) 0.6 V, (c) 0.8 V, (d) 1.0 V, (e) 1.2 V, (f) +1.4 V

Electrochromic switching behaviors of the films were investigated by recording absorption spectrum while stepping the potential between 0.5 V-1.0 V for P(DATE) and 0.4V-1.4V for P(DATE-co-Th) for a switching time of 5 seconds. The optical contrast of P(DATE) was measured as 18 % at 432 nm wavelength. Switching time was measured as 1.3 s. In case of P(DATE-co-Th) the contrast measured was 44.3 % and the switching time was 0.9 s at 476 nm wavelength (Figure. 3.27). Upon 1000 cycles there was only 3.5 % loss in optical contrast. Results implied the superior properties of the copolymer over homopolymer on the basis of both stability and switching times. Thus, utilization of copolymerization during the synthesis of electrochromic material could be considered as a powerful approach to achieve desired properties.

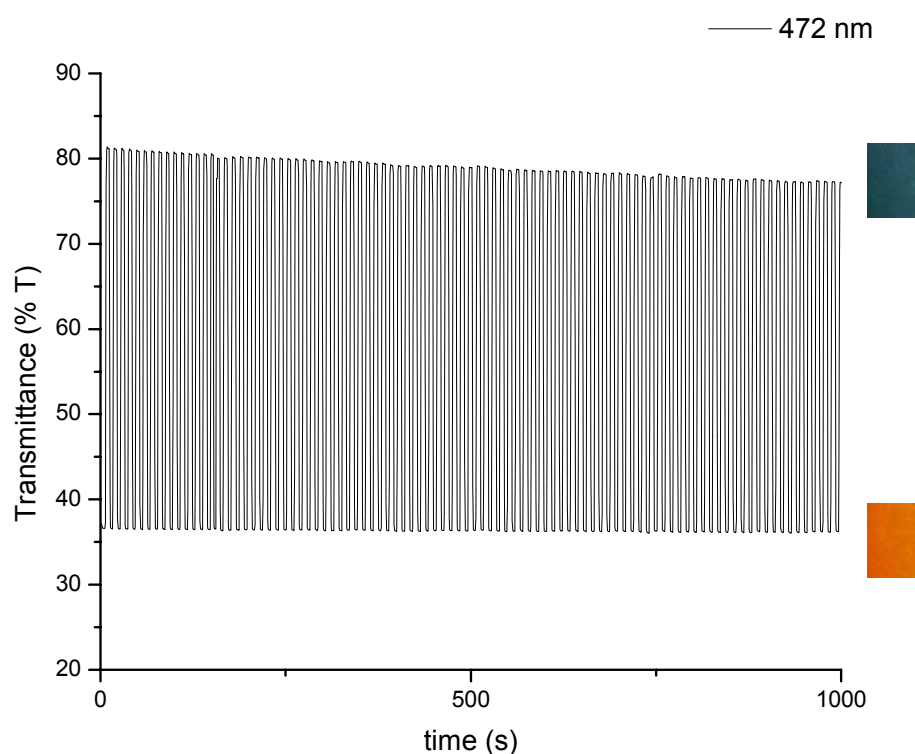


Figure 3.27 Electrochromic switching of P(DATE-co-Th)

3.5. Fine Tuning of Color

There are various strategies to tune the color of the material. Controlling the band gap of the polymer via substitution, blending, copolymerization and lamination are the techniques that are applied to achieve desired properties. The aim of the work presented in this part of the thesis is to control the color change observed in an electrochromic material in a predictable and reproducible manner via copolymerization and lamination.

3.5.1. Copolymerization

Copolymerization is an easy, facile method to combine the electrochromic properties of the comonomers. [102] Copolymerization of distinct monomers, can lead to an interesting combination of the properties observed in the corresponding homopolymers.[71] In order to investigate such properties and tune the color of the conducting polymers we performed constant potential electrolysis at 1.5 V with various feed ratio of comonomers

Figure 3.28 depicts the UV-Vis studies of the copolymers synthesized with various stock ratios in 0.1 M TBAFB/ACN in the presence of BFEE at 1.5 V. Spectral studies were performed in the same but monomer free electrolytic media, where before each measurement each polymer was reduced to its neutral state via application of -0.5 V. The colors of these polymers could also be seen in Figure 3.29. The homopolymer of DATE and Th reveal maximum absorption at 437 and 498 nm respectively. As the content of Th with in the stock solution increases, λ_{\max} of the resulting polymers increases progressively, along with the variation of the color.

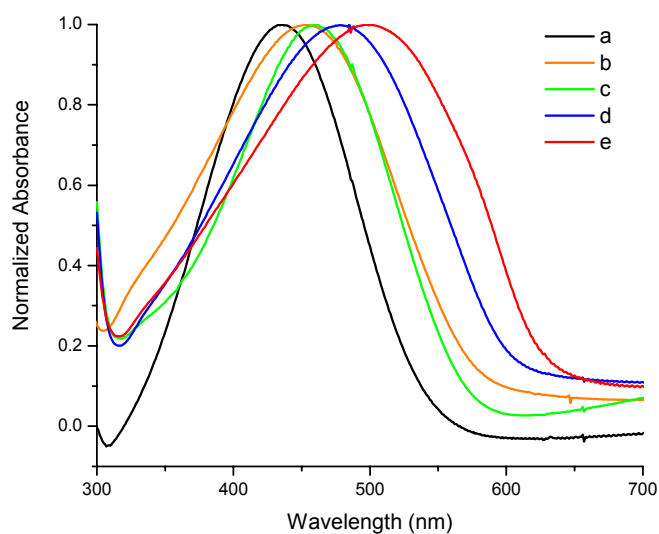


Figure 3.28 UV-Vis spectra of the dedoped conducting polymers synthesized with feed ratio of a) 0, b) 0.1, c) 0.15, d) 0.25, e)1 (w/w) in 0.1 M TBAFB/ACN in the presence of BFEE at 1.5 V

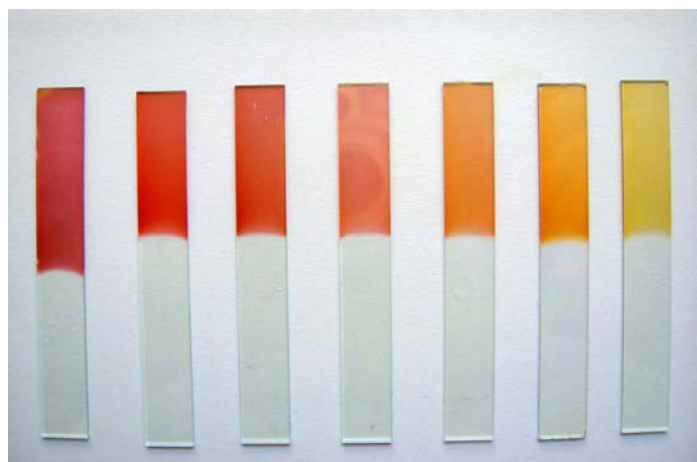


Figure 3.29 Colors of the polymers synthesized with feed ratio of 1, 0.5, 0.25, 0.15, 0.1, 0 % (w/w) in 0.1 M TBAFB/ACN in the presence of BFEE at 1.5 V (from left to right)

In order to investigate the composition changes, FTIR spectra of the polymers were recorded. During these studies the peaks around 1730 and 1640 cm^{-1} were

considered as the finger print of C=O band (originating from the monomer) and polyconjugation respectively. As seen in Figure 3.30 there is a progressive decrease in the ratio of the peak heights of the C=O band with respect to polyconjugation band as the feed ratio changes from 1 to 0. At this point, it is important to note that copolymerization of DATE with Th was found to have a significant effect on the conductivity of the resultant polymer which could be associated with the polyconjugation [100].

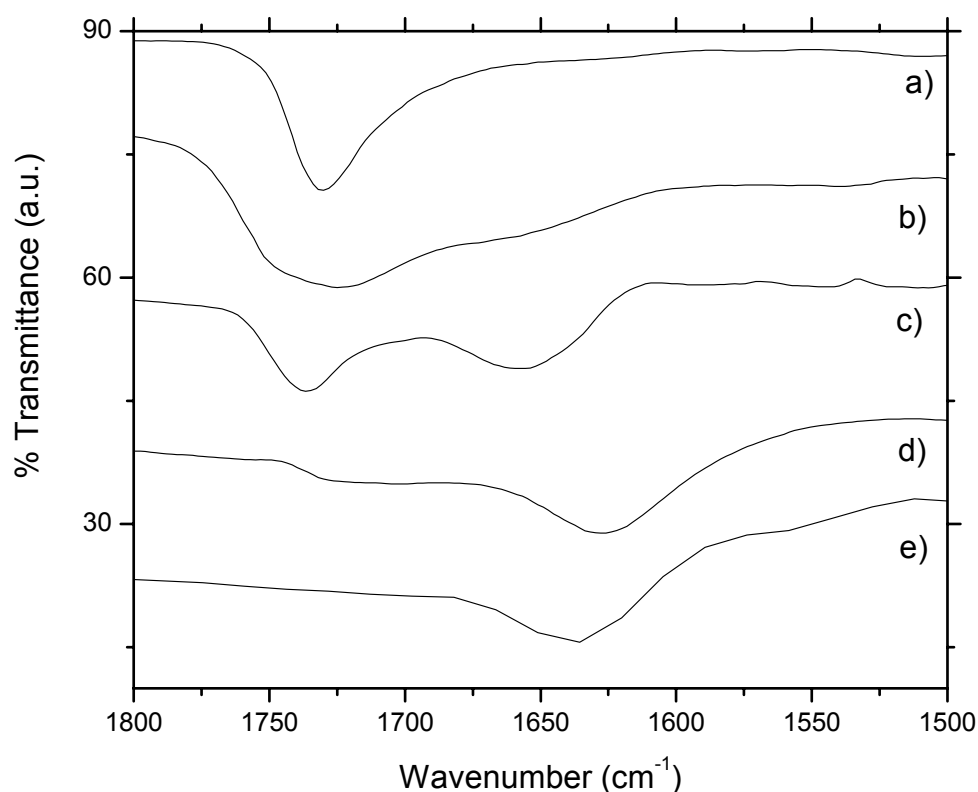


Figure 3.30 FTIR spectra of a) pure homopolymer, copolymer synthesized with the feed ration of c).0.15. d) 0.25 e) 0.5 and e) pure polythiophene

In the light of the studies like UV-Vis and FTIR studies, it was shown that it is possible to tune the color of the polymer between yellow, orange and red in a predictable, controlled and detectable manner via alternation of the feed ratio of the stock solution during electrochemical polymerization at a fixed potential.

3.5.2. Green: The Missing Color- Lamination

Other than copolymerization, lamination can be used to tailor the electrochromic response of electrochromic electrode by using different homopolymers. Selected homopolymers should display well defined electrochromic properties so that layering them on top of each other would provide desired color. The natural vegetation colors like green or brown in *neutral state* are desired in order to simulate the full color spectrum. Here the neutral and doped state colors of such laminated electrodes would follow basic color addition theories, so that by careful choice of the homopolymers, facile color control of the device can be achieved. We have fabricated laminated electrodes using poly(3,4-ethylenedioxythiophene), PEDOT, a polymer that undergoes a transition from blue to colorless upon oxidation, and PHABTE, a polymer that changes color from yellow to blue upon oxidation.

A three-electrode cell containing ITO-coated glass slide as the working electrode, a platinum flake as the counter electrode, and a silver wire as the pseudo-reference electrode were used for deposition of polymer films in a single compartment cell. First layer of bilayered electrochromic electrode, poly(3,4-ethylenedioxythiophene) (PEDOT), was synthesized at 1.5 V in TBAFB containing ACN solution. Second layer (PHABTE) was polymerized on top of this layer in the presence of TBAFB in ACN/BFEE (8:2, v/v) (Figure 3.31). Electrochromic behavior of this electrode was investigated in TBAFB containing ACN solution via spectroelectrochemistry studies.

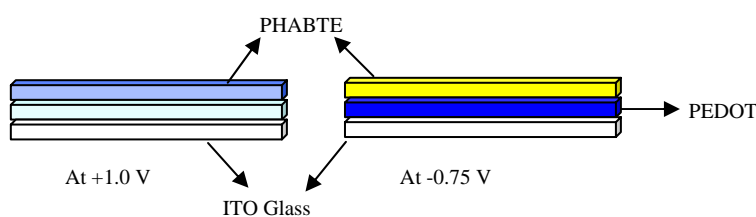


Figure 3.31 Schematic representation of lamination and color of the electrochromic layer at +1.0 and -0.75 V

Figure 3.32a reflects the UV-Vis spectra of PEDOT/PHABTE bilayer electrochromic electrode` at various potentials. Generally, UV-Vis spectra of the laminated electrode could be considered as the rough summation of the spectral behavior of the electrochromic layers. At 1 V laminated electrode displays a broad absorption centered at 1052 nm where the electrode appears as light blue. At this stage both polymers are expected to be in their oxidized state, where PHABTE and PEDOT reveal blue and transmissive color in single layer systems respectively. As the potential is decreased to 0 V, the peak corresponding to the $\pi-\pi^*$ transition of the PHABTE layer appears at 436 nm signifying the reduction of this layer. At this point, PEDOT layer is still in oxidized form without any significant absorption within the visible region. Yet, the electrode appears as yellow due to dominant effect of PHABTE. As the applied potential decreased further, there is a progressive increase in the intensity of the band at 600 nm, which corresponds to $\pi-\pi^*$ of PEDOT (Figure A.10), along with the already existing 436 nm absorption. Starting from -0.75V, laminated electrochromic electrode displays a true green color. According to literature [103], to observe green color, there has to be at least two simultaneous absorption bands within both red-yellow and blue regions. The appearance of green color, starting from -0.5 V, is considered to be due to the presence of transitions originating from $\pi-\pi^*$ of both PHABTE and PEDOT layers.

Within the light of these studies it was shown that lamination of different polymer layers in accordance with the color mixing theory is a powerful approach to achieve different colors especially those that require two or more absorptions like green. By using a simple 3-substitued thiophene ester and commercially available EDOT one is able to achieve green color in the neutral state. As seen in Figure 3.32,33,34,35 it is possible to achieve quite a number of different colors by copolymerization and lamination of these simple monomers.

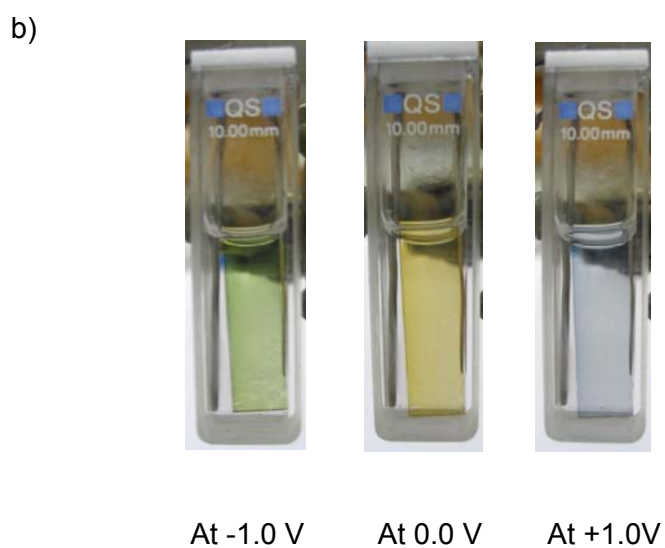
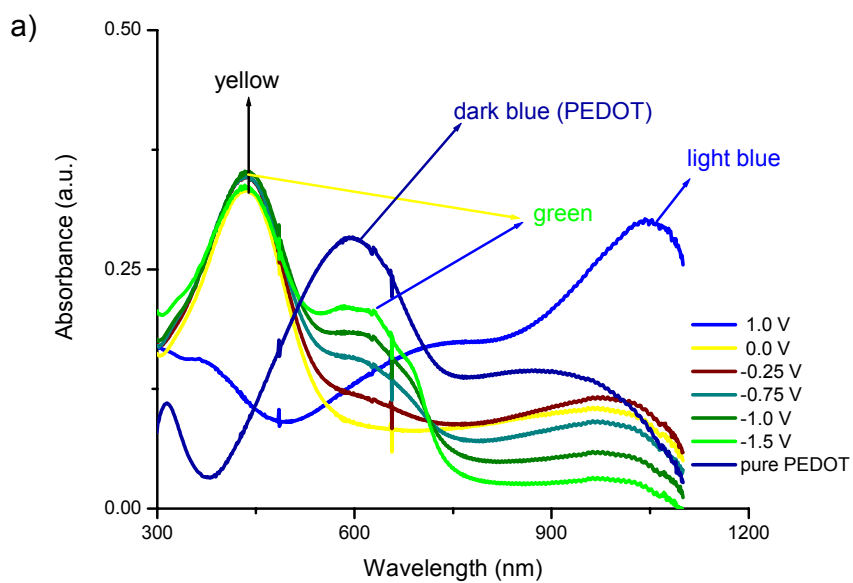


Figure 3.32 a) Spectroelectrochemistry studies of laminated electrode in 0.1 M TBAFB containing ACN b) colors of the electrochromic electrode at different potentials

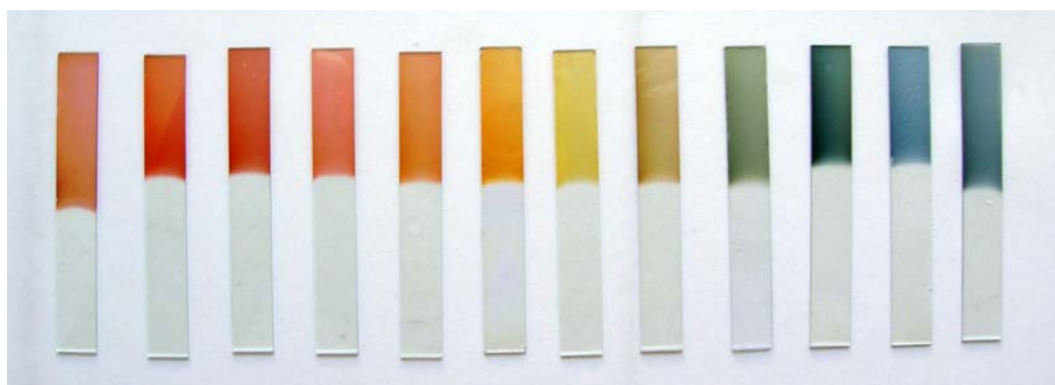


Figure 3.33 Colors of the electrochromic electrodes of HABTE based polymers at different comonomer ratios and potentials

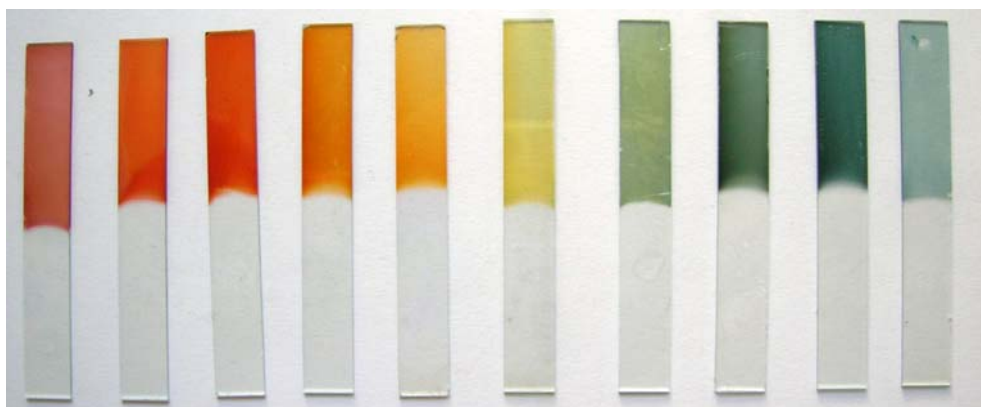


Figure 3.34 Colors of the electrochromic electrodes of DATE based polymers at different comonomer ratios and potentials



Figure 3.35 Colors of the electrochromic electrodes of POTE at different potentials

3.6. Electrochromic Device Application

The most versatile way of exploiting electrochromic properties of conducting polymers is to construct electrochromic devices, which, being in solid state, are suitable for daily life applications like smart windows etc. For this purpose, dual type polymer electrochromic devices based on homopolymers and copolymers of 3-ester substituted thiophenes were constructed against poly(3,4-ethylenedioxythiophene), where the former functioned as anodically and the later functioned as cathodically coloring layer. Before assembling the devices, it was important to balance the charge capacities of the electrochromic layers in order to prevent incomplete electrochromic reaction and residual charges that may remain during the coloring/bleaching processes. To minimize the effect of charge imbalances in ECD, we matched the redox charges of the two complementary polymer films by chronocoulometry and we provided a balanced number of redox sides for switching. Before sealing the electrochromic device, anodically coloring polymer films were fully reduced and the cathodically coloring polymer PEDOT was fully oxidized in order to achieve complementary operating conditions. To provide the ion exchange between the electrochromic layers we coated ITOs with gel electrolyte and ITOs were positioned in a way to face electrochromic layers to each other.

3.6.1. Electrochromic Devices of HABTE Based Polymers

We assembled the dual transmissive/absorptive type devices of PHABTE or P(HABTE-co-Th) with PEDOT using transparent ITO electrodes. ITO's were coated with anodically coloring materials (PHABTE or P(HABTE-co-Th)) at 1.5 V in the presence of 0.2 M TBAFB ACN/ BFEE (8:2,v/v). Cathodically coloring polymer was electrochemically deposited onto the ITO-coated glass from a 0.1 M solution of EDOT in 0.1M ACN at +1.5V.

3.6.1.1. Spectroelectrochemistry

Spectroelectrochemical studies of the ECDs' were performed to examine the spectral changes that occur during redox switching which are important for electrochromic applications. Optoelectrochemical spectra of the dual-type PHABTE/PEDOT ECD as a function of applied voltage are shown in Figure 3.36a. The wavelength for maximum electronic absorption was 448 nm at 0.2 V where the color of the device was yellow. The yellow color was attributed to the absorption of reduced PHABTE (π - π^* transition), since PEDOT was in its oxidized form (highly transparent- appendix Figure A10). Upon application of positive potentials, PHABTE layer started to oxidize and the intensity of the peak due to π - π^* transition decreased and there appears to be a second absorption at around 800 nm due to the formation of charge carrier bands. At this point, both anodically and cathodically coloring polymers were in their partially oxidized states. Further positive potentials results in the evolution of the new peak around 619 nm due to π - π^* transition of PEDOT itself, which was followed by the decrease in the intensity at π - π^* transition of anodically coloring electrochromic layer. At this stage the color of the device started to alter from yellow to blue. At 1.8 V, PEDOT and PHABTE layers were in fully reduced and oxidized states respectively.

Similar type of spectroelectrochemical behavior was observed in the case of P(HABTE-co-Th)/PEDOT device. Figure 3.36b presents spectroelectrochemistry of the P(HABTE-co-Th)/PEDOT device, which clearly shows absorbance features of both PEDOT and P(HABTE-co-Th). At 0.0V the entire device was in orange color (λ_{\max} = 467nm due to π - π^* transition of P(HABTE-co-Th)). The color of device changed to blue (λ_{\max} = 646 π - π^* transition of PEDOT) upon further applied positive potentials. From 1.0 V to 1.6 V, the gradual coloration was primarily due to the reduction of PEDOT. In fact, at 0.0V, the spectrum of P(HABTE-co-Th)/PEDOT ECD appeared very similar to that of P(HABTE-co-Th) in the reduced state and at 1.6 V device spectrum appeared very similar to that of PEDOT in reduced state. The relative luminance (L) and the a (hue), b (saturation) values of the devices (Table 3.6) were measured at bleached and colored state. The color

of the PHABTE/PEDOT switches from a yellow to blue and P(HABTE-co-Th)/PEDOT switched between orange to blue.

Table 3.6 Colorimetry Data for PHABTE/PEDOT and P(HABTE-co-Th)/PEDOT ECDS

Electrochromic Device	Color	L	a	b
PHABTE/PEDOT	Blue (at 1.8 V)	30	7	-39
	Yellow (at 0.2 V)	54	7	57
P(HABTE-co-Th)/PEDOT	Blue (at 1.6 V)	27	1	-31
	Orange (at 0.0 V)	47	31	46

3.6.1.2. Switching Characteristics

The kinetics of color changes within devices were investigated performing fast spectral scans in situ while applying the potential step square wave form. This technique provides information about the kinetics of color-switching as depicted in Figure.3.37 (a) and (b) which demonstrate the transmittance change at a selected wavelength (maximum contrast; at 619 nm and 646 nm for PHABTE/PEDOT and P(HABTE-co-Th)/PEDOT ECD respectively). During the experiment, potentials were stepped between +0.2 and +1.8V for PHABTE/PEDOT, 0.0 and +1.6 V for P(HABTE-co-Th) /PEDOT device with a residence time of 5 s. Results showed that time required to reach 95 % of ultimate % T was 1.8 s and 1.9 s for PHABTE/PEDOT and P(HABTE-co-Th) /PEDOT electrochromic devices respectively. The optical contrast was measured as the difference between %T in the bleached and colored states and was found to be 25.3 % and 24 % for PHABTE/PEDOT and P(HABTE-co-Th)/PEDOT ECD respectively.

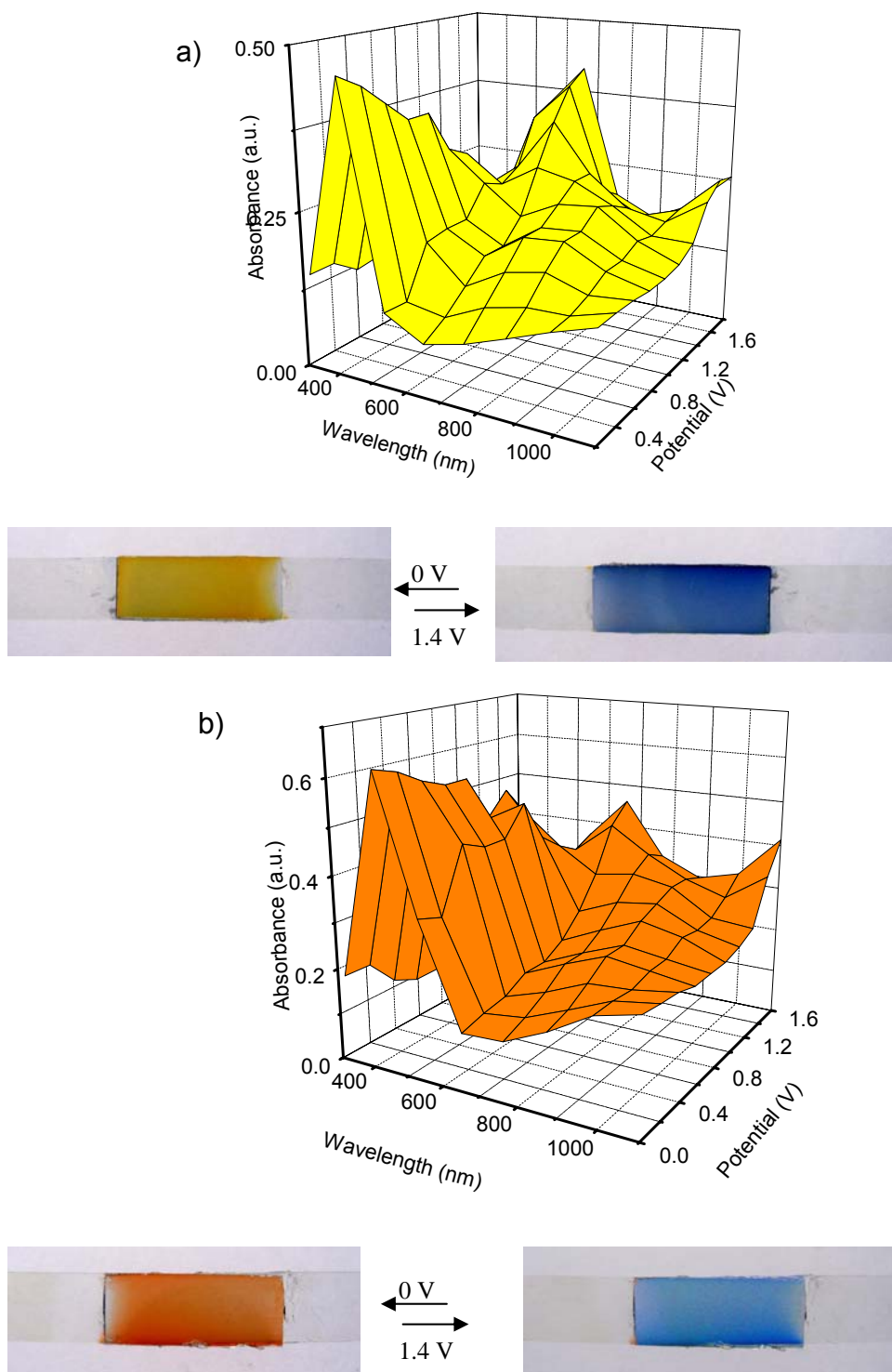


Figure 3.36 Optoelectrochemical spectra of (a) PHABTE/PEDOT ECD at applied potentials between 0.2 and +1.8 V (b) P(HABTE-co-Th)/PEDOT ECD at applied potentials between 0.0 and +1.6 V

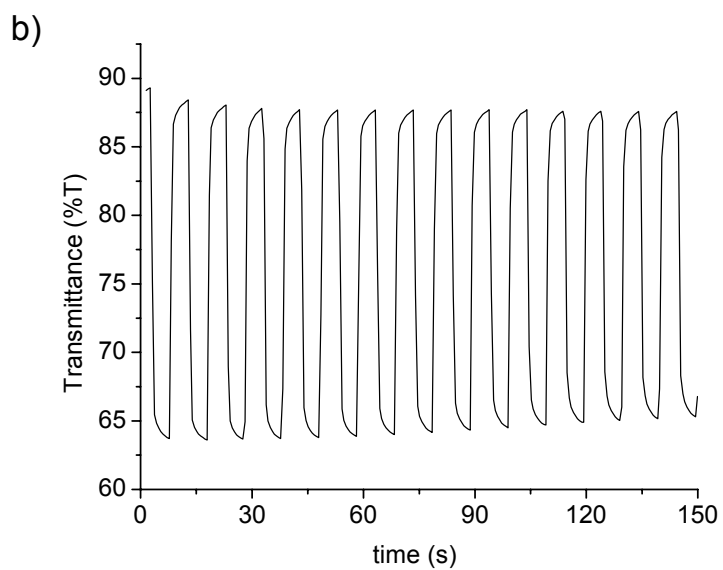
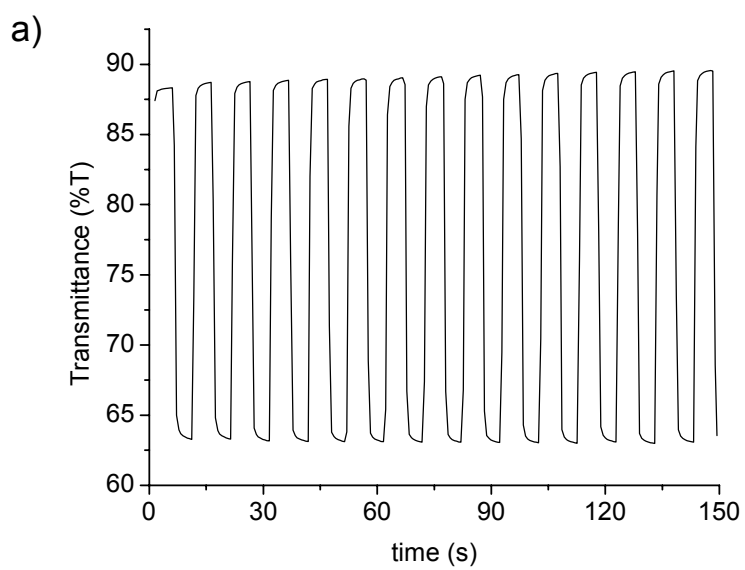


Figure 3.37 (a) Electrochromic switching, optical absorbance change monitored at 619 nm for PHABTE/PEDOT ECD between 0.0 V and 1.4 V (b) Electrochromic switching, optical absorbance change monitored at 646 nm for P(HABTE-co-Th)/PEDOT between 0.0 V and 1.4 V

3.6.1.3. Electrochromic Memory

Electrochromic memory, defined as the ability of an ECD to retain its color and/or optical density while the current is off. In order to investigate electrochromic memory of the devices, the experiment was performed by polarizing the devices in their two extreme states (yellow/blue and orange/blue for PHABTE/PEDOT and P(HABTE-co-Th)/PEDOT respectively) by an applied pulse (0.2/1.8 V and 0.0/1.6 V for PHABTE/PEDOT and P(HABTE-co-Th)/PEDOT respectively) for 1 second and kept at open circuit conditions for 200 s. The variation of the optical spectrum was simultaneously followed at 646 and 619 nm for P(HABTE-co-Th)/PEDOT and PHABTE/PEDOT respectively as a function of time under open circuit conditions. (Figures 3.38 a and b). When P(HABTE-co-Th)/PEDOT were polarized in the blue colored state, initially device presents % T = 65.0 %, while after 200 s it decreases to 66.5 % under open circuit conditions, which is remarkable. Similar but less pronounced effect was observed for the case of PHABTE/PEDOT. PHABTE/PEDOT device, results indicate that this system does not truly reach to equilibrium under open circuit conditions. However, this matter can be overcome by application of current pulses to freshen the fully colored state. For both devices at bleached states, namely yellow and orange colored states, a true permanent memory effect was observed.

3.6.1.4. Stability

Redox stability is an important requirement for production of reliable electrochromic devices with long life times. Main reasons for device failure are different applied voltages and environmental conditions. In this study, CV was exploited as a method to evaluate the stability of the devices. For this purpose, we performed non-stop cycling of the applied potential between 0.0-2.0 V for both ECDs with 500 mV/s scan rate. As seen in Figures 3.39 a and b, even after 1000th run both devices revealed only a slight decrease (9%) in electroactivity accompanied by unperturbed color change from bleached to colored state, where P(HABTE-co-Th)/PEDOT seems to be more stable upon switching for longer times. These results showed that both ECDs' have good environmental and redox stability which make them promising materials for future applications.

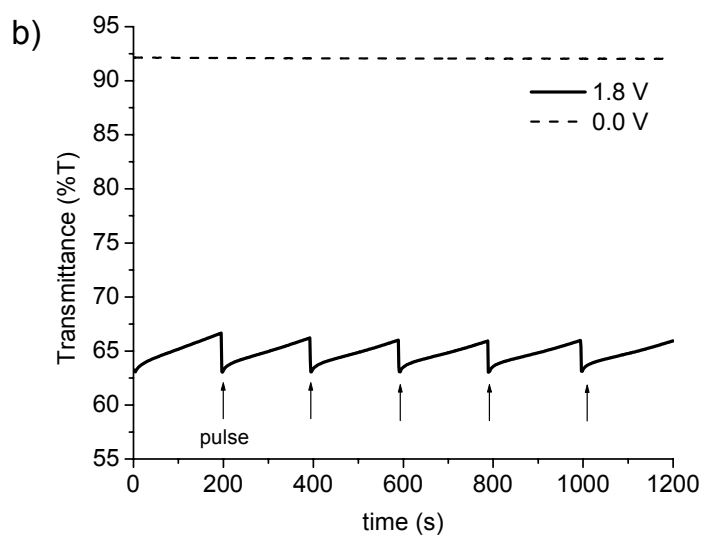
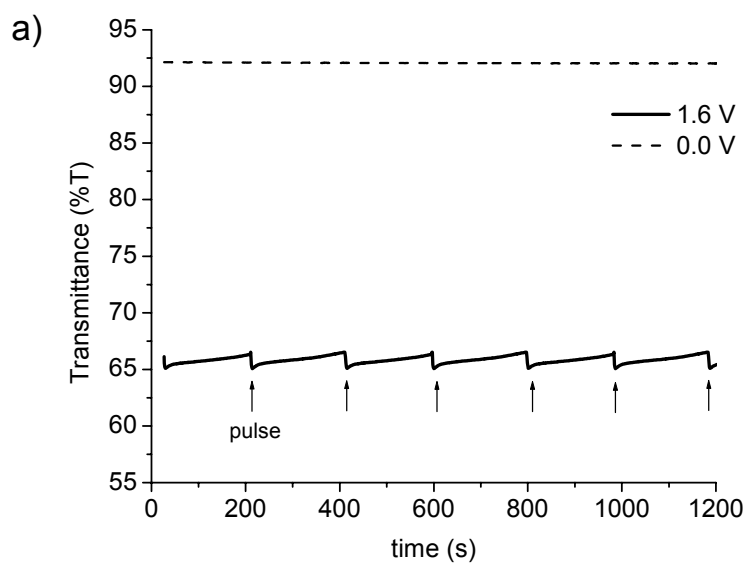


Figure 3.38 Open Circuit Memory of (a) P(HABTE-co-Th)/PEDOT (b) PHABTE/PEDOT monitored by single-wavelength absorption spectroscopy at a) 646 nm +1.6 and 0.0 V b) 619 nm +1.8 and 0.2V, pulses are applied for 1 second for every 200 seconds to recover the initial transmittance

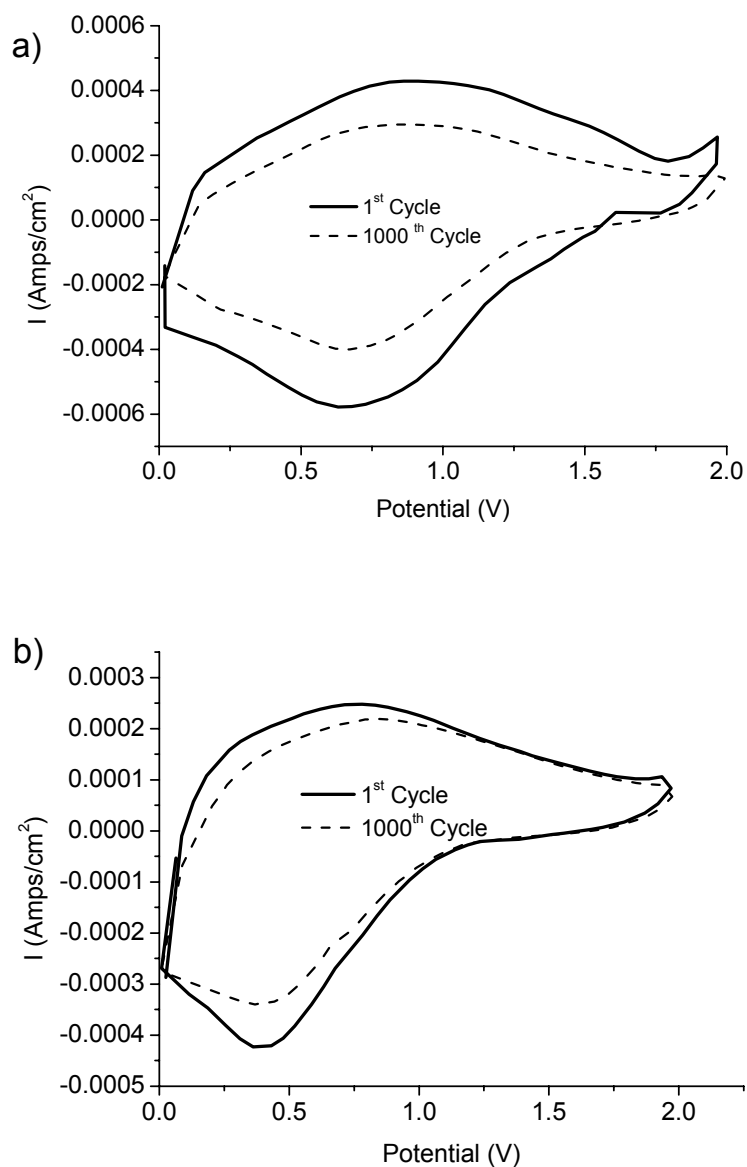


Figure 3.39 Cyclic Voltammogram of (a) PHABTE/PEDOT (b) P(HABTE-co-Th)/PEDOT electrochromic devices as a function of repeated scans 500 mV/s: 1st cycle and after 1000th cycles

3.6.2. Electrochromic Devices of POTE and PDATE

We assembled the device POTE or PDATE /PEDOT using transparent ITO electrodes coated via potentiodynamic switching of the electroactive monomers

between 0.0 -1.6 V in the presence of 0.2 M TBAFB in ACN/ BFEE (8:2). As to the synthesis of the anodically coloring electrochromic layers, we made use of the BFEE, as an effective approach to succeed in synthesizing uniform films with better electrochemical cycling stability, which was attributed to the decrease in the oxidation potential of the monomer due to an increase in the interaction strength and decreased aromaticity [33].

3.6.2.1. Spectroelectrochemistry

Spectroelectrochemical studies of the ECDs' were performed to obtain information on the electronic structure and to examine the spectral changes that occur during redox switching; both of these are important for electrochromic applications. Optoelectrochemical spectra of dual type ECD as a function of applied potential are given in Figures 3.40 a,b. Upon stepwise increase of the applied potential from 0.0 to 1.6 V, alternation of the color from yellow to blue was observed. UV-Vis Spectroscopy results implied that at 0.0V bias to POTE or PDATE layer, anodically coloring electrochromic materials, dominated in the features of the device, revealing brownish yellow and yellow color respectively. Thus, there were maximum absorptions at 434 nm and 427 nm due to $\pi-\pi^*$ transition of the electrochromic layers, POTE and PDATE respectively. At this potential PEDOT layer was in its oxidized state revealing transparent sky blue color. Upon application of further positive potentials, both POTE and PDATE layers started to get oxidized and the intensity of the peak due to $\pi-\pi^*$ transition decreased and there appears to be a second intense absorption at around 800 nm due to the formation of charge carrier bands.

At potentials beyond + 0.8 V, device starts to reflect the PEDOT dominance, declared by the alternation of the color to blue and evolution of the new peak around 635 nm due to $\pi-\pi^*$ transition of PEDOT itself all of which was accompanied by the decrease in the intensity at $\pi-\pi^*$ transition of anodically coloring electrochromic layer.

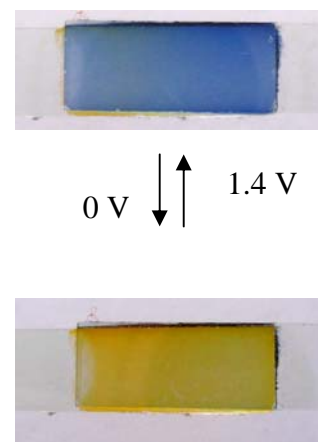
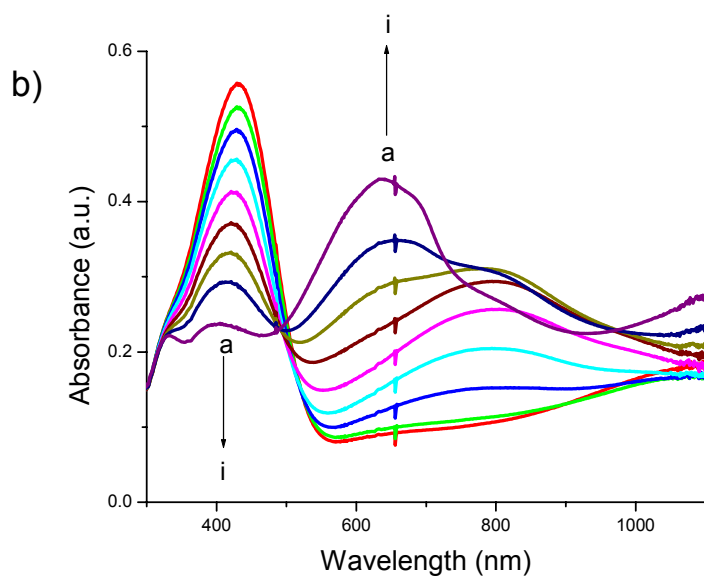
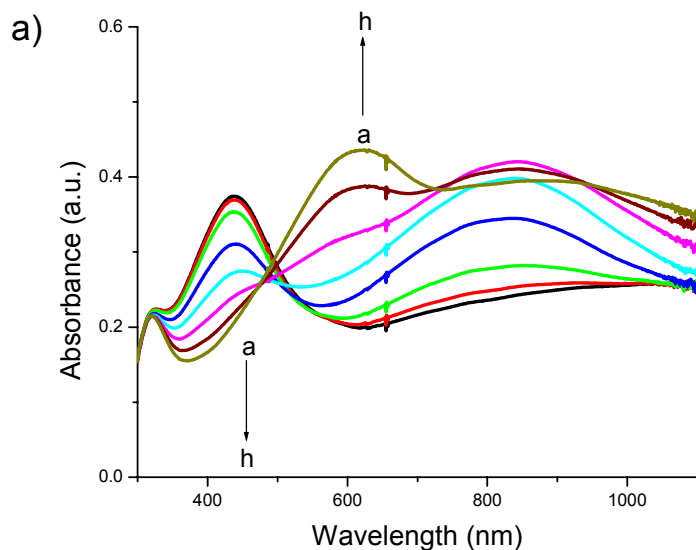
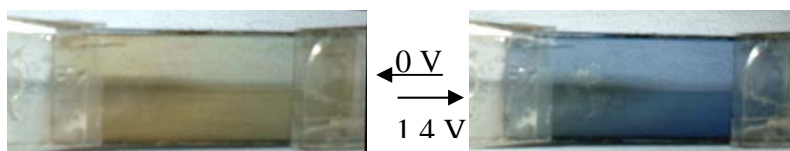


Figure 3.40 Optoelectrochemical spectrum of a) P(OTE)/PEDOT ECD at applied potentials between 0.0 and +1.4 V (a)+ 0.0 V, (b)+ 0.2 V, (c)+ 0.4 V, (d)+ 0.6 V, (e)+ 0.8 V, (f)+ 1.0 V, (g)+ 1.2V, (h)+ 1.4 V b) Optoelectrochemical spectrum of PDATE/PEDOT ECD at applied potentials between 0.0 and +1.4 V (a) + 0.0 V, (b)+ 0.2 V, (c)+ 0.4 V, (d) + 0.6 V, (e)+ 0.8 V, (f)+ 1.0 V, (g)+ 1.2 V (h)+ 1.3 V (i)+ 1.4 V

Table 3.7 Colorimetry Data for PDATE/PEDOT and POTE/PEDOT ECDs

Electrochromic Device	Dominant Layer	Color	L	a	B
PDATE/PEDOT	PEDOT	Blue (at 1.4V)	48	-7	-6
	PDATE	Yellow (at 0 V)	70	-8	36
POTE/PEDOT	PEDOT	Blue (at 1.4V)	50	-6	-13
	POTE	Brownish Yellow (at 0 V)	66	-2	12

3.6.2.2. Switching

A double potential step experiment was performed in order to evaluate the response time of the device and its stability during repeated cycles. Potential was stepped between 0 and +1.6V with a residence time of 5 s. During the experiment, the % transmittance (T %) at the wavelength of maximum contrast was measured by using a UV-Vis spectrophotometer. The optical contrast (ΔT , %) was monitored with switching of devices between 0.0 V and 1.4 V at 632 and 427 nm for POTE/PEDOT and PDATE /PEDOT respectively. The contrast was measured as the difference between %T in the reduced and oxidized forms and was found to be 14% and 20% for POTE/PEDOT and PDATE /PEDOT ECDs respectively (Figures 3.41 a,b). Results showed that time required to reach 95 % of ultimate % T was less than 1 s for POTE/PEDOT device and 1.2 seconds for the PDATE /PEDOT device.

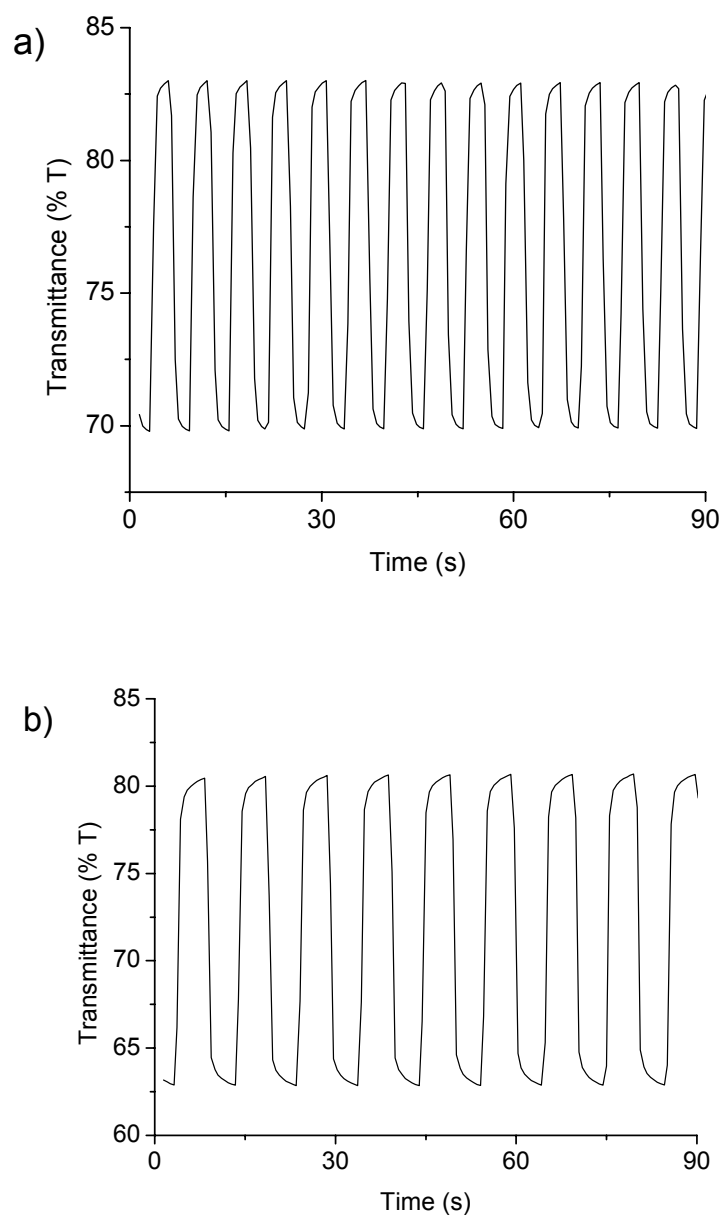


Figure 3.41 a) Electrochromic switching, optical absorbance change monitored at 632 nm for POTE/PEDOT ECD between 0.0 V and 1.4 V b) Electrochromic switching, optical absorbance change monitored at 427 nm for PDATE/PEDOT between 0.0 V and 1.4 V

3.6.2.3. Stability

Cyclic voltammetry studies showed that the ECDs stably operated with an applied voltage of -0.5 - 1.6 V under atmospheric conditions. In this study CV was

exploited as a method to evaluate the stability of the devices. For this purpose we accomplished non-stop cycling of applied potential between 0.0-1.6 V and -0.5 - 1.6 V PDATE /PEDOT and POTE/PEDOT respectively with 500 mV/s scan rate. As seen in Figures 3.42 a,b even after 1000th run both devices showed only a slight decrease in electroactivity accompanied by unperturbed color change from yellow to blue. Although POTE/PEDOT had shorter switching times, PDATE /PEDOT seems to be more stable upon switching for longer times. These results showed that both ECDs' have good environmental and redox stability, which make them promising materials for future applications.

3.6.2.4. Open Circuit Stability

The color persistence in the electrochromic devices is an important feature since it is directly related to aspects involved in its utilization and energy consumption during use [104]. Experiment was performed by polarizing the POTE/PEDOT device in the yellow/blue states by an applied pulse (0.0 /1.4 V, yellow/blue colored states respectively) for 1 second and kept at open circuit conditions for 200 s. Simultaneously the optical spectrum at 432 nm as a function of time at open circuit conditions was monitored. (Figure 3.43.). When polarized in the blue colored state initially device presents % T = 85 %, while after 200 s it changes to 80%. These results indicate that this system does not reach equilibrium under open circuit conditions. It presents good optical memory in blue colored state, however, POTE is not that stable in reduced (brownish yellow) state.

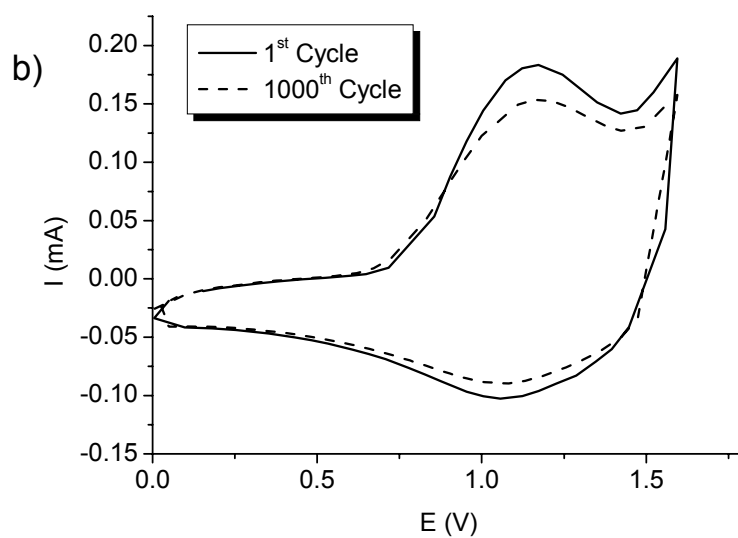
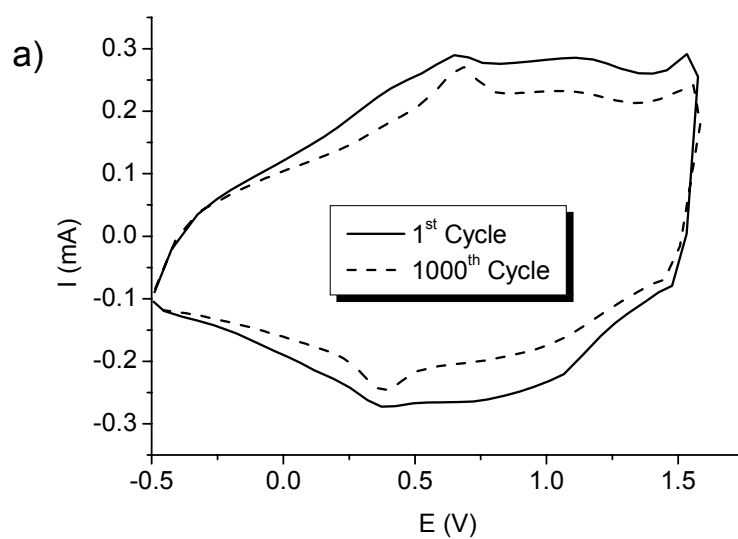


Figure 3.42 Cyclic Voltammogram of a) POTE/PEDOT b) PDATE/PEDOT electrochromic devices as a function of repeated scans 500 mV/s: after 1st cycle (plain), after 1000th cycles (dash)

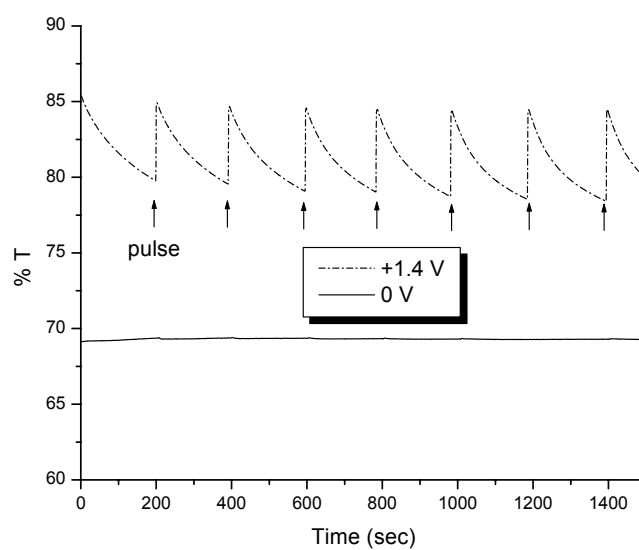


Figure 3.43. Open Circuit memory of a POTE/PEDOT ECD monitored by single-wavelength absorption spectroscopy at 430 nm. +1.4 and 0.0 V pulses are applied for 1 second every 200 seconds to recover the initial transmittance

CHAPTER IV

CONCLUSIONS

In this study three different 3-ester substituted thiophene monomers were synthesized via esterification reaction of 3-thiophene ethanol with adipoyl chloride or sebacoylchloride or octanoyl chloride in the presence of triethylamine at 0^oC. Synthesized monomers were characterized by several techniques like ¹H-NMR, ¹³C-NMR, FTIR, DSC, TGA.

Cyclic voltammetry was utilized as the major characterization technique to acquire qualitative information about electrochemical behavior of monomers. Preliminary studies were performed in TBAFB/ACN supporting electrolyte/solvent system. 3-Ester substituted thiophene monomers revealed an irreversible electroactivity at around 2 V which sharply decreased upon consecutive scans. Similar type of an experiment was performed by addition of borontrifluoride diethyletherate (BFEE). In all cases upon scanning between 0.0 to 1.6 V it was possible to synthesize polymer film which was monitored by the increase in the polymer's anodic and cathodic peak currents. Studies revealed the astonishing effect of BFEE on the polymerization, where free standing films of the homopolymers could be synthesized. Use of pure BFEE as the electrolytic system resulted even in better film formation, where the oxidation potential of monomer (OTE) decreased down to 1 V.

Copolymers of the monomers with thiophene or 3-methyl thiophene were synthesized in the presence and absence of BFEE at constant potential electrolysis and the resultant polymers were characterized by CV, FTIR, DSC,

TGA, SEM and conductivity measurements. Copolymerizations were proven by the drastic difference in the voltammograms such as the presence of characteristic peaks that belonged to both comonomers. Difference in thermal behavior and morphology of the films compare to those of two parent homopolymers supported the above argument. In general both the conductivity and the thermal stability of the copolymers are higher than their corresponding homopolymers.

Second part of the study was devoted to investigate one of the most interesting property of conducting polymers, electrochromism. In recent years there has been a growing interest in the application of conducting polymers in electrochromic devices. Thus, electrochromic properties of the synthesized conducting polymers were investigated by several techniques like spectroelectrochemistry, kinetic and colorimetry studies.

Spectroelectrochemistry experiments were performed in order to investigate key properties of conjugated polymers such as band gap, maximum absorption wavelength, the intergap states that appear upon doping and evolution of polaron and bipolaron bands. Formation and recombination of polarons to bipolaron were also investigated by ESR studies. Generally, the homopolymers displayed color changes between yellow, green and blue colors upon variation in applied potentials.

Switching time and optical contrast of the homopolymers and copolymers were evaluated via kinetic studies. Polymers exhibited similar switching times and optic contrast that are around 1 second and 25% respectively. Results implied the possible use of these materials in electrochromic devices due to their satisfactory electrochromic properties like short switching time and stability. Especially the copolymers tend to reveal higher stability against long term switching times.

Fine tuning of the colors of the polymers were accomplished by techniques like copolymerization and lamination. Via copolymerization. we were able to tune the color of the polymers between different tones of yellow and orange and red in neutral state. This color variation was followed by UV-Vis spectroscopy where

gradual shift of the λ_{\max} was observed. Similarly, compositional changes upon copolymerization were evaluated via FTIR spectroscopy. Results implied the progressive decrease in the ratio of the peak heights of the C=O band with respect to polyconjugation band as the feed ratio changes.

Other than copolymerization, lamination was used yet as another technique to tailor the color of electrochromic electrode by using two different homopolymers. We have fabricated laminated electrodes using poly(3,4-ethylenedioxythiophene), PEDOT, a polymer that undergoes a transition from blue to colorless upon oxidation, and PHABTE, a polymer that changes color from yellow to blue upon oxidation. The bilayer electrode revealed green in reduced, yellow in neutral and blue in oxidized state. Yet, lamination of different polymer layers in accordance with the color mixing theory was found to be a powerful approach to achieve different colors especially those that require two or more absorptions like green.

As the last part of the study, dual type electrochromic devices based on polymers of 3-ester substituted thiophenes with PEDOT were constructed, where the former and the later functioned as anodically and cathodically coloring layers respectively. Spectroelectrochemistry, switching ability, stability, open circuit memory and color of the devices were investigated. POTE/PEDOT and PDATE/PEDOT devices revealed brownish yellow and yellow colors at 0.0 V respectively. PHABTE and P(HABTE-co-Th) devices revealed yellow and orange colors respectively. Among the homopolymer based devices, POTE/PEDOT revealed the shortest switching time, whereas, the devices of PHABTE and P(HABTE-co-Th) revealed the highest optical contrast, stability and memory along with satisfactory switching times.

REFERENCES

- [1] C.K. Chiang, C.R Fincher, Y.W. Park, A.J. Heeger, H .Shirakawa, F.J. Louis, S.C. Gau, A.G. MacDiarmid, Phys. Rev. Lett., 1977, 39,1098.
- [2] K.Doblhofer, K.Rajeshwar, Handbook of Conducting Polymers. eds T.A. Skotheim, R.A .Elsenbaumer, J.R. Reynolds, New York: Marcel Dekker, 1998. Ch 20
- [3] J. I. Reddinger, J. R. Reynolds, Advances in Polymer Science, 1999, 45, 59.
- [4] K. Shimamura, F.E. Karasz, J.A.Hirsch, J.C. Chien, Makromol. Chem. Rapid Commun. 1981, 2, 443.
- [5] R. Hoffmann, Angew. Chem. Int. Ed., 1987, 26, 846.
- [6] M. Salmon, A.F. Diaz, A.J. Logan, M. Krounbi, J. Bargon, J Mol. Cryst. Liq. Cryst., 1983, 83,1297.
- [7] V. Sexena, B. D. Malhotra, Handbook of Polymers In Electronics, ed B.D.Malhotra, Shawbury UK, Rapra Technology 2002,Ch. 1
- [8] G. Tourillon, D. Gourier, P. Garnier, D. Vivien, J. Phy. Chem., 1984, 88, 1049.
- [9] P. Chandrasekhar, Conducting Polymers Fundamentals and Applications, Boston, Kluwer Academic Publishers, 1999, Ch. 2
- [10] A. J. Heeger, J. Phys. Chem. B, 2001, 105, 8475.

- [11] W. R. Salaneck, I. Lundstrom, W. S. Huang, A. G. MacDiarmid, *Synth. Met.*, 1986,13, 291.
- [12] P. J. Nigrey, A. G. MacDiarmid, A. J. Heeger, *J. Chem. Soc. Chem. Commun.*, 1979, 594.
- [13] J. J. Apperloo, R. A. J. Janssen, M. M. Nielsen, K. Bechgaard, *Adv. Mater.*, 2000,12, 1594.
- [14] I. F. Perepichka, D. F. Perepichka, H. Meng, F. Wudl, *Adv. Mater.*, 2005, 17, 1.
- [15] Y. Yamamoto, K. Sanechika, A. Yamamoto, *J. Polym. Sci. Polym.*, 1980, 18,9.
- [16] J. W. P. Lin, L.P. Dudek, *J. Polym. Sci. Polym. Chem.*, 1980, 18, 2869.
- [17] K. Yoshino, S. Hayashi, R. Sugimoto *Jpn. J. Appl. Phys. Part 2*, 1984, 23, 899.
- [18] S. Amou, O. Haba, K. Shirato, T. Hayakawa, M. Ueda, K. Takeuchi, M. Asai, *J. Polym. Sci. Part A Polym. Chem.*, 1999, 37, 1943.
- [19] R.D. McCullough, R.D. Lowe, M. Jayaraman, D.I. Anderson, *J. Org. Chem.*, 1993, 58, 904.
- [20] L. B. Groenendaal, G. Zotti,P. H. Aubert, S. M. Waybright, J. R. Reynolds *Adv. Mater.*, 2003, 15, 855.
- [21] J. Roncali, *Chem. Rev.*, 1992, 92, 711.
- [22] R. J. Waltman, J. Bargon, *Tetrahedron*, 1984, 40, 3963.
- [23] A.F. Diaz, K.K. Kanazawa, G.P. Gradini, *J. Chem. Soc. Chem. Commun.*,1079, 14, 635.

- [24] S. Hotta, T. Hosaka, W. Shimotsuma, *Synth. Met.*, 1983, 6, 319.
- [25] A. F. Diaz, J. Bargon, *Handbook of Conducting Polymers*, ed. T. J. Skotheim, Marcel Dekker, New York, 1986, p. 81.
- [26] P. Marque, J. Roncali, F. Garnier *J. Electroanal. Chem.*, 1987, 218, 107.
- [27] Y. Li, J. Yang, *J. Appl. Polym. Sci.*, 1997, 65, 2739.
- [28] M. Ogasawara, K. Funahashi, T. Demura, T. Hagiwara, K. Iwata, *Synth. Met.*, 1986, 14, 61.
- [29] B. Krische, M. Zagorska *Synth. Met.*, 1989, 28, 263.
- [30] M. Gratzl, D. F. Hsu, A. M. Riley, J. Janata, *J. Phys. Chem.*, 1990, 94, 5973.
- [31] A. Yassar, J. Roncali, F. Garnier *Macromolecules*, 1989, 22, 804.
- [32] B. Krische, M. Zagorska, *Synth. Met.*, 1989, 28, 257.
- [33] G. Shi, S. Jin, G. Xue, *Science*, 1995, 267, 994.
- [34] S. Jin, G. Xue, *Macromolecules*, 1997, 30, 5730.
- [35] D. Zhang, J. Qin, G. Xue, *Synth. Met.*, 1999, 106, 161.
- [36] D. Zhang, J. Qin, G. Xue, *Synth. Met.*, 1999, 100, 285.
- [37] J. K. Xu, G. Q. Shi, L. T. Qu, J. X. Zhang, *Synth. Met.*, 2003, 135, 221.
- [38] C. Li, G. Shi, Y. Liang, Z. Sha, *Polymer*, 1997, 38, 6421.
- [39] X. Wang, G. Shi, Y. Liang, *Electrochem. Commun.*, 1999, 1, 536.

- [40] C. Li, G. Shi , Y. Liang, J. Electroanal. Chem., 1998, 455, 1.
- [41] J. Xu, G. Shi , Z. Xu, F. Chen, X. Hong, J. Electroanal. Chem. 2001, 514, 16.
- [42] D.D.Eley, Chemistry of Cationic Polymerization, ed. P.H. Plesh, Macmillan, Newyork, 1963.
- [43] S. Alkan, C. A. Cutler, J. R. Reynolds, Adv. Func. Mater., 2003, 13, 331.
- [44] L. P. Hammett, J. Am. Chem. Soc., 1937, 59, 96.
- [45] L. P. Hammett, Chem. Rev., 1935, 17, 125.
- [46] R. J. Waltman, J. Bargon , A. F. Diaz, J. Phys. Chem., 1983, 87, 1459.
- [47] M.A. Sato, S. Tanaka, K. Kaeriyama, J. Chem. Soc., Chem. Commun., 1985, 713.
- [48] W. Helfrich, W.G. Schneider, Phys. Rev. Lett., 1965, 14, 229.
- [49] C.W. Tang, S. A .Vanslyke, Appl. Phys. Lett., 1987, 51, 913.
- [50] J.H. Burroughes, D.D.C. Bradley, A.R Brown, R.N Marks, K. Mackay, R.H Friend, P.L Burn, A.B Holmes, Nature, 1990, 347, 539.
- [51] A. Moliton, C. R. Hiorns, Polym. Int., 2004, 53, 1397.
- [52] V. Saxena, B.D. Malhotra, .Current Applied Physics, 2003, 3, 293.
- [53] C. J. Brabec, N. S. Sariciftci, J. C. Hummelen, Adv. Funct. Mater., 2001, 11, 15.
- [54] A. Cravino, N. S. Sariciftci, J. Mater. Chem., 2002, 12, 1931

- [55] C. J. Brabec, N. S. Sariciftci, *Monatshefte fuer Chemie*, 2001, 132, 421.
- [56] A. Cravino, N. S. Sariciftci, *J. Mater. Chem.*, 2002, 12, 1931.
- [57] A. Shah, P. Torres, R. Tscharnner, N. Wyrsh, *Science*, 285,1999, 692.
- [58] J. Kline, M. D. Mcgehee, E. N. Kadnikova, J. Lui, J. Frechet, *Adv. Mater.*, 2003, 15 ,1519.
- [59] J. H. Burroughes, C. A. Jones, R. H. Friend, *Nature*, 1988, 335, 137.
- [60] A. R. Brown, C. P. Jarrett, D. M. De Leeuw, *M. Matters, Synth. Met.*, 1997, 88, 37.
- [61] Z. Bao, A. Dodabalapur, A. J. Lovinger, *Appl. Phys. Lett.*, 1996, 69, 4108.
- [62] G.G. Wallace, M. Smyth, H. Zhao, *Trends in Analytical Chemistry*, 1999, 18, 245.
- [63] T. Hanawa, S. Kuwabata, H. Hashimoto, H. Yoneyama, *Synth. Met.*, 1989, 30, 173.
- [64] J. C. Vidal, E. G. Ruiz, J. R. Castillo, *Microchim. Acta*, 2003, 143, 93.
- [65] M. Leclerc, K. Faid *Handbook of Conducting Polymers*. eds T.A. Skotheim, R.A .Elsenbaumer, J.R. Reynolds, New York: Marcel Dekker, 1998 Ch 24.
- [66] G.H. Brown, *Photochromism*, John Wiley & Sons Inc., New York 1971
- [67] I. Levesque, M. Leclerc, *Synth. Met.*, 1997, 84, 203.
- [68] T. Kaniowski, W. Luzny, S. Nizioł , T. M. Sanetraj, *Synth Met.*, 1998, 92,

- [69] K. Ihn, J. Moulton, P. Smith, J. Polym. Sci. Part B, Polym. Phys., 1993, 31, 735.
- [70] J. Mardelen, E. Samuelsen, A. Pendersen, Synth. Met., 1993, 55, 378.
- [71] P. R. Somani, S. Radhakrishnan, Mat. Chem. Phys., 2002, 77, 117.
- [72] S.K. Deb, J.A. Chopoorian, J. Appl. Phys., 1968, 37, 4818.
- [73] H.J. Byker, Gentex Corporation, Us Patent No. 4902108.
- [74] D. R. Rosseinsky, R. J. Mortimer, Adv. Mater., 2001, 13, 783.
- [75] R.J. Mortimer, Electrochimica Acta, 1999, 44, 2971.
- [76] M A. De Paoli, W. A. Gazotti, J. Braz. Chem. Soc., 2002, 13, 410.
- [77] G. Sonmez, I. Schwendeman, P. Schottland, K. Zong, J. R. Reynolds Macromolecules, 2003, 36, 639.
- [78] K. Fesser, A. R. Bishop, D. K. Campbell, Phys. Rev. B, 1983, 27, 4804.
- [79] B.C. Thompson, P. Schottland, G. Sonmez, J.R. Reynolds, Synth. Met., 2001, 119, 333.
- [80] J. Roncali, Chem. Rev., 1997, 97, 173.
- [81] J. L. Bredas, J. Chem Phys., 1985, 82, 3808.
- [82] F. Wudl, M. Kobayashi, A. J. Heeger, J. Org. Chem., 1984, 49, 3382.
- [83] R.D. McCullough, Adv. Mater., 1998, 10, 93.
- [84] S. A. Jenekhe, Macromolecules, 1991, 24, 1.

- [85] G. A. Sotzing, J. L. Reddinger, A. R. Katritzky, J. Soloducho, R. Musgrave, J. R. Reynolds, *Chem. Mater.*, 1997, 9, 1578.
- [86] F. Jonas, I Schrader, *Synth Met.*, 1991, 41-43, 831.
- [87] A. Kumar , D. M. Welsh, M.C. Morvant, F. Piroux, K. A. Abbound, J. R. Reynolds, *Chem. Mater.*, 1998, 10, 896.
- [88] S. A. Sapp, G.A. Sotzing, J. R. Reynolds, *Chem. Mater.*, 1998, 10, 2101.
- [89] P. Schottland, K. Zong, C. L. Gaupp, B. C. Thompson, C. A. Thomas, I. Giurgiu, R. Hickman, K. A. Abound, J. R. Reynolds, *Macromolecules*, 2000, 33, 7051.
- [90] G. A. Sotzing, J. L. Reddinger, A. R. Katritzky, J. Soloducho, R. Musgarave, J. R. Reynolds, *Chem. Mater.*, 1997, 9, 1578.
- [91] G. A. Soltzing ,J. R. Reynolds, *J Chem. Soc. Chem. Commun.*, 1995, 703.
- [92] C. G. Granqvist, A. Azens, A. Hjelm, I. Kullman, G. A. Niklasson, D. Ronnow, M. Strømme Mattsson, M. Veszelei, G. Vaivars, *Solar Energy*, 1998, 63, 199.
- [93] I. Schwendeman, R. Hickman, G. Sonmez, P. Schottland, K. Zong, D. Welsh J. R. Reynolds, *Chem. Mater.*, 2002, 14, 3118.
- [94] J. Wang, *Analytical Electrochemistry*, Wiley, NY, 2001
- [95] I. Schwendeman, PhD. Thesis, University of Florida, 2002.
- [96] R. F. Lane, A. T. Hubbard, *J. Phys. Chem.*, 1973, 77, 1401.
- [97] E. Lavion, *J. Electroanal Chem.*, 1972, 39, 1.

- [98] R. Silverstein, G.C. Bassler Spectrometric Identification of Organic Compounds, 5th Edition New York: Wiley, 1999.
- [99] C. L. Gaupp, J. R. Reynolds, *Macromolecules* ,2003, 36, 6305.
- [100]M. E. Nicho, H. Hu, C.Lopez-Mata, J. Escalante, *Sol. Energy Mater.Sol. Cells.*, 2004, 82, 105.
- [101]B.Sankaran, J.R Reynolds, *Macromolecules*, 1997, 30, 2582.
- [102]J.P. Ferraris, D.G. Guerrero Handbook of Conducting Polymers. eds T.A. Skotheim, R.A .Elsenbaumer, J.R. Reynolds, New York: Marcel Dekker, 1998.Ch 10.
- [103]G.Sonmez *Chem. Commun.*, 2005, 5251.
- [104]E. M. Giroto, M. De Paoli *J. Braz. Chem. Soc.*, 1999, 10, 394.

APPENDIX A

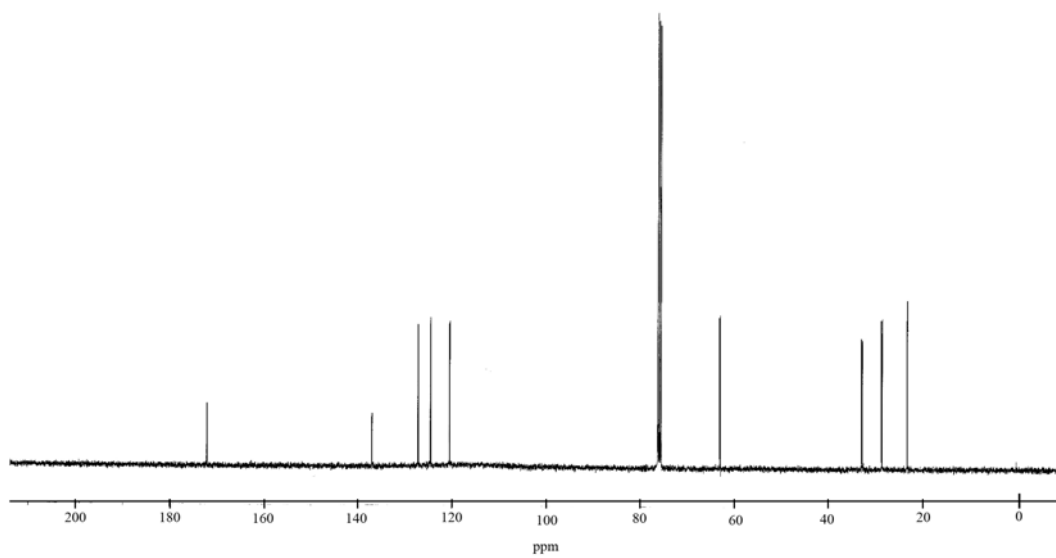


Figure A 1. ^{13}C -NMR of HABTE

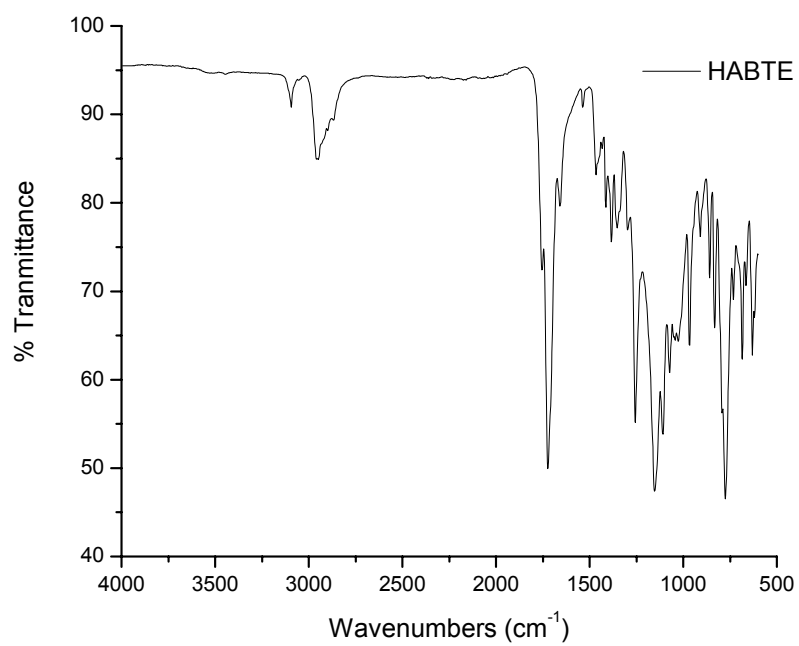


Figure A 2. FTIR of HABTE

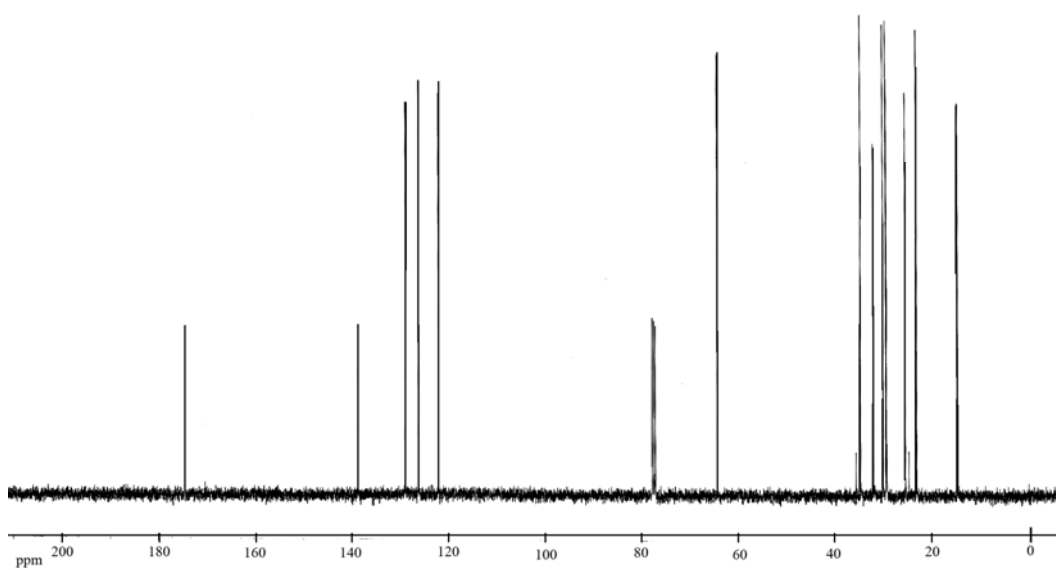


Figure A 3. ¹³C-NMR of OTE

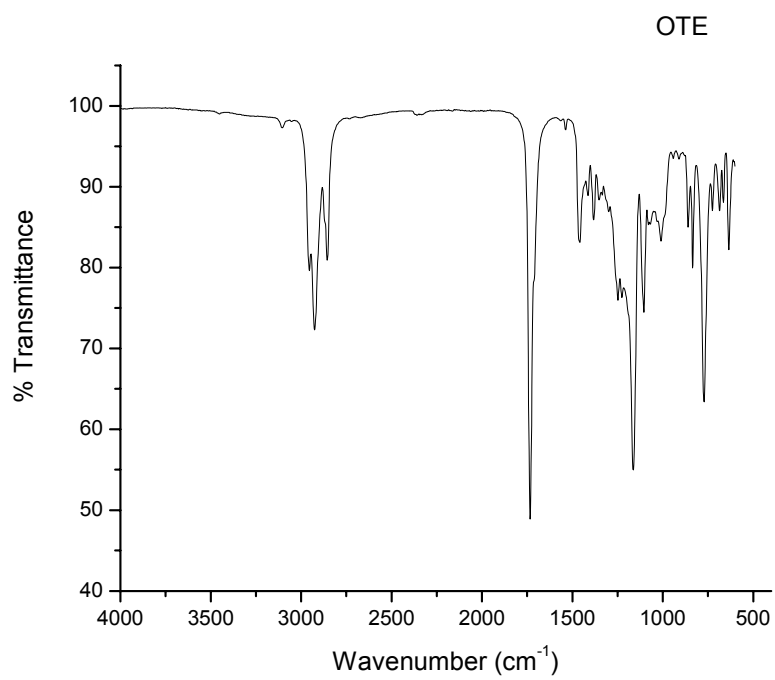


Figure A 4. FTIR of OTE

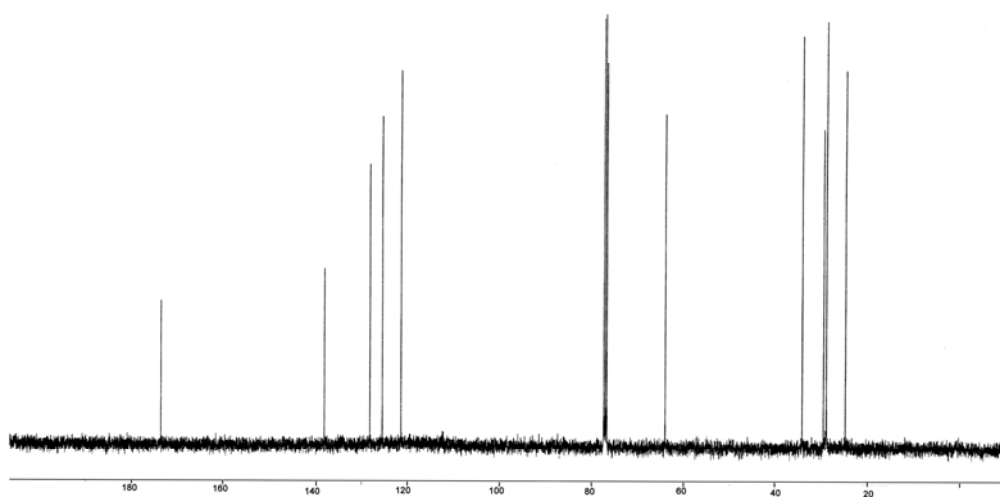


Figure A 5. ¹³C-NMR of DATE

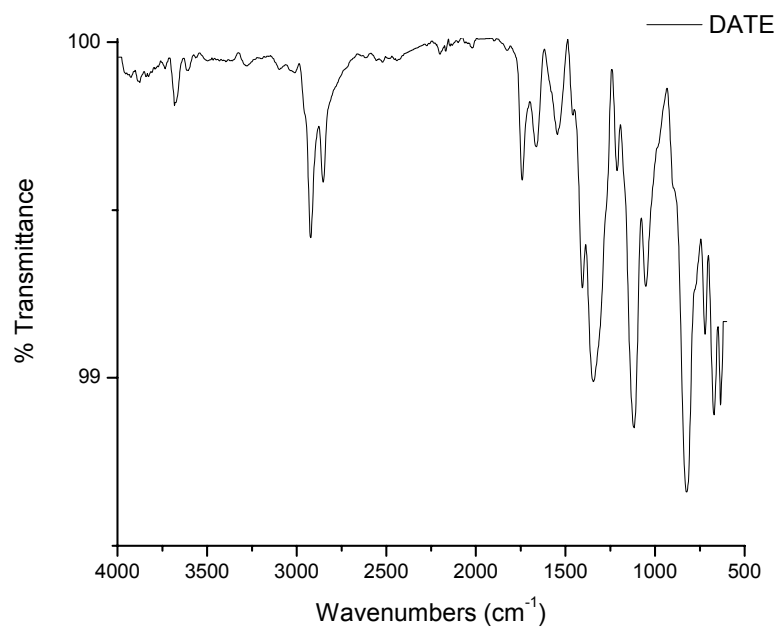


Figure A 6. FTIR of DATE

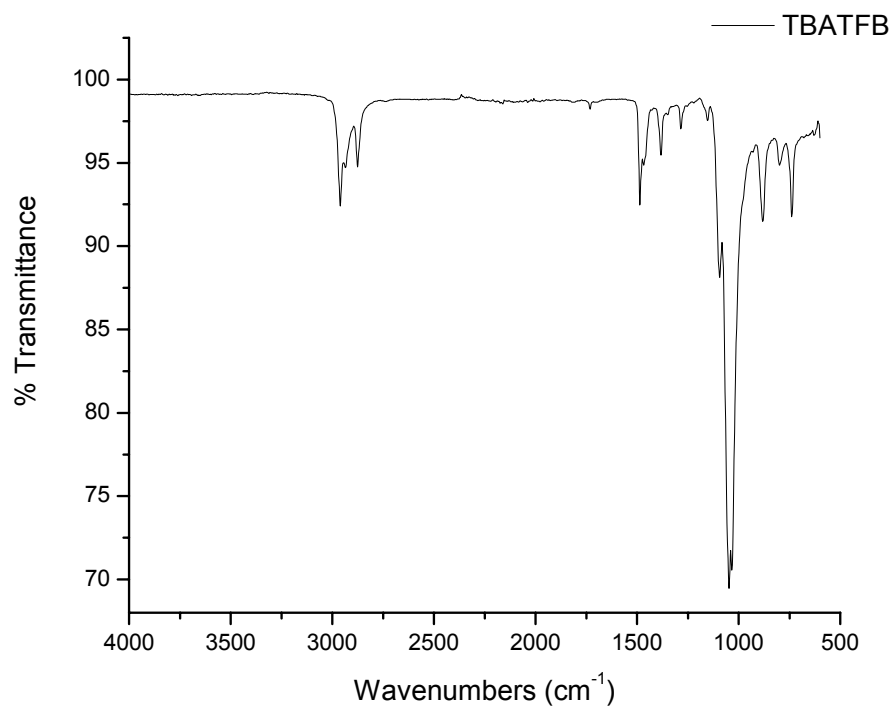


Figure A 7. FTIR of TBAFB

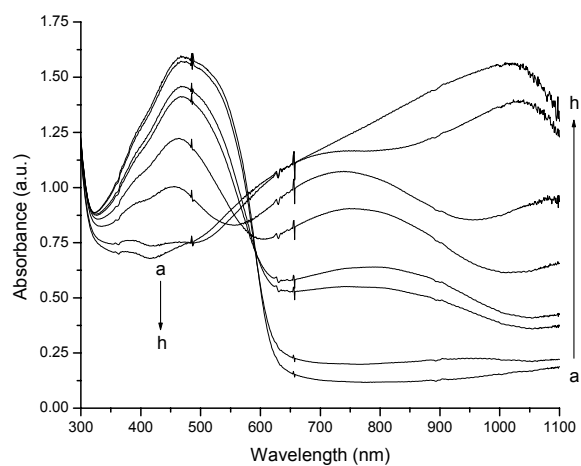


Figure A 8. Spectroelectrochemistry of PTh as a function of applied voltage: (a)0.2V, (b)0.4V, (c)0.5V, (d)0.6V, (e)0.7V, (f)0.8V, (g)1.0V, (h)1.2V

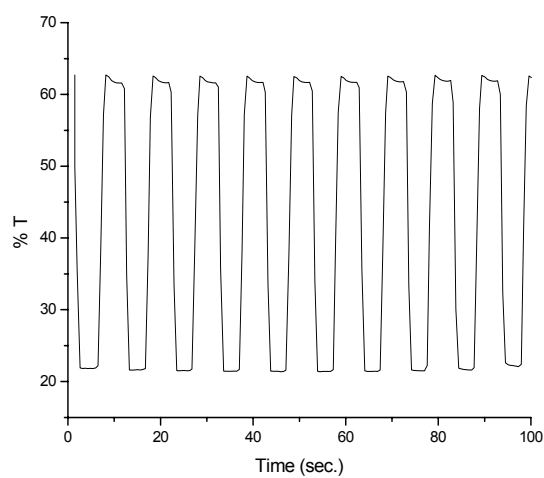


Figure A 9. Electrochromic switching at $\lambda_{\text{max}} = 500\text{nm}$ as the voltage is stepped between -0.5V and 1.5V

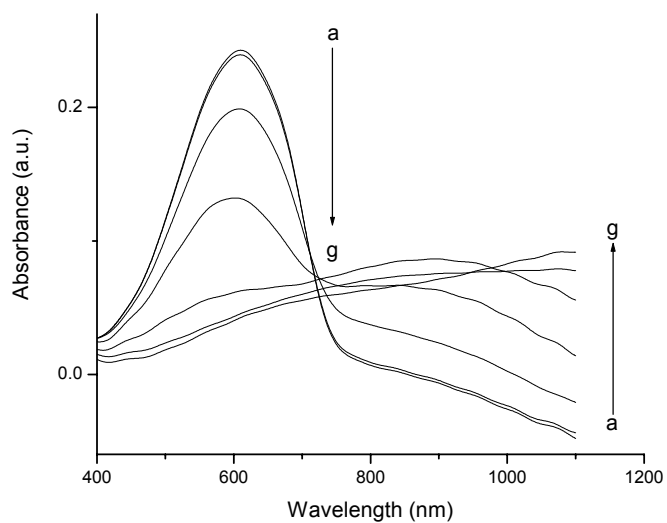


Figure A 10. Spectroelectrochemistry of PEDOT as a function of applied voltage: (a)- 1.0 V, (b) -0.5 V, (c) -0.3 V, (d) 0.0 V, (e) 0.2 V, (f) 0.4 V, (g) 0.6 V

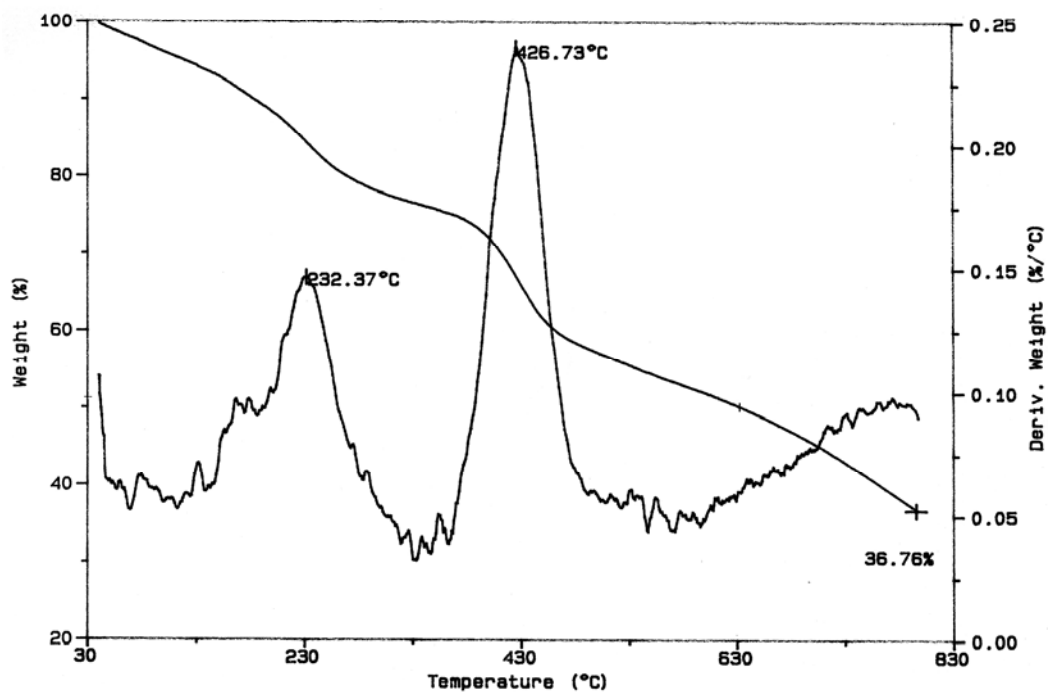


Figure A 11. TGA thermogram of P(HABTE/Th)

VITA

Pınar amurlu was born in Ankara on 19th June 1978. She graduated from TED Ankara College in 1995. She received her B.S. degree at the Chemistry Department, in Middle East Technical University (METU) in 1999 and joined the Department as a research assistant in the same year. She completed her M.S. degree in February 2002 under the supervision of Prof. Dr. Duygu Kısakürek in the field of “Synthesis and Characterization of Poly(dibromophenyleneoxide)s Through Thermal Decomposition of Various Transition Metal Complexes”. She began her PhD. study in 2002 under the supervision of Prof. Dr. Levent Toppare in the field of conducting polymers and electrochromism. In 2003 she joined the Academic Human Resources Program (ÖYP), which is supported by State Planning Organization, and she continued her studies in METU on behalf of Akdeniz University. She worked as a visiting scientist at CNR-ISMAL in Italy on the topic of light emitting diodes. Up to date she has published eleven papers in international journals.